SMALL AND LARGE INTESTINAL STEM CELLS AND THEIR RELATION TO CANCER

by

Julie Marie Cramer

B.S. in Biology, Youngstown State University, 2003

M.S. in Biology, Youngstown State University, 2005

Submitted to the Graduate Faculty of

School of Medicine in partial fulfillment

of the requirements for the degree of

Doctor of Philosophy

University of Pittsburgh

2013

UNIVERSITY OF PITTSBURGH

SCHOOL OF MEDICINE

This dissertation was presented

by

Julie Marie Cramer

It was defended on

December, 13, 2013

and approved by

Marie DeFrances, MD, PhD, Associate Professor, Pathology

David Hackam. MD, PhD, Professor, Surgery and Cell Biology and Physiology

Kacey Marra, PhD, Associate Professor, Plastic Surgery and Bioengineering

Tom Smithgall, PhD, Professor, Microbiology and Molecular Genetics

Jian Yu, PhD, Associate Professor, Pathology and Radiation Oncology

Dissertation Advisor: Eric Lagasse, PharmD, PhD, Associate Professor, Pathology

SMALL AND LARGE INTESTINAL STEM CELLS AND THEIR RELATION TO CANCER

Julie Marie Cramer, MS, PhD

University of Pittsburgh, 2013

The epithelial layers of the small intestine (SI) and large intestine (LI) are generated via self-renewal and differentiation of tissue-specific stem cells (SCs). Failure of intestinal SCs to respond properly to proliferation and differentiation signals can lead to the formation of cancer, almost exclusively found in the LI in humans. We hypothesize that there are distinct resident SCs in the SI versus LI leading to an increased frequency of human LI (colon) cancer. While fleeting observations of differences between SI and LI have been made in the past, a robust study of the origin of their differences has yet to be done. Here we show dramatic intrinsic differences between normal human SI and LI SCs that may have important implications for the disparity in their susceptibilities to cancer. Primary human fetal SI and LI cells were isolated and expanded *in vitro* using conditions that selected for SCs. Flow cytometry and limiting dilution analysis indicated differential SC marker expression as well as disparate populations of colony-forming cells. Gene array analysis showed separate hierarchical clustering and differential expression of transcripts involved in differentiation, proliferation and disease pathways of the SI and LI. Using a three-dimensional *in vitro* differentiation assay, SI and LI SCs formed organoids with architecture and cellular hierarchy similar to that found *in vivo*. Immunostaining and real-time PCR indicated that both SI and LI SCs retain the ability to differentiate into mature cells of the intestine. We also found that well-known proliferation and differentiation pathways in SI- and LI-derived organoids responded differently when exposed to the same exogenous stimuli.

Notably, upon exposure to differentiation cues, an expected decrease in SC marker LGR5 in SI SCs was met with an unexpected increase in LI SCs. We also demonstrate similarities between human LI SCs and colon cancer SCs not present in SI SCs, supporting the notion that normal intestinal SCs are the cell of origin of cancer. Our characterization of human fetal SI and LI SCs revealed critical intrinsic differences that may affect their susceptibility to diseases such as cancer. Further elucidation of pathway differences may allow the exploitation of protective mechanisms to prevent or treat human colon cancer.

TABLE OF CONTENTS

LIST OF TABLES

LIST OF FIGURES

PREFACE

First thanks go to God, my strength. Without which, I would not have survived the last six years. Sometimes we walked together, but mostly, He carried me.

Thank you to my husband, Liam. If you did not encourage me to follow my aspirations, I would not have decided to take on such a challenge. Your support and patience over the past six years has kept me going when I thought I was done. Your willingness to take on nearly ALL of the responsibilities normally shared between a husband and wife is a testament of your dedication and love. I would never have chosen to travel this road without you. I am truly blessed to have you as my partner in life.

Thanks to my family for supporting my decision to pursue a PhD. As the first of both my husband's and my siblings to move out of Youngstown, it was not easy. But the constant communications and pictures of our 8 nieces and nephews kept us close at heart. Thanks for always asking how school was, even though you feared that the answer might take an hour. Your constant love and support was more than appreciated, it was necessary!

I may be blessed with the most diverse set of friends anyone has ever known. Thank you for providing me with constant entertainment and unwavering love, for tear-stained shoulders and a swift kick in the pants when I needed it. My life is better because of you.

I would like to thank my mentor Eric Lagasse for his guidance over the past six years. After a rocky start, you built your lab to be a place of support and mutual respect. You let me

find my own way, but your door was always open when I got lost. The opportunities you provided have given me key insights into the world of industry and academia. You taught me the importance of collaborations and encouraged me to step out of my comfort zone.

I would also like to thank my Thesis Committee: Drs. Jian Yu, David Hackam, Marie DeFrances, Kacey Marra and Tom Smithgall for their support. Their positive words of encouragement always made me want to reach further.

Thanks to Drs. Chet Cooper, Gary Walker and Tom Kim, the Three Amigos. They helped me get my start in science at Youngstown State University. It was in their collaborative lab that the other Lab Goddesses (Heather and Erin) and I learned how to play well with others in the lab. Thank you for teaching me how to teach others and for providing me plenty of opportunities to do so. You saw more potential in me than I did in myself and encouraged me to keep going forward. Thank you for being a constant support system as I moved on to my PhD training at the University of Pittsburgh. Now excuse me, as I must get back to work… Daylight's burnin'!

1.0 INTRODUCTION

Colon cancer, or cancer of the large intestine (LI), remains third in the list of estimated new cases and estimated deaths when considering all cancer sites [1]. While its 5-year survival rate is 90.3% if diagnosed at the local stage, this drops to 12.5% at the metastatic stage [2]. Current treatments for metastatic disease, focused on treating rapidly dividing cells, can lead to toxicity and ultimately poor patient outcome. The genetic model for sporadic colorectal tumorigenesis is defined as an accumulation of mutations and modifications, building on one another with increased chromosomal instability which ultimately ends in the formation of a carcinoma and often times metastasis [3]. These initial mutations are likely to occur in a population of cells that already possess many advantageous characteristics for cancer cells. Therefore, recent evidence has implicated the normal intestinal SC as the cell of origin of LI cancer, which seems to follow a similar differentiation pattern compared to normal tissue [4]. Only in recent years have we begun to understand the intricate niche of the normal intestinal SC and its regulation [5]. Our current knowledge of intestinal SCs and their niche has largely come from experiments performed in the SI with the assumption that the results would likely hold true in the LI. However, based on their functional and structural differences *in vivo*, it is likely that their homeostatic mechanisms and response to transformative events differ and are reflected in their cancer incidence, mortality and 5-year survival rates (**Table 1**) [2].

Table 1: Small versus large intestinal cancer statistics

Statistic	Small Intestine	Large Intestine
Incidence rate*	2.1	45
Mortality*	0.4	16.4
5-yr survival rate with diagnosis at metastatic stage	42.1%	12.5%

*per 100,000 per year

Statistics were taken from the National Cancer Institute's SEER Stat Fact Sheets

1.1 INTESTINAL ORGANIZATION

A myriad of cells contribute to the normal function and maintenance of adult tissues. Some cells, are terminally differentiated and will die serving the tissue. Other rare and undifferentiated cells, SCs, are instead responsible for replenishing the pool of differentiated cells while maintaining an adequate supply of themselves through the process of self-renewal. SCs can divide asymmetrically to produce one daughter cell that is more committed to a specific cell lineage, a transit amplifying (TA) cell, and one that retains stemness. SCs have a slower cycling time, on the order of one per day, whereas TA cells have a limited life span and self-renewal potential while re-populating the differentiated cells of the tissue [6]. TA cells divide every 12-16 hours, surviving for 48 hours and go through approximately 5 rounds of division before being exhausted [7]. Differentiated cells have completely lost the ability to self-renew and succumb to apoptosis after their role is absolved.

The intestine is organized in this hierarchical fashion and its epithelium is renewed every five days in humans [8]. In this very dynamic process lies a complex collection of epithelial cell lineages along with an intricate set of molecular mechanisms to maintain order. The intestine is functionally divided into two sections, the SI and the LI. Both are structurally organized in an elegant network of invaginations, termed crypts. Villi, present only in the SI, provide a higher

surface area to aid in optimal digestion of food and absorption of nutrients. The LI is void of villi and is responsible for absorption of water and waste removal. SCs of both the SI and LI are located at the crypt base and produce epithelial cells that are committed to three to four different cell lineages. These differentiated cells are the absorptive enterocytes, mucus-secreting goblet cells and hormone-secreting enteroendocrine cells that will migrate up the crypt wall to form the intestinal epithelium (**Figure 1**, left). A fourth cell, the Paneth cell, is only present in the SI and occupies the base of the crypt among the SCs [9].

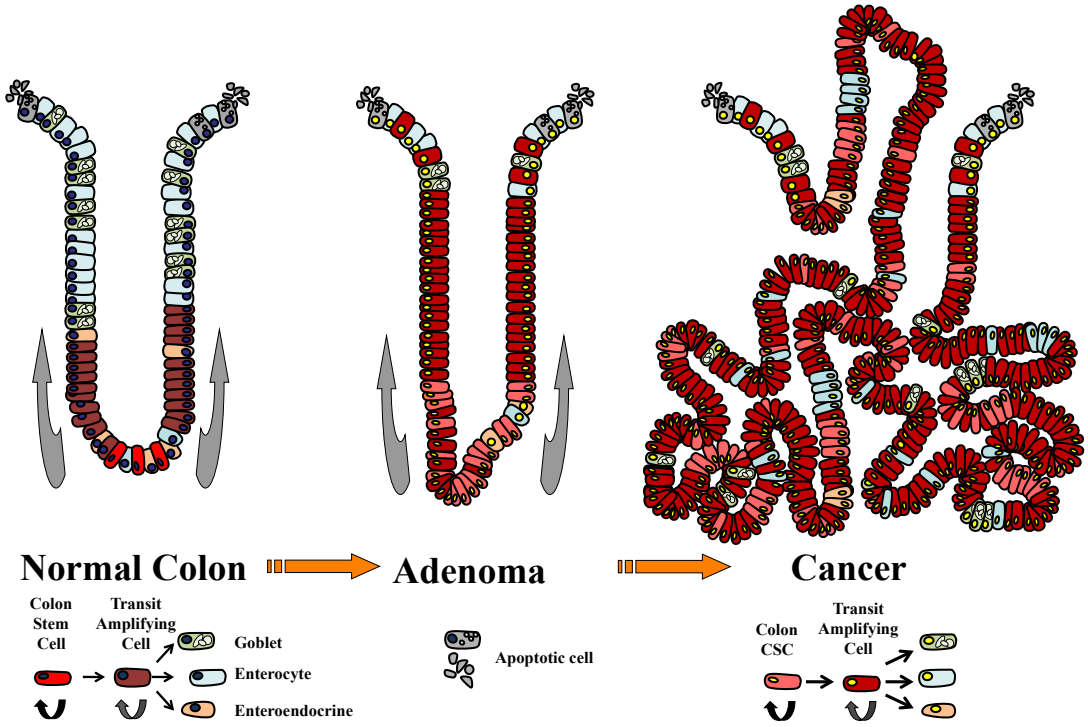

Figure 1: Organization of intestinal crypts and their transformation to cancer. Intestinal SCs are located at the base of the crypt in normal SI and LI and produce more differentiated cells as they migrate up the sides of the crypt. An adenoma will develop in the LI upon deregulation of SC homeostasis. Upon further neoplastic injuries, SCs will transform into cancer stem cells (CSCs) with some limited ability to differentiate [10].

1.1.1 Intestinal SC niche

In 1978, Schofield observed that hematopoietic cells derived from the spleen have decreased proliferative potential when compared to those from bone marrow, the first description of a SC niche [11]. It followed that there may be specialized environments that maintain proliferative potential but limit differentiation, the perfect combination for homeostatic regulation of SCs. It was not until 2007, thanks to the improvement of lineage tracing strategies, that the SI SC niche was fully described in mammals, containing vascular components, fibroblasts and Paneth cells providing factors such as Wnt, Bone Morphogenetic Protein (BMP) and Notch [6].

Paneth cells, which are interspersed between SCs and the surrounding subepithelial mesenchyme in the SI, express many factors believed to be intricately involved in niche maintenance including EGF, Wnt3 and Notch ligands Delta-like ligands Dll1 and Dll4 [12]. However, Wnts and EGFs are also produced by sub-epithelial mesenchyme [13] in addition to BMP inhibitors, not produced by Paneth cells [14]. Finally, Rspondins are required for maintenance of intestinal organoid cultures *in vitro*, but their *in vivo* source is yet unknown [5].

While multiple experimental evidences indicate the importance of Paneth cells in the intestine [9, 15], these studies are limited to the SI, as the LI is void of lysozyme-expressing Paneth cells. This raises the question of differential regulation of SCs in the two compartments of the intestine. However, Paneth cells in the SI reportedly express CD24 and a similar cell, previously described as a non-goblet secretory cell was found to express CD24 in the LI crypt [9, 16]. This may be a cell providing similar signals to LI SCs in the absence of a true Paneth cell, but it has not been definitively identified.

1.1.2 Intestinal SCs

Before the discovery of intestinal SCs, a model for repopulation of the intestinal epithelium was being formed. The idea that cells flowed from crypts to villi in a "conveyor belt" mechanism was first demonstrated by autoradiography [17-19]. The identity of the crypt base columnar (CBC) cell, following the Unitarian Theory that all cells in an intestinal crypt are derived from one cell, was not investigated until 1974 [20]. Elementary lineage tracing of radioactive phagosomes indicated that differentiated lineages were derived from CBC cells [21]. Later, chemical mutagenesis allowed other groups to visualize ribbons of cells moving from crypt to villous tips with long-lived clones, presumably the fully differentiated compartment, and short-lived clones, presumably the TA compartment [22, 23]. Some controversy began with Potten's identification of a label-retaining cell (LRC) at the +4 position in the intestinal crypt [7, 24]. Label retention suggests mitotic quiescence and stemness, however, other groups have since shown that these cells cycle every day and their label retention is due to their asymmetric segregation of old (labeled) DNA and new (unlabeled) DNA [7, 25]. This is unlike CBC cells, which segregate their chromosomes randomly [26-28].

The identification and regulation of SCs in the intestine has evolved rather rapidly in recent years. More sophisticated *in vivo* lineage tracing studies have identified leucine-rich repeat-containing G-protein coupled receptor 5 $(LGR5)^{+}$ SCs in the mouse as cells capable of generating all the epithelial cells of the intestine, dividing every day, and forming crypt-like structures *in vitro* [5, 6]. Their ability to divide every day *in vivo* and complete 1,000 cell divisions in a lifetime allows them to exceed the Hayflick limit in appropriate *in vitro* settings without evidence of transformation or senescence [5, 29]. In this tightly controlled system, growth factors

and three-dimensional matrix support the growth of epithelium with structures resembling that found *in vivo*.

These studies confirmed and expanded the idea that the Wnt pathway is critical for homeostatic crypt formation and maintenance in the intestine [30]. Interestingly, LGR5, a serpentine receptor is a facultative member of the Wnt receptor complex that responds to secreted Wnt pathway agonists such as Rspondins [31-34]. Not only is LGR5 a Wnt receptor, it is also a Wnt target, repressed upon inhibition of the pathway [6]. It is evident that the SCs of the intestine are intricately controlled by Wnt signals via their expression of LGR5 and synergistic signal transduction.

In addition to the $LGR5^+$ CBC SC, a population of +4 cells has recently been characterized as slow cycling, therefore different from Potten's fast cycling +4 cell, and able to proliferate, expand, self-renew and give rise to all differentiated cells of the intestine [35]. Further, upon ablation of $Lgr5^+$ cells, crypt homeostasis seemed unperturbed, owing to $Bmi1^+$ cells repopulating the epithelium [36]. Therefore, some have proposed a model in which Lgr5 SCs are responsible for homeostatic maintenance of the intestine while $Bmi1^+$ cells are responsible for injury-induced regeneration [32]. However, it is important to note that the $Bmi1^+$ population of SCs was only found in the SI, indicating the lack of a second SC population in the LI if the LGR5 SC is lost due to injury or transformation.

1.1.3 Differentiated cells of the intestine

The differentiated cells of the intestine work in concert as a specialized ecosystem to carry out the functions of the intestine. This specialized layer protects the host from a myriad of insults from the harsh contents of the intestinal lumen. In the SI, digestive enzymes work to digest food

and absorb nutrients before the LI eliminates indigestible food particles. Four main cell types are present in the SI, while one, the Paneth cell is absent from the LI [21].

Enterocytes are by far the most numerous of the intestinal cell types and make up a majority of the epithelial lining [21]. Their cell polarity and structural properties give the intestinal epithelium its integrity, while being able to take up and process antigens that penetrate the protective mucin layer [37].

Goblet cells produce a variety of high molecular weight glycoproteins, called mucins [37-39]. Mucins provide a viscous extracellular layer for defense and defects in this mucous layer can increase bacterial adhesion, permeability, inflammation and cancer [40]. Most importantly, the mucin layer functions to allow adhesion of resident microbiota while preventing the attachment of pathogenic microorganisms [39].

Enteroendocrine cells export peptide hormones from secretory granules [37, 41, 42]. They act as luminal surveyors, responding at their basolateral side to nutrient sensing at the apical surface [43]. This results in the control of physiological functions such as glycemia, exocrine pancreatic secretion, growth and repair of the gut epithelium, motility of the gut wall and gastric emptying [44, 45]. It has been reported that the Notch-Hes axis (discussed below) is pivotal in enteroendocrine cell differentiation, with Hes1 antagonizing expression of enteroendocrine cell-specific neurogenin3 and blocking differentiation to that lineage [44, 46].

Lastly, Paneth cells secrete antimicrobial cryptdins or defensins, digestive enzymes and growth factors [37]. Unlike the other three cell types, these cells migrate down to the base of the crypt, rather than in an upward direction, becoming part of the SI SC niche. Even though separated spatially from goblet cells, Paneth cells also play a role in enteric defense, producing antimicrobial peptides [42]. Wnt and Notch signaling work in concert to regulate Paneth cell

differentiation [47, 48]. With such important roles, it is interesting that the LI can avoid injury without this cell population, however, it may explain why it is more susceptible to cancer formation, especially since cancer is likely to arise from inflammation-plagued epithelium.

1.2 SIGNALING PATHWAYS IN INTESTINAL HOMEOSTASIS

The two main signaling pathways responsible for homeostasis in the intestine, the Wnt pathway and the Notch pathway have extensive cross-talk with their involvement in cell fate decisions, proliferation, differentiation and tumorigenesis [48, 49]. Thus far, a majority of studies elucidating these pathways in the intestine have not made clear distinctions between the SI and LI.

1.2.1 Wnt Pathway

Wnt signaling is one of the driving forces of crypt formation and maintenance in the colon [30]. In the absence of Wnt signals, a destruction complex sequesters beta-catenin in the cytoplasm with axin, adenomatous polyposis coli (APC) and glycogen synthase kinase 3 (GSK3) beta [50, 51]. This complex marks beta-catenin for degradation and leads to a decrease in Wnt targeted transcription. When Wnt proteins bind Frizzled/LRP receptors, the canonical Wnt pathway ensues. This involves the disruption of the destruction complex and allows beta-catenin to enter the nucleus and in concert with transcription factor 4 (TCF4), trigger transcription of Wnt targets [52, 53] (**Figure 2**). Two of the known Wnt targets are cyclin D1 and c-myc oncogene, both overexpressed in colon cancer [54, 55].

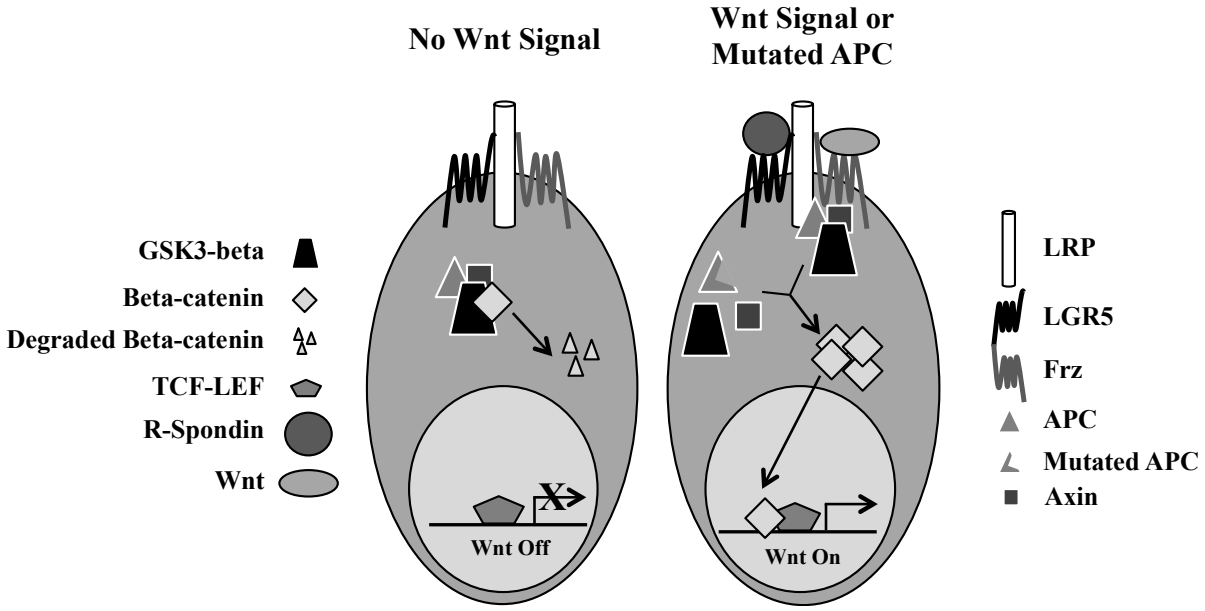

Figure 2: The Wnt Pathway. In the absence of Wnt signals (left), the APC destruction complex leads to the degradation of beta-catenin. When Wnt signals bind to Wnt receptors or APC is mutated (right), disruption of the complex allows beta-catenin to move into the nucleus for transcriptional regulation of Wnt genes in concert with TFC transcription factors.

The dysregulation of the Wnt pathway and its role in self-renewal as well as differentiation have been shown to be required for the development of cancer [30]. Mutations in APC have been implicated in both the sporadic and inherited forms of colorectal cancer, causing an accumulation of beta-catenin in the nucleus and enhanced Wnt signaling [56-60]. Therefore, if aberrantly active, the Wnt pathway could result in an expanded progenitor population and colon cancer (**Figure 1**).

1.2.2 Notch Pathway

The Notch pathway determines cell fate decisions in the intestinal crypt. Upon binding of a Notch ligand on one cell to a Notch receptor on another cell, gamma-secretase cleaves the intracellular tail of the Notch receptor, the Notch Intracellular Domain (NICD), which translocates to the nucleus for transcriptional signaling[61]. The most well-known targets of Notch are the hairy/enhancer of split (HES) family of transcription factors, principally HES1 for its involvement in the intestine [46, 62]. Notch receptors 1 and 2 are expressed on SCs and TA cells in intestinal crypts and mediate the expression of HES1, blocking transcription of atonal homolog 1 (ATOH1) and differentiation [48, 63, 64]. DLL1 and DLL4 are ligands for these receptors and can be found on the surface of Paneth cells in the SI [65]. While activation of the Notch pathway represses secretory cell differentiation [66], inhibition of Notch leads to activation of ATOH1 promoting goblet cell differentiation in intestinal crypts and adenomas [48, 67] (**Figure 3**). Again, it is important to note that a majority of these studies have been carried out in the SI. Therefore, it has largely been assumed that the same holds true for the LI.

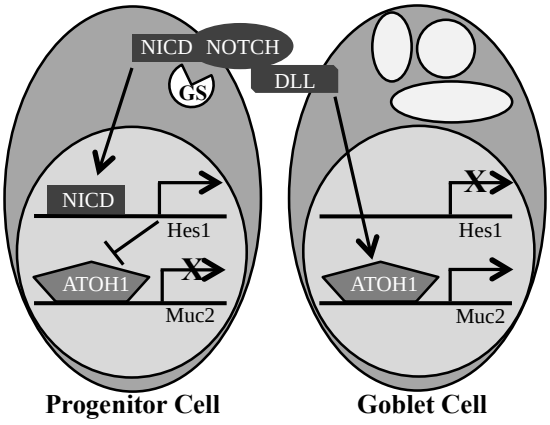

Figure 3: Notch signaling in intestinal cells. Lateral inhibition via expression of Notch receptor on one cell and Notch ligand on a neighboring cell. GS = gamma secretase.

The manipulation of the Notch pathway via drug intervention is an attractive approach to target CSCs. Gamma-secretase inhibitors have been shown to reduce cancer growth, inhibit CSC self-renewal and increase differentiation to goblet cells [67]. Similar results were found with small molecule and RNA knockdown studies, showing that the inhibition of Notch leads to increased apoptosis, decreased self-renewal and increased secretory cell lineage differentiation of CSCs in colon cancer [66]. In yet another study, inhibition of DLL4 inhibited the expression of Notch targets and reduced tumor initiating cell frequency [68]. These targeted therapies may enhance the efficacy of chemotherapeutic drugs when used in sequence or combination [69]. However, these are mechanisms shared with normal intestinal SCs and may lead to toxicity.

1.3 SMALL INTESTINE VERSUS LARGE INTESTINE

Even though the SI and LI vary greatly in their function and structure, comprehensive studies have not been done to explain the origin of these differences and their relation to disease. An accumulation of evidence of their differences may prove to be important to intestinal disease susceptibility.

1.3.1 Cycling time

In mouse intestinal lineage tracing assays, LI SCs seem to cycle slower than their SI SC counterparts as evidenced by LacZ cells remaining restricted to the crypt base after 5 days, when in the SI, full ribbons of cells were observed [6]. Full ribbons of LacZ positive cells did increase in later days, indicating the ability of LI SCs to self-renew long-term. The difference in rate of

epithelial turnover between the SI and LI may be an indication of differential intrinsic responses to environmental cues.

1.3.2 Resistance differences

SCs are charged with the task of maintaining genomic integrity and tissue homeostasis. Therefore, their resistance to damage must be higher than more differentiated cells. This is a distinguishing factor between SCs of the intestine. The quiescent +4 cell in the SI crypt is sensitive to ionizing radiation, while its rapid cycling counterpart, the $LGR5^+$ CBC SC, is more resistant [6, 7, 70]. The surviving $LGR5^+$ SCs, presumably with better DNA repair mechanisms, can then repopulate the SI after injury. Thus, even if +4 $Bmi1^+$ cells serve as a reserve SC in the SI, but are absent from the LI, $LGR5^+$ SCs are still able to rescue the tissue. Additionally, LI SCs seems to be more resistant than their SI SC counterpart, possibly contributing to therapy resistance and higher occurrence of LI cancer over SI cancer [71].

Prior to well-defined lineage tracing and specific identification of +4 ($Bmi1^+$) and CBC ($LGR5^+$) SCs in the intestine, apoptotic differences in SC positions were observed between SI and LI crypts. Spontaneous and irradiation-induced apoptosis were higher in the SI compared to the LI and were maximal at position 4. In the LI, apoptosis was not confined to the crypt base or the +4 position, but was distributed along the length of the crypt [72]. Similarly, the apoptotic and mitotic index of the LI are 50-60% and 45-70% of the values for the SI, respectively [73]. This may be due in part to differential expression of bcl-2, an inhibitor of apoptosis. While bcl-2 is expressed in CBC cells of the LI, it is absent from SI crypts. Therefore, when apoptosis was observed in bcl-2 null mice, it rose significantly at the base of LI crypts, while remaining unchanged in SI crypts [72]. It has also been reported that LI SCs have lower expression of p53, a

tumor suppressor and DNA damage responder [74, 75]. Since apoptosis is a mechanism by which damaged cells are removed from the epithelium, a decrease in apoptosis in the LI may predispose its SCs to propagate damaged cells, which may lead to transformation. Once transformation occurs, the newly firmed CSCs likely have inherited the resistance of the cells of origin.

1.3.3 Wnt pathway differences

As mentioned above, the Wnt pathway is the most perturbed pathway in LI cancer and is responsible for homeostasis in the normal intestine. It is generally accepted that upon Wnt activation, beta-catenin translocates to the nucleus where is binds to TCF factors (namely TCF4), entering into a transactivation complex to enhance the expression of downstream targets of Wnt. As mentioned before, most of these studies have been carried out in the SI and it was not until the expression of TCF4 (encoded by *Tcf7l2*) was assessed along the entire intestine, that its expression was seen to be limited to the SI. A KO in this gene had no affect on the phenotype of LI crypts, but the SI lacked proliferative compartments completely [30]. The expression of *Tcf7l1* (TCF3) is thought to have functional redundancy in the intestine and may be the mechanism used to transmit Wnt signals in the LI [30, 76]. TCF3 has an unconventional interaction with beta-catenin. When beta-catenin binds to TCF3, it reduces TCF3 chromatin occupancy and causes degradation of TCF3, thus releasing its repressor role, and allowing for the transduction of Wnt signaling [77]. These interactions demonstrate a delicately controlled system of Wnt signals in the LI. Furthermore, there is controversy as to the function of TCF4 as a tumor suppressor or oncogene [78]. In any case, differences between human and mouse as well as SI and LI must be investigated further to truly understand the involvement of TCF factors in small and large intestinal homeostasis and carcinogenesis.

1.4 NORMAL STEM CELLS VERSUS CANCER STEM CELLS

Since the hallmarks of SCs are their ability to self-renew and differentiate, investigators were prompted to explore the similarities and differences that exist between normal SC maintenance of tissues and organs and the uncontrolled proliferation of cancer [79]. Abnormal cellular behavior in this tightly controlled system can occur via genetic alterations such as tumor suppressor loss or gene destabilization that result in incremental neoplastic gains and disruption of the homeostatic system [80]. In essence, tumors can be viewed as small aberrant organs containing a hierarchy of progenitor cells and differentiated cells (**Figure 1**). Albeit dysfunctional in the bodily view, they maintain their own abnormal proliferation and survival mechanisms [81]. If tumors are indeed aberrant organs, then there is a program by which the system is controlled, however loosely it might be. Therefore, in the cellular hierarchy of a tumor, there is a differentiation mechanism from CSC to tumor progenitor cell to mature cancer cell that ends in apoptosis and turnover [82].

1.4.1 Intestinal SCs as the cell of origin of cancer

The CSC theory presents a situation where a cancerous cell, formed from mutations in a normal SC, inherits the characteristics of the cell of origin. This concept was nicely demonstrated after deletion of APC in $LGR5^+$ intestinal SCs, which led to rapidly growing adenomas, suggesting that normal SCs are the cell of origin of intestinal cancer[4]. Furthermore, murine adenomas revealed continual $LGR5^+$ SC activity, providing functional evidence of a SC population in these pre-cancerous intestinal lesions [83]. Alternatively, the +4 $Bmi1^+$ SCs were also able to generate adenomas upon the induction of a stable form of beta-catenin, similar to the LGR5 CBC SC. The

protective mechanisms meant to preserve the SC pool become part of the CSC repertoire of repair and resistance. These studies provide important evidence of the relation between normal and cancer SCs.

To strengthen the relation between normal and cancer SCs, an intestinal SC signature was found on colon CSCs displaying robust tumor-initiating capacity and long-term self-renewal potential that also correlated with disease relapse [84]. This intestinal SC signature was validated *in situ* using a human colorectal gene expression database looking at colorectal adenocarcenomas [85]. The similarities found between normal LI SCs and colon CSCs support the hypothesis that transformative events in LI SCs produce colon CSCs capable of fueling cancer growth and assumes differences between SI SCs and LI SCs contribute to the higher frequency of LI cancer.

1.4.2 Intrinsic versus extrinsic factors

In any cellular environment there are extrinsic factors, including matrix, neighboring cells and secreted factors that can alter a cell's behavior, telling it to proliferate, differentiate, move or die. There are also intrinsic factors that determine the cellular response to these environmental cues. The same cues could lead to differential responses in two differently programmed cells. In LI cancer, intrinsic resistance in cancer cells determines response to treatment [86]. Colitis-associated carcinogenesis may be triggered by an intrinsic defect in Maltripase, an important component of tight junctions, leading to a compromised permeability barrier [87]. Loss of APC and activation of KRAS, followed by nuclear beta-catenin accumulation, as the first steps from adenoma to carcinoma sequence, are considered intrinsic alterations causing an effect in cellular behavior [88]. In normal intestinal crypts, it is Wnt, Notch and BMP signaling that determines SC proliferation and differentiation, and upon transformation, an altered maintenance of colon CSCs [89, 90].

Alternatively, normal intestinal crypts and their resident SCs may be extrinsically maintained. If SCs divide symmetrically [91], it may be their surroundings, such as neighboring cells, that determine their fate instead of intrinsic mechanisms laid out at the birth of a cell [92]. Extrinsically, the leading edge of a growing cancer is inundated with signals from the microenvironment. Myofibroblasts produce extracellular matrix, secrete cytokines and growth factors that signal for proliferation and invasion of tumor cells [93]. Furthermore, HGF, often found in the tumor microenvironment, enhances tumor growth and invasion via Wnt/beta-catenin signaling, an example of the intrinsic working with the extrinsic for survival of the fittest cancer cell [94, 95]. Other extrinsic factors can be derived from pathogens or cellular damage, but it is the intrinsic cell programming for molecules such as receptor for advanced glycation end products (Rage) that determines the response to such signals [96]. Therefore, it is a synergistic battleground of intrinsic versus extrinsic signaling that ultimately determines cellular response. Either set of signals or a combination of the two can determine differences between two cell populations.

2.0 EXPANSION OF NORMAL HUMAN SMALL AND LARGE INTESTINAL EPITHELIAL CELLS

Few methods allow the successful expansion of undifferentiated SCs of the human intestine. To overcome this limitation, we used feeder cells as a stromal layer to provide cell-cell interactions and promote epithelial cell growth [97]. Our lab has previously used this system to expand CSCs from human metastatic colon cancer [98]. Here, we isolated human fetal SI and LI cells from primary tissue and plated bulk intestinal cells on the feeder layer, allowing colonies to form from the SC population. In this approach, only the cells with SC characteristics such as colony-formation and self-renewal propagate. Therefore, there is no bias in identification of SCs via markers, only identification and characterization of cells with SC properties. Most importantly, we compared SI and LI cells isolated from the same donor tissue, minimizing potential discrepancies due to genetic variability.

2.1 REQUIRED CULTURE CONDITIONS AND INITIAL OBSERVATIONS

2.1.1 Intestinal epithelial cell expansion required the addition of R-Spondin 2

Human fetal SI and LI cells from primary tissue were isolated and plated on the feeder layer as was done with the human metastatic colon cancer [98]. However, the plating efficiency was very

low with cells surviving only about a week in culture, unable to be passaged. The Wnt pathway has previously been shown to be integral to the growth of intestinal cells *in vitro* [5]. We found that maintenance of normal human intestinal cells required the addition of R-spondin 2, a Wnt agonist (**Figure 2**). Within one week after plating, intestinal cells formed visible colonies among the feeder cells that were sustainable up to ten passages.

2.1.2 Small and large intestinal epithelial cells differ in morphology

There are dramatic differences in the SI and LI architecture *in vivo* (**Figure 4A**). While both the SI and LI have invaginations called crypts, only the SI has protrusions called villi. This structure is related to function. The structure of the SI lends to absorption and digestion of food. The structure of the LI allows for the absorption of vitamins and water as well as removal of waste from the body. When the colonies began to form *in vitro*, differences between SI and LI colony density, cell growth, size and shape were observed (**Figure 4B**). The SI cells formed more dispersed colonies with cells of various shapes and sizes while the LI cells formed more compact colonies with cells of homogeneous shape and size.

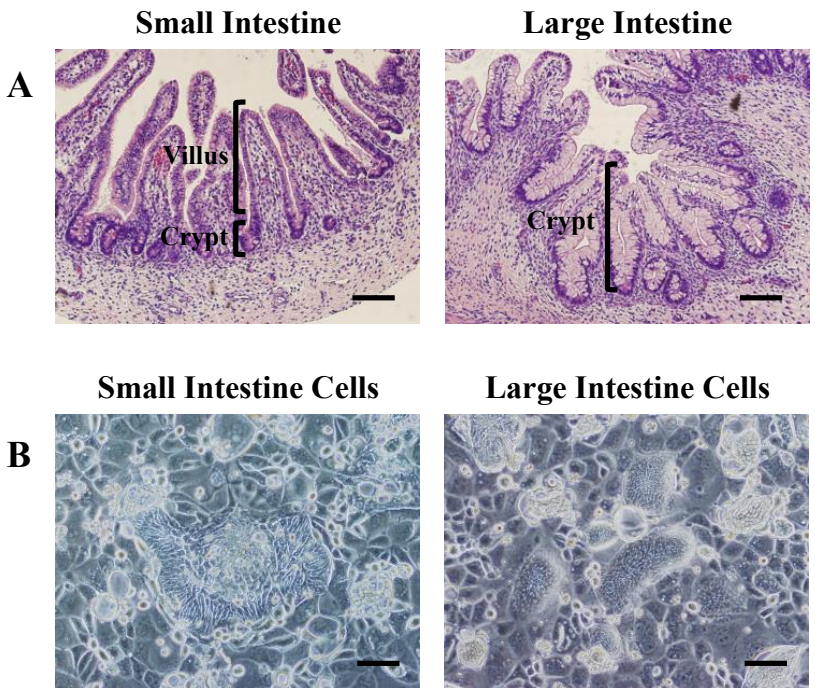

Figure 4: Primary human intestinal cells expand on the feeder layer. (A) Hematoxylin and eosin paraffin sections of normal fetal SI (left) and LI (right). (B) SI (left) and LI (right) SCs expanding on the feeder layer *in vitro*. Scale bar = 100μm.

2.1.3 Expanded intestinal cells are epithelial

Flow cytometry analysis revealed that even though bulk intestinal cells were plated *in vitro*, including blood, muscle and mesenchymal cells, expansion of the cells increased the proportion of epithelial cells, as marked by Epithelial Cell Adhesion Molecule (EpCAM), from 21.6 and 34.3% to 92.3 and 92.4% in primary SI and LI respectively (**Figure 5A & B**), indicating the feeder cells provided an environment that selects for and allows the expansion of intestinal epithelial cells.

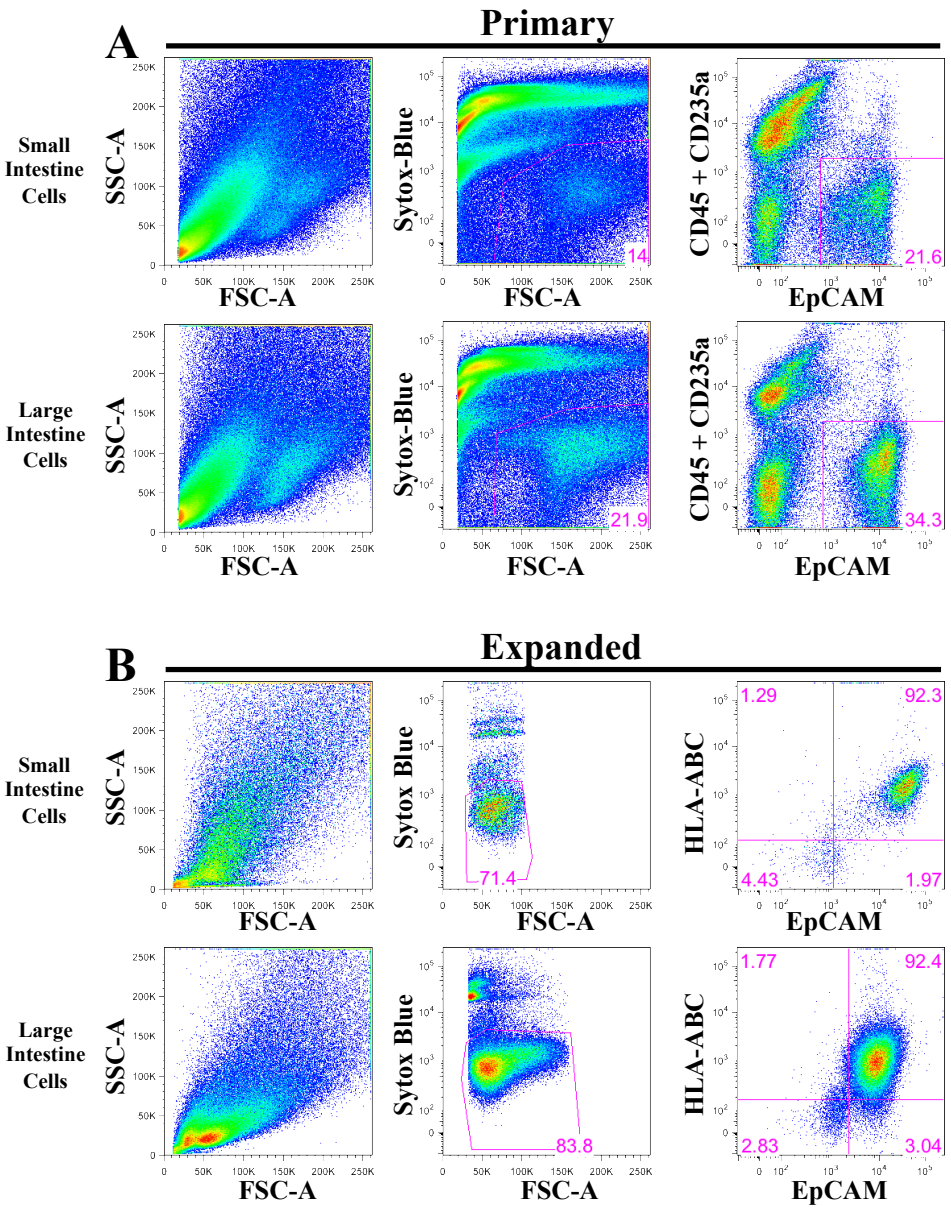

Figure 5: Cells expanded on feeder layer are EpCAM^{+}. (A) Normal human SI and LI cells freshly isolated from tissue and analyzed by flow cytometry for EpCAM, excluding blood cells (EpCAM^{+}CD45^{-}CD235a^{-}). (B) Normal SI and LI epithelial cells expanded *in vitro* retain EpCAM marker, excluding feeder layer (HLA^{+}EpCAM^{+}).

2.2 EXPANDED INTESTINAL CELLS ARE NOT TRANSFORMED

2.2.1 Expanded intestinal cells do not form tumors in mice

Since the Wnt pathway is also known to play a role in cancer [99] and we used a Wnt agonist to propagate them, we wanted to ensure that the cells were not transformed. Expanded intestinal cells that had been treated with R-Spondin 2 were injected into the subcutaneous space of immunocompromised, Rag-$2^{-/-}/\gamma c^{-/-}$, mice. These normal cells failed to form tumors in every case. As a control, human colon CSCs (Tu22 from Odoux [98]) were also injected and formed xenograft tumors in every case (**Table 2**). This is an indication that the normal intestinal cells expanded in the feeder layer system are not transformed.

Table 2: Normal intestinal SCs did not form tumors *in vivo*

Cell Type	Frequency of Tumor Formation
Colon CSC	5/5
SI SC	0/5
LI SC	0/6

2.3 DISCUSSION

While human CSCs from primary tissue can be expanded on our feeder layer culture system without additional exogenous growth factors, the same system appeared futile for the expansion of normal human intestinal cells. However, understanding the importance of the Wnt pathway in intestinal crypt maintenance, the addition of R-Spondin 2 greatly enhanced the plating efficiency. The initial observations of growth differences between SI and LI cells prompted us to investigate

the possibility that the SI and LI are propagated from two different SC populations. To begin these studies, it was imperative to first identify the type of cells expanding in our system from the bulk primary cells. EpCAM was first discovered as an adhesion molecule, but has since been found to play a role in cell cycle and proliferation [100]. The enrichment of $EpCAM^+$ cells in both SI and LI cultures validated that these cells were in fact epithelial in nature and could be separately characterized from the feeder layer using this marker. EpCAM has long been found to be overexpressed on cancer cells and cancer-initiating cells, but more recently, its expression and role has been investigated in the context of normal SCs [101-103]. This was the first indication that these cells may be of SC nature.

3.0 CHARACTERIZATION OF EXPANDED INTESTINAL EPITHELIAL CELLS

Many studies of SCs focus on cell surface markers as a way of identification. This identification is often linked to SC properties within a specific cell population. Therefore, it was imperative to identify cell surface markers present on the expanded intestinal epithelial cells to further characterize them as SCs. A panel of markers was selected for their previous identification in SC studies of various tissues. Each expanded intestinal cell sample was subjected to panel analysis by flow cytometry. While there were some variations within the two groups most likely due to genetic variation, many similar and repeatedly disparate patterns emerged between the expanded SI and LI cells. These markers were subsequently used in limiting dilution analysis (LDA) studies to test their role in self-renewal and colony formation. Furthermore, quantitative flow cytometry was used to demonstrate the dramatic growth rate differences between the two SC populations. Through these studies, it became apparent that there are intrinsic differences between SI and LI SCs that warrant further investigation.

3.1 CELL SURFACE MARKER PROFILE

Primary and expanded SI and LI epithelial cells (13 SI and 8 LI) were screened against 16 antibodies. The marker profile gave rise to many patterns while also showing the effect of genetic variation between samples. Three matched SI and LI are shown in **Table 3** in comparison

to freshly isolated primary cells. While many of the matched samples did share markers within SI and LI groups (ex. CD44, CD49b), some were variable (ex. CD227, CD13). When comparing primary cells to expanded cells, some apparent selection has occurred (ex. CD166, CD133.1, CD66c, CD49f), indicating enrichment for a particular population of cells.

Table 3: Phenotypic profile of primary and expanded intestinal cells.

Primary and expanded SI and LI cells were screened against 16 antibodies. For primary cells, blood cells were eliminated by CD235 and CD45, then EpCAM was used to gate on epithelial cells prior to marker profiling. For expanded cells, HLA was first used to distinguish the human cells from the rat feeder layer, then EpCAM was used to gate on epithelial cells prior to marker profiling. One representative primary sample is presented here for primary cells and three matched SI and LI samples for expanded cells. +/- indicates more cells are expressing the marker than are not expressing the marker, -/+ indicates more cells are not expressing the marker than are expressing the marker, low+ indicates that the expression of that marker was low.

Marker	Primary SI	Expanded SI 1	Expanded SI 2	Expanded SI 3
CD9	+	+	+	+
CD13	+	+	+/-	+
CD24	-	low+	low+	low+
CD26	+/-	+	+	+
CD29	+/-	low+	+	low+
CD34	-	-	-	-
CD44	-	-	-	-
CD49b	+	+	+	+
CD49f	-	+	+	+
CD54	-	-	-	-
CD66c	-/+	+/-	+/-	+
CD90	-	-	-	-
CD133.1	-/+	-/+	+/-	-/+
CD133.2	-/+	+/-	+/-	-/+
CD166	-	+	+	+
CD227	-	-/+	-/+	-

Marker	Primary LI	Expanded LI 1	Expanded LI 2	Expanded LI 3
CD9	+	+	-	low+
CD13	+/-	-/+	+/-	+/-
CD24	-	+	+	low+
CD26	+/-	+	+	+/-
CD29	-/+	+	+	+
CD34	-	-	-	-
CD44	-	-	-	-
CD49b	+	+	+	+
CD49f	low+	+	low+	+
CD54	-	+/-	-/+	-
CD66c	+/-	-/+	-/+	-/+
CD90	-	-	-	-
CD133.1	-/+	+	+	+
CD133.2	-/+	+	+	+
CD166	-	+	+	+
CD227	-/+	+	-	-

3.1.1 Small and large intestinal cells share many cell surface markers, including markers of SCs

Analysis by flow cytometry indicated that intestinal cells co-cultured with the feeder layer expressed several putative SC markers. CD133.1 (CD133 AC133) has long been accepted as a marker of colon CSCs [104]. While primary SI and LI cells contained less than 1% CD133.1^{+} cells, the expanded cells comprised 69.4 and 73.8% CD133.1^{+} cells for the SI and LI, respectively (**Figure 6A**). Other putative SC markers showed similar expression profiles, including CD166 [105], CD24 [106] and CD49f [107] (**Figure 6B**).

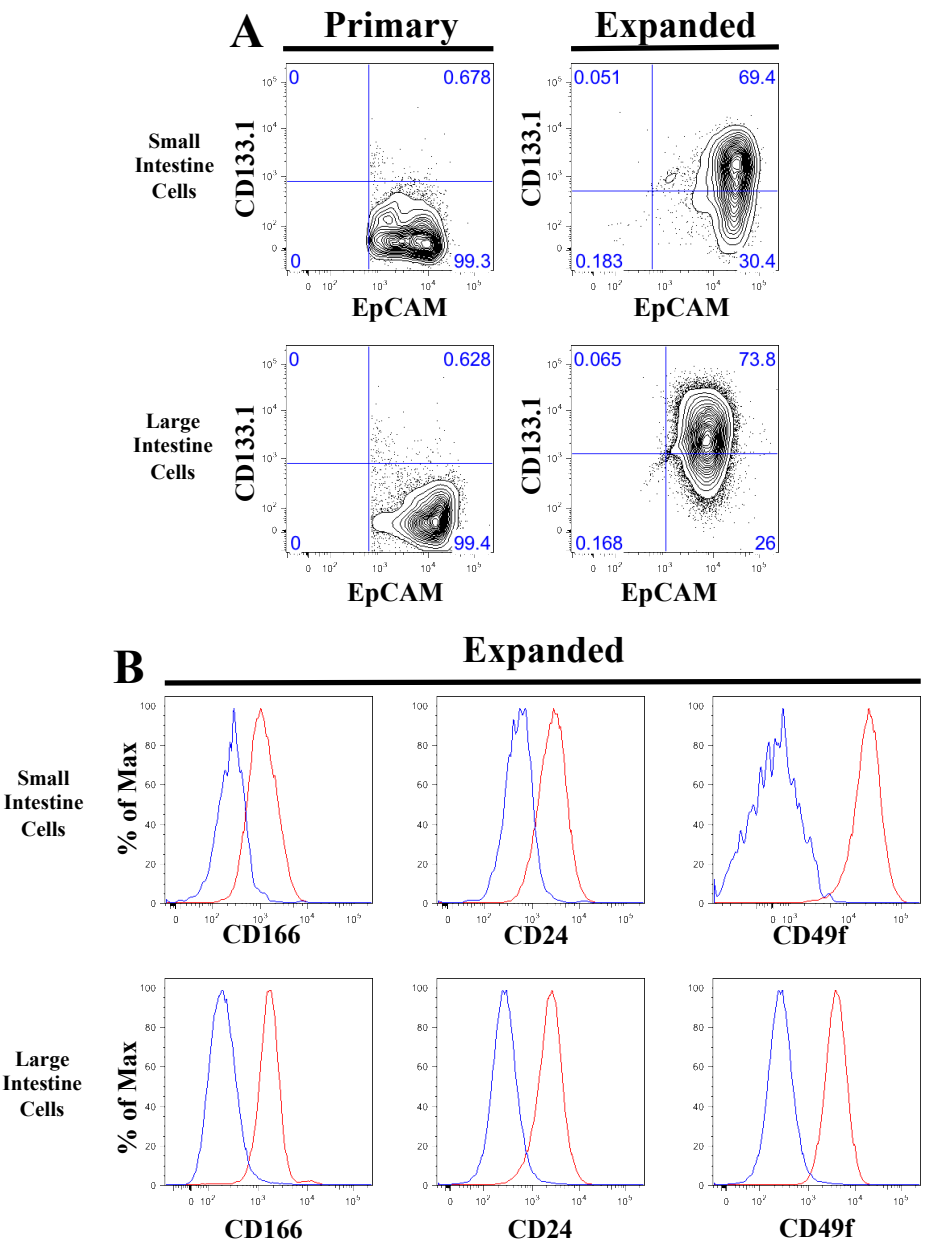

Figure 6: Culture system enriches for intestinal SCs. (A) Flow cytometric analyses of EpCAM$^+$ primary SI and LI cells indicate <1% population of CD133.1$^+$ cells (left), as seen in contour plots. Analysis of EpCAM$^+$ SI and LI cells expanded on the feeder layer indicates an enrichment of CD133.1+ population (right), as seen in contour plots. (B) Expanded SI and LI cells express other putative SC surface markers. Histograms represent unstained control (blue) and stained cells (red).

3.1.2 Normal intestinal SCs versus colon CSCs

The same SC markers that were expressed on both SI and LI SCs (**Figure 6A & B**) were also expressed by CSCs derived from human metastatic colon cancer (**Figure 7A**). Notably, CD44, a cell surface glycoprotein involved in cell-cell interactions and thought to be related to distant metastasis of colorectal cancer (CRC) [108], was consistently negative on both normal SI and LI SCs but positive on colon CSCs grown under the same conditions (**Figure 7B**). This indicates that CD44 may play a key role in cancer as suggested by other groups that targeted CD44 with shRNA, reducing cell growth and invasion and increasing apoptosis [109].

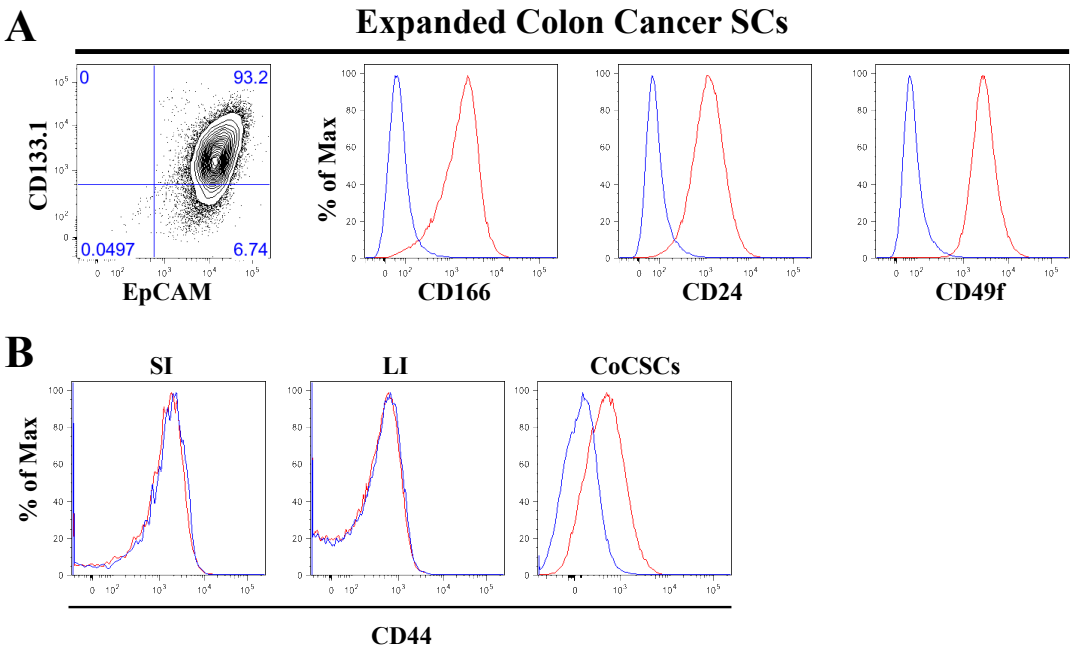

Figure 7: Shared and disparate expression of SC markers between normal intestinal SCs and colon CSCs: (A) Flow cytometric analysis indicating expression of CD133.1 (contour plot), CD166, CD24 and CD49f (histograms) on previously characterized colon CSCs (Tu22) [98]. (B) CD44 is consistently negative on normal intestinal SCs and positive on colon CSCs. Histograms represent unstained control (blue) and stained cells (red).

3.1.3 Differential expression of specific cell surface markers indicates fundamental differences between SI and LI SCs

Flow cytometry analyses of CD133.1, CD13, and CD66c expression revealed reproducible differences between SI and LI SCs expanded *in vitro* (**Figure 8A & B**). CD133.1 expression was higher in LI cells compared to a low, broad expression in SI cells. We found an opposite expression profile using CD13, an aminopeptidase whose expression decreases from ascending to descending colon and possibly plays a role in the different cancer incident rates of these two segments [110]. CD66c, also known as carcinoembryonic antigen cell adhesion molecule 6 (CEACAM6), was notably different between the SI and LI SCs, where 79.8% of the expanded SI cells expressed high levels of CD66c and 89.4% of the expanded LI cells expressed CD66c at a low level (**Figure 8A**). Three paired SI and LI samples showed reproducible expression differences of CD133.1, CD13 and CD66c using flow cytometry staining index as the output (**Figure 8B**).

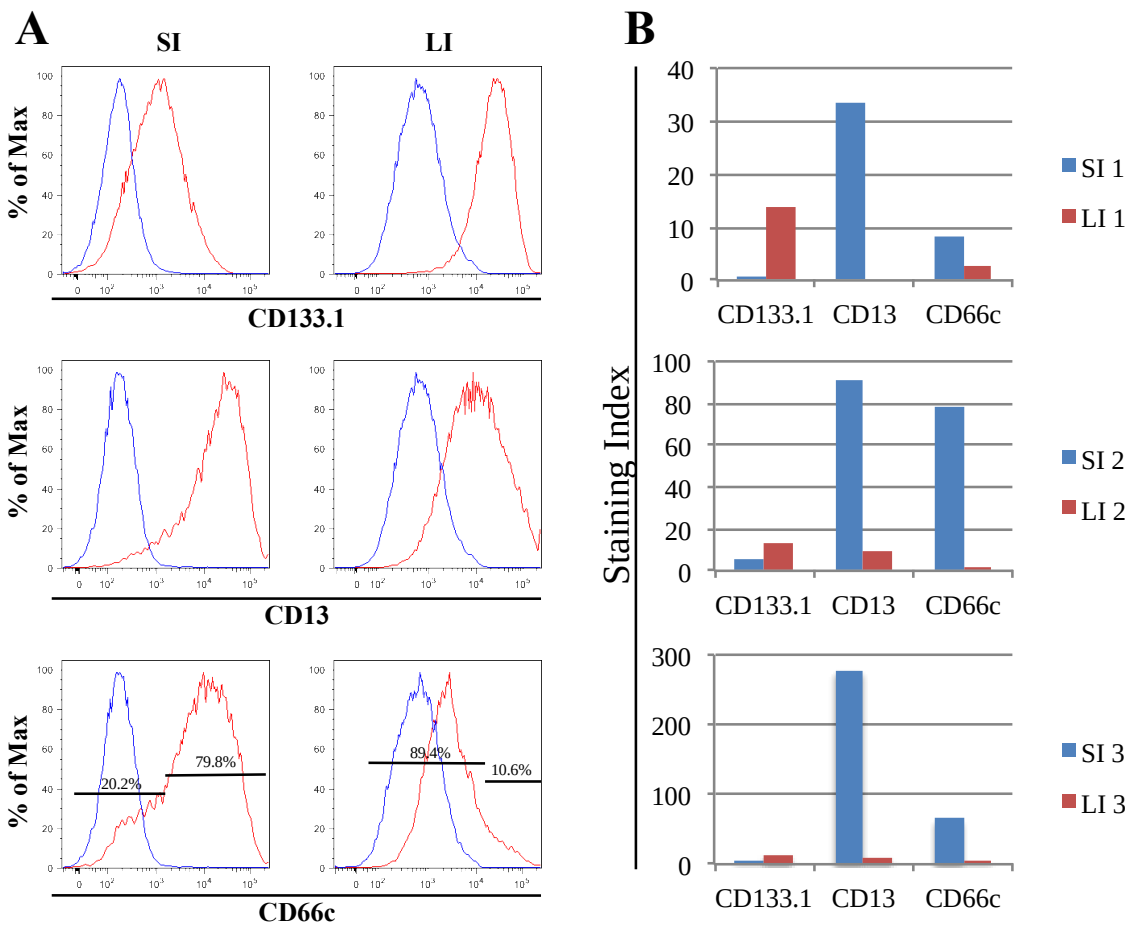

Figure 8: Small and large intestinal SCs differ by cell surface marker expression. (A) Flow cytometry shows differential expression between paired intestinal SCs of CD133.1, CD13 and CD66c as seen in histograms with expression of $CD66c^{lo}$ comprising 20.2% in SI and 89.4% in LI, and $CD66c^{hi}$ comprising 79.8% in SI and 10.6% in LI. Histograms represent unstained control (blue) and stained cells (red). All markers were PE-labeled. The same control was used for SI CD13 and CD66 as well as LI CD133 and CD13 because they were analyzed on the same day. (B) Corresponding staining index of paired samples (staining index = D/W, where D is the distance between the positive and negative populations and W is two standard deviations of the negative population).

3.2 SELF-RENEWAL AND GROWTH RATE

3.2.1 CD66c expression distinguishes SI from LI SCs

LDA was used to assess the clonogenic potential of SI and LI SC populations. LDA is a quantitative measurement that can determine the colony-forming frequency of a specific cell population. Increased colony-forming frequency correlates with stem cell activity [111]. Using Fluorescence Activated Cell Sorting (FACS), we sorted three different tissue-matched cultures of SI and LI SCs in limiting dilution based on $HLA^+/EpCAM^+$ expression. Four weeks after plating, we calculated the colony-forming unit (CFU) frequency of the cells by linear regression [112]. The frequency of the $EpCAM^+$ colony-forming SI and LI SCs was similar, and ranged from 1/10 to 1/106 (**Table 4**).

Table 4: CFU Frequency of $HLA^+/EpCAM^+$ cells. LDA was carried out on expanded $HLA^+/EpCAM^+$ SI and LI SCs. CFU frequency ± SE (L-Calc) for SI and LI SC cultures indicated a high potential for colony formation among this cell population.

LDA	CFU Freq.	SE Range in CFU Frequency
SI 1	1/60	1/15-1/8
SI 2	1/10	1/17-1/9
SI 3	1/25	1/16-1/8
LI 1	1/22	1/32-1/18
LI 2	1/106	1/279-1/160
LI 3	1/38	1/103-1/58

Next, we sorted the same set of cultures in limiting dilution based on differing CD66c expression levels. Interestingly, SI SCs that expressed low levels of CD66c had a higher CFU frequency than $CD66c^{hi}$ cells, while LDA results for LI cells were reversed (**Table 5**). This reveals a fundamental difference between SCs of the SI and LI.

Table 5: CD66c distinguishes SI from LI SCs. LDA was carried out on expanded $HLA^{+}/EpCAM^{+}$ $CD66c^{hi}$ versus $CD66c^{lo}$ SI and LI SCs. CFU frequency ± SE (L-Calc) for SI SC cultures indicated the $CD66^{lo}$ fraction is enriched with colony forming cells while the LI SC cultures show the opposite result with the $CD66^{hi}$ fraction enriched with colony forming cells.

LDA	Population	CFU Freq.	SE Range in CFU Frequency
SI 1	CD66c lo	1/11	1/15-1/8
	CD66c hi	1/78	1/103-1/58
SI 2	CD66c lo	1/12	1/17-1/9
	CD66c hi	1/25	1/30-1/18
SI 3	CD66c lo	1/11	1/16-1/8
	CD66c hi	1/34	1/45-1/25
LI 1	CD66c lo	1/24	1/32-1/18
	CD66c hi	1/9	1/13-1/7
LI 2	CD66c lo	1/211	1/279-1/160
	CD66c hi	1/15	1/20-1/11
LI 3	CD66c lo	1/77	1/103-1/58
	CD66c hi	1/13	1/18-1/10

3.2.2 LI SCs have a higher growth rate than SI SCs

Next, flow cytometry was used to quantitatively measure intestinal SC proliferation *in vitro*. We plated SI and LI SCs from three paired samples in triplicate with a defined number of cells (day 0) and counted the number of $EpCAM^{+}$ cells on days 1, 4, 8 and 11. For all three paired samples, LI SCs showed significantly greater cell numbers than the SI SCs at each time point (**Figure 9**).

This is in contrast to previous *in vivo* results, indicating that the mouse SI turns over at a higher rate than the LI [6]. This result demonstrates one important difference between mouse and human intestinal homeostasis.

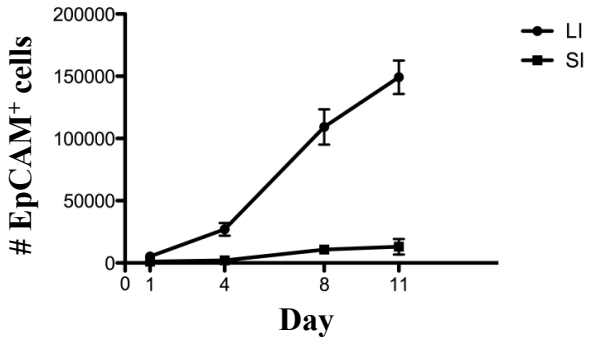

Figure 9: LI SCs have a higher growth rate than SI SCs. Quantitative flow cytometry was used to count the number of EpCAM$^+$ cells at 1,4,8 and 11 days after plating 93,750 cells/well in triplicate on day 0. One representative pair of two examined is shown here.

3.3 DISCUSSION

This set of experiments not only characterized the normal SI and LI epithelial cells as SCs, but also began to decipher key differences between the two cell populations. The broad panel of markers showed that the culture system selected for a defined population of EpCAM$^+$ epithelial cells expanded from primary bulk cells and that the cells were more homogenous than cells from primary tissue. This can be seen in the movement from a +/- or -/+ in **Table 3** to a + or – expression pattern for most markers. This identifies the strength of the culture system, demonstrating that it selects for a homogenous population having the ability to form colonies and

eliminating those that cannot. The expression of CD166, CD24 and CD49f not only further verify their SC identification, but also the similarities of SI and LI SCs to one another.

In contrast, the expression of CD133.1, CD13 and CD66c began to identify differences between SI and LI SCs. The enrichment of CD133.1^{+} populations laid the groundwork for future SC studies and their relation to cancer since this marker has been studied extensively in the CSC field [102, 104, 113]. This is of particular interest since CD133.1 is reproducibly more highly expressed in the LI SCs than the SI SCs (**Figure 8B**). Considering its relation with CSCs, a higher expression of CD133.1 on LI SCs may indicate a predisposition to neoplastic transformation compared to SI SCs.

While the ascending and descending segments of the LI were not separated here, there have been some studies indicating differences in gene expression. CD13 was expressed at a higher degree in the ascending colon versus the descending colon [110]. If this pattern continues proximal, into the SI, this can explain the higher expression found in the SI SCs compared to the LI SCs.

Furthermore, we specifically compared normal intestinal SCs with colon CSCs and found very similar SC marker expression among all three cell types. This indicates that normal intestinal SCs may be the cell of origin for cancer. This was more directly demonstrated in mice where APC was specifically deleted in LGR5+ ISCs, leading to rapidly growing adenomas. This indicated that SC specific loss of APC could be one of the initial hits on the way to cancer formation [4]. Importantly, while both normal SI and LI SCs shared many markers with colon CSCs, they lacked expression of CD44 (**Figure 7**). Due to its role in distant metastasis of colorectal cancer [108], lack of CD44 expression on normal cells provided another indication that these cells were not transformed, in addition to their failure to form tumors *in vivo* (**Table 2**).

An unexpected finding was that the disparity in expression of CD66c identified opposing populations of SI and LI SCs capable of forming colonies (**Table 5**). We used the difference in expression, and sorted the hi- and low-expressing populations, finding that the minority population in each case (10.6% of $CD66c^{hi}$ for LI SCs and 20.2% of $CD66c^{lo}$ for SI SCs) was the population that held the most self-renewal potential. In addition, although most markers are homogenously expressed on the expanded cells, this marker alone identifies a subset that most likely separates the progenitor cells from the true SCs in this system. A recent study showed that high expression of CD66c was associated with colon CSCs and silencing CD66c blocked tumor growth [114]. The LDA result was reproducible for three paired samples and is likely a conserved and important phenomenon. Like CD133.1, high CD66c expression in LI SCs may indicate why these SCs are more susceptible to transformation than their SI counterparts expressing low levels of CD66c.

Even though it seems that $EpCAM^{+}$ SI and LI SCs have nearly equal colony formation ability, the expanded human LI SCs have a significantly higher growth rate when compared to SI SCs (**Figure 9**). This is in contrast to previous *in vivo* results, indicating that the mouse SI turns over at a higher rate than the LI [6]. This result may identify important differences between mouse and human intestinal homeostasis. Lineage tracing in mice indicated that while at 5 days, entire crypts were lineage marked from the $LGR5^{+}$ SCs in the SI, lineage marking was still restricted to the crypt bottom in the LI, indicating more quiescence in the LI compared to the SI [6]. Therefore, in the mouse, SI SCs seem to divide more readily than the LI SCs, an opposing result to our human intestinal SC data. Interestingly, the APC/min mouse, with a heterozygous loss for APC, develops ten times more SI tumors than LI tumors, whereas humans develop twenty times more LI cancer than SI cancer [115, 116] (**Table 1**). The discrepancy in location of tumors between mouse

and human seems to be related to the difference in proliferation rates. A higher proliferation rate in the mouse SI may be related to higher incidence of SI cancer, whereas a higher proliferation rate in the human LI may be related to a higher incidence of LI cancer. Entire studies have been performed using tumors generated in the mouse SI, a fact that is generally only disclosed in the methods section [117]. If the origin of mouse intestinal cancer, the SI SC, is different from the LI SC, their mechanisms of tumorigenicity and responses to therapy may differ. Only recently have mouse models of colon cancer emerged. Even these rely on inflammation induction of colon cancer, which has a very different progression from normal epithelium to cancer [118]. The differences between SI and LI SCs may change the way researchers use mouse models and relate them to human colon cancer.

4.0 MOLECULAR DIFFERENCES BETWEEN SMALL AND LARGE INTESTINAL STEM CELLS

While important for identification and live cell sorting, cell surface marker expression gives a limited view of the inner workings of SCs. Complex intracellular mechanisms give the cells their identity and function. Interestingly, researchers agree that normal SCs and CSCs share many characteristics. They both have the ability to self renew and differentiate into the multiple cell lineages of their parent organ while having a higher clonogenicity than other, more differentiated cells[90].

As discussed above, Wnt signaling is a driving force of crypt formation and maintenance of the intestine [30] via its many targets, including LGR5, but its disruption is also what is responsible for the transformation of human intestinal epithelial cells [119]. Likewise, the Notch pathway is not only involved in the maintenance of progenitor cells of the intestine [48], but also in the cell fate decisions [67]. Changes in these gatekeeper pathways in SI and LI would have a great impact on their regulation and susceptibility to disease.

To better understand the molecular characteristics and functional aspects of SI and LI SCs, they were subjected to gene array analysis. For a robust comparison, the samples consisted of four matched SI and LI SC samples and two sets that were unmatched.

4.1 DIFFERENTIAL GENE EXPRESSION PATTERNS INDICATE SEPARATE MOLECULAR SIGNATURES IN SMALL AND LARGE INTESTINAL SCS

Gene array analysis provided a glimpse into the molecular signature of the SI and LI SCs. Of the thousands of significantly different transcripts, 1118 had a fold change greater than 1.5. The two different cell types clustered separately using unsupervised hierarchical clustering methods where the distances are defined linearly (left axis, **Figure 10**). This reinforces the inherent similarities within each group, while still demonstrating clear differences between SI and LI SCs. It is important to note that feeder cells were also subjected to gene array analysis to ensure they were profoundly different from the SI and LI SCs. Indeed, in both cases, most of the transcripts are expressed at significantly different levels when comparing SI (19,647) and LI (18,873) SCs to feeders. This gives us confidence that the SI and LI SCs are phenotypically very different from the feeders and that the feeders likely represent a constant background of gene expression in both cases.

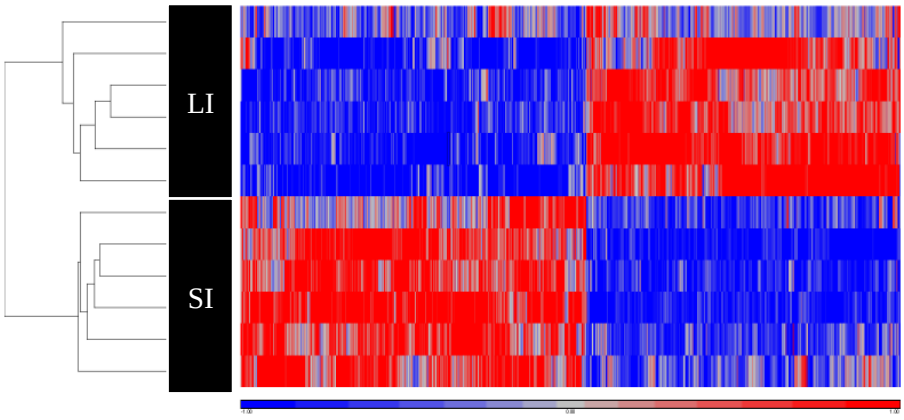

Figure 10: Heat map indicating differences between SI and LI SCs at a molecular level. Heat Map of differentially expressed transcripts in SI versus LI samples. Unsupervised clustering was performed on log2 gene

expression values (K-means algorithm) with q<0.05 (FDR=5%) cutoff. Expression values are scaled for minimum (blue) and maximum (red) intensity values. SI and LI samples formed distinct clusters based on cell origin.

4.2 GENES ASSOCIATED WITH PROLIFERATION AND MIGRATION ARE AMONG THE MOST SIGNIFICANTLY CHANGED TRANSCRIPTS BETWEEN SMALL AND LARGE INTESTINAL SCS AND ARE PREDICTED TO CONTRIBUTE TO FUNCTION

Predictive function analysis predicts the effect that expression changes in the dataset have on biological processes and disease. Ingenuity software indicated functional differences in gene expression between LI and SI SCs that most frequently appeared in cancer and gastrointestinal diseases (**Table 6**). In the category of cancer, significantly changed genes in epithelial neoplasia (301), intestinal cancer (89) and metastasis (55) are predicted to translate to biological function. Likewise, functions in gastrointestinal diseases such as digestive organ tumor (127), colorectal cancer (88) and metastatic colorectal cancer (24) were among the most significant. Cellular development, cellular movement, cellular growth and differentiation and cell-to-cell signaling and interaction finish off this selected list among many others with functions in neoplasia of tumor cell lines (30), cell movement (142), tumorigenesis of tumor cell lines (20) and binding of cells (49). All of these selected functions have a p-value of less than 0.00001.

At first glance, it is concerning that so many of the predicted functions are cancer-related. However, when considering that cancer is initiated from normal tissue, it follows that shared pathways are likely perturbed upon cancer formation.

Table 6: Predictive function analysis of 2-fold differentially expressed genes. Genes with fold changes greater than or equal to 2 were analyzed in Ingenuity Pathway Analysis (Ingenuity Systems, www.ingenuity.com). The functional analysis identified the biological functions and/or diseases that were most significant to the dataset. Right-tailed Fisher's exact test was used to calculate a p-value determining the probability that each biological function and/or disease assigned to that dataset is due to chance alone.

Category	Functions Annotation	p-Value	Molecules	# Molecules
Cancer	epithelial neoplasia	1.39E-07	ABCA5,ABCC1,ABCC2,ABP1,ACE2,ACP5,ADCY9,AFP,AGR2,AHSG,AKAP13,ALCAM,ALDH8A1,AMACR,ANPEP,APOBEC1,AREG/AREGB,ARL4C,ATP1B3,BANK1,BBS10,BCHE,BCL11A,BICC1,BMP2K,BPGM,C3,C6,CADM1,CAPN3,CCND1,CCND2,CCNG2,CD24,CD44,CDH12,CDH2,CDH6,CDK14,CDX2,CEP170,CFB,CHGA,CHKA,CHST4,CKAP4,CKB,CNTNAP2,COBLL1,COL18A1,COL5A2,CPE,CPS1,CRYL1,CSE1L,CSGALNACT2,CTGF,CTSC,CTSL2,CX3CL1,CXCL1,CXCL6,CXCR4,CYP2B6,CYP4F11,CYP51A1,CYR61,DAB2,DAPK1,DDC,DEFB1,DENND1A,DFNA5,DHRS11,DHRS7,DKK1,DMBT1,DPP4,DPY19L1,DST,DUSP4,DUT,E2F8,EGF,EHF,ENAH,EPB41L3,ETNK1,ETV5,EXPH5,F2R,FAIM,FAM13A,FAM149A,FAM184A,FAM198B,FAM5C,FAR2,FARP1,FAS,FCGBP,FGFR2,FOLH1,FOLH1B,FOLR1,FRZB,FXYD3,GALC,GATA4,GCNT1,GDF15,GEM,GLDC,GLRB,GNAS,GPSM2,GREB1,GSTM1,GUCY2C,HEPH,HES1,HHEX,HIF1A,HK2,HMOX1,HOXC6,HPN,HRG,HSPA13,HSPB8,HTRA1,ICK,ID4,IFI30,IFI44,IFITM2,IFITM3,IFT81,IGFBP1,IGFBP3,IL6ST,IL8,INSIG1,ISG20,ITIH2,KCTD14,KIAA1199,KLK10,KRT19,KRT23,KRT7,LAMA4,LAMP3,LCN2,LCT,LEPR,LGALS2,LIMCH1,LPCAT1,LRP12,LXN,MACF1,MAF,MAOA,MAP4K4,MAX,MCAM,ME1,MEP1A,MGAT4A,MITF,MMP7,MREG,MSMO1,MSN,MTUS1,MUC13,MUC5B,MYL9,MYO1A,MYRF,NAAA,NAP1L1,NBN,NCOA1,NDRG2,NEDD9,NELL2,NME1,NOTCH2,NR2F2,NR5A2,NRP1,NRXN3,NT5E,NTS,OGG1,OSR2,PADI2,PCSK1,PDGFC,PDZK1IP1,PGAP1,PHLDA1,PID1,PITX2,PLAGL2,PLCE1,PLOD2,PLXNC1,POF1B,PRKAR1A,PRKCH,PRKG2,PRLR,PRNP,PRODH,PROM1,QPCT,RAB11FIP2,RAMP1,RANBP6,RARRES2,RELN,RPGRIP1L,S100A10,SAA4,SALL1,SCNN1A,SCRN1,SCUBE2,SEMA5A,SEMA6A,SEPP1,SERPINA3,SERPINA5,SERPINE2,SERPINF1,SERPING1,SKAP2,SKP2,SLC16A1,SLC16A4,SLC19A2,SLC26A2,SLC26A3,SLC36A1,SLC38A6,SLC39A6,SLC3A1,SLC44A4,SLC46A3,SLC4A7,SLC5A12,SLC6A8,SLC7A7,SLC7A8,SLC7A9,SLCO1B3,SMARCA2,SNRPN,SOAT2,SOX4,SPP1,SRPX,STAT1,STC1,SULT1B1,SULT2A1,SYNE2,TACSTD2,TBC1D8,TBL1X,TDP2,TGFA,TGFB2,TGFBR3,THSD7A,TMEM106C,TMPRSS3,TMX4,TNFAIP2,TNS1,TPM1,TRAM1,TRHDE,TRIM22,TSPYL5,TTR,TUBA1A,TUBB6,TUSC3,UGT8,UHRF1BP1L,UNC93A,VAV3,VGLL1,VIPR1,VTCN1,WWTR1,XK	301
	intestinal cancer	7.68E-07	ABCA5,ABP1,AKAP13,ALCAM,AMACR,ANPEP,AREG/AREGB,BANK1,CAPN3,CCND1,CCND2,CD24,CD44,CDH12,CDH2,CDH6,CDX2,CNTNAP2,COBLL1,CRYL1,CSE1L,CTGF,CXCL1,CXCR4,CYR61,DKK1,DPP4,EGF,ENAH,EPB41L3,F2R,FAS,FCGBP,FGFR2,FOLH1,GATA4,GDF15,GNAS,GPSM2,GREB1,GSTM1,GUCY2C,HIF1A,HMOX1,HOXC6,HTRA1,IGFBP3,IL8,INSIG1,ISG20,KIAA1199,KLK10,LCN2,LEPR,LGALS2,MAP4K4,MCAM,MEP1A,MMP7,MUC13,MYO1A,NAAA,NEDD9,NRP1,NTS,PITX2,PLOD2,PRKCH,PRNP,PROM1,QPCT,SERPINA3,SERPINE2,SLC16A1,SLC26A2,SLC26A3,SLC38A6,SLCO1B3,SPP1,SRPX,STAT1,TACSTD2,TDP2,TGFB2,TGFBR3,TNS1,TTR,UGT8,VIPR1	89
	metastasis	4.36E-06	AGR2,AHSG,ANPEP,CCND2,CD24,CD44,CD47,CDH2,CDH6,COL18A1,CSE1L,CTGF,CXCL1,CXCL6,CXCR4,CYR61,DAPK1,DKK1,EGF,ENAH,EPB41L3,F2R,FGFR2,GDF15,GREB1,HIF1A,HMOX1,HOXC6,HRG,HTRA1,KIAA1199,LCN2,LGALS2,MCAM,MITF,MMP7,NDRG2,NEDD9,NME1,NT5E,PITX2,PLOD2,PRNP,PROM1,QPCT,RDX,RELN,SLC38A6,SPP1,SRPX,SSX2IP,TGFA,TGFB2,TGFBR3,TUBA1A	55
Gastrointestinal Disease	digestive organ tumor	1.87E-07	ABCA5,ABCC1,ABCC2,ABP1,AFP,AKAP13,ALCAM,AMACR,ANPEP,AREG/AREGB,ATP1B3,BANK1,BICC1,CAP2,CAPN3,CCND1,CCND2,CD24,CD44,CDH12,CDH2,CDH6,CDK14,CDX1,CDX2,CNTNAP2,COBLL1,COL18A1,CRYL1,CSE1L,CTGF,CTSC,CTSL2,CXCL1,CXCR4,CYR61,DAPK1,DDC,DKK1,DPP4,E2F8,EGF,ENAH,EPB41L3,F2R,FAIM,FAS,FCGBP,FGFR2,FOLH1,FXYD3,GATA4,GDF15,GNAS,GPSM2,GREB1,GSTM1,GUCY2C,HIF1A,HMOX1,HOXC6,HRG,HTRA1,IFT81,IGFBP3,IL8,INSIG1,ISG20,KIAA1199,KLK10,KRT19,KRT7,LAMA4,LCN2,LEPR,LGALS2,MAOA,MAP4K4,MCAM,MEP1A,MMP7,MTUS1,MUC13,MYO1A,NAAA,NAMPT,NBN,NEDD9,NME1,NOTCH2,NR5A2,NRP1,NTS,OGG1,PDGFC,PITX2,PLOD2,PRKAR1A,PRKCH,PRNP,PROM1,QPCT,SAA4,SERPINA3,SERPINE2,SLC16A1,SLC16A4,SLC26A2,SLC26A3,SLC38A6,SLCO1B3,SOAT2,SOX4,SPP1,SRPX,STAT1,TACSTD2,TDP2,TGFA,TGFB2,TGFBR3,TNS1,TRAM1,TTR,TUBA1A,UGT8,VIPR1	127
	colorectal cancer	1.21E-06	ABCA5,ABP1,AKAP13,ALCAM,AMACR,ANPEP,AREG/AREGB,BANK1,CAPN3,CCND1,CCND2,CD24,CD44,CDH12,CDH2,CDH6,CDX2,CNTNAP2,COBLL1,CRYL1,CSE1L,CTGF,CXCL1,CXCR4,CYR61,DKK1,DPP4,EGF,ENAH,EPB41L3,F2R,FAS,FCGBP,FGFR2,FOLH1,GATA4,GDF15,GNAS,GPSM2,GREB1,GSTM1,GUCY2C,HIF1A,HMOX1,HOXC6,HTRA1,IGFBP3,IL8,INSIG1,ISG20,KIAA1199,KLK10,LCN2,LEPR,LGALS2,MAP4K4,MCAM,MEP1A,MMP7,MUC13,MYO1A,NAAA,NEDD9,NRP1,NTS,PITX2,PLOD2,PRKCH,PRNP,PROM1,QPCT,SERPINA3,SERPINE2,SLC16A1,SLC26A2,SLC38A6,SLCO1B3,SPP1,SRPX,STAT1,TACSTD2,TDP2,TGFB2,TGFBR3,TNS1,TTR,UGT8,VIPR1	88
	metastatic colorectal cancer	9.24E-06	ANPEP,CCND2,CDH2,CDH6,CTGF,DKK1,EPB41L3,F2R,FGFR2,GDF15,GREB1,HMOX1,HOXC6,HTRA1,KIAA1199,LGALS2,PITX2,PLOD2,PRNP,QPCT,SLC38A6,SRPX,TGFB2,TGFBR3	24
Cellular Development	neoplasia of tumor cell lines	2.30E-08	AREG/AREGB,CCND1,CD24,CDH2,CDX1,CDX2,COL18A1,CSE1L,CXCL1,CXCR4,CYR61,DAPK1,DKK1,DPP4,E2F8,EGF,F2R,GNAS,HMOX1,IL8,MCAM,NEDD9,NME1,PDZK1IP1,PRKAR1A,PRLR,PRNP,PROM1,SKP2,STAT1	30
Cellular Movement	cell movement	1.57E-06	ABCA1,ABCC1,AGR2,AHSG,ALCAM,ANPEP,AREG/AREGB,BID,C3,C6,CADM1,CCL25,CCND1,CCRL2,CD24,CD44,CD47,CDH2,CDK14,CDX1,CDX2,CFB,CHGA,CHST4,CKLF,CNTNAP2,COL18A1,CPB2,CSE1L,CTGF,CTSC,CTSL2,CX3CL1,CXCL1,CXCL5,CXCL6,CXCR4,CYR61,DAB2,DEFB1,DKK1,DMBT1,DPP4,DPYSL3,DST,EGF,ENAH,ETV5,F2R,FAM5C,FAS,FERMT2,FGFR2,FNDC3B,FOLR1,GALNT1,GCNT1,GDF15,GIP,GLRB,GNAS,GUCY1B3,HEBP1,HHEX,HIF1A,HMOX1,HRG,HSPB1,HTRA1,IGFBP1,IGFBP3,IL6ST,IL8,KRT19,LCN2,LGMN,LITAF,MAP4K4,MAX,MCAM,MITF,MMP7,MSN,MYRF,NAMPT,NDP,NDRG2,NEDD9,NEU1,NEUROD1,NME1,NOTCH2,NR2F2,NRP1,NT5E,NTS,PITX2,PLXNC1,PRKAR1A,PRLR,PRNP,QPCT,RARRES1,RARRES2,RELN,S100A10,SCNN1A,SCPEP1,SDC2,SEMA3E,SEMA5A,SEMA6A,SERPINA3,SERPINA5,SERPINE2,SERPINF1,SERPING1,SGPP1,SKAP2,SKP2,SLC16A4,SPA17,SPP1,STAT1,STC1,SYNE2,TACSTD2,TDP2,TGFA,TGFB2,TGFBR3,TNS1,TPBG,TPM1,TSPO,TUBA1A,TUSC3,VAV3,VIPR1,VTCN1,WASF1,WWTR1	142
Cellular Growth and Proliferation	tumorigenesis of tumor cell lines	1.69E-06	AREG/AREGB,CCND1,CD24,CDX1,CDX2,CXCR4,CYR61,DKK1,DPP4,E2F8,EGF,GNAS,IL8,PDZK1IP1,PRKAR1A,PRLR,PRNP,PROM1,SKP2,STAT1	20
Cell-To-Cell Signaling and Interaction	binding of cells	2.17E-06	ABCA1,ALCAM,AREG/AREGB,C3,CCL25,CD24,CD44,CD47,CDH2,CHST4,CKAP4,COL18A1,CX3CL1,CXCL1,CXCR4,CYR61,DAPK1,DKK1,DPP4,EGF,F2R,FAS,FERMT2,FOLH1,GCNT1,GNAS,HLA-DMA,IGFBP3,IL8,LAMA4,LEPR,MSN,NOTCH2,NRP1,NT5E,OXTR,PRNP,RAMP1,RELN,S100A10,SDC2,SERPINA5,SERPINF1,SERPING1,SPA17,SPP1,TGFA,TGFB2,VIPR1	49

The transcripts with the highest positive fold changes in LI SCs compared to SI SCs were related to proliferation, adhesion and migration with known function in cancer and metastasis. A few selected molecules were of particular interest. Secreted phosphoprotein 1 (SPP1; better known as osteopontin (OPN)) (142-fold increase), CD44 (7-fold increase) and matrix metalloproteinase-7 (MMP-7) (37-fold increase) made several appearances in **Table 6** with functions in epithelial neoplasia, intestinal cancer, metastasis, digestive organ tumor, colorectal cancer and cell movement. In our analysis, these three molecules are among those with the highest fold changes when comparing LI SCs to SI SCs, indicating a higher likelihood of LI SCs to transform over their SI SC counterparts.

Interestingly, when investigating those transcripts with the highest expression in SI SCs compared to LI SCs, the disease-related functions were more limited. Carbamoyl phosphate 1 (CPS1) showed one of the most dramatically down-regulated expressions (25-fold decrease) in LI SCs compared to SI SCs. While it does appear in **Table 6** under epithelial neoplasia, it is more widely known to be specific for the SI and for its tumor suppressive effects [120]. Retinoic acid receptor responder 1 (RARRES1) (10-fold decrease), as its name suggests, is a retinoid regulated gene. Vitamin D, a pro-differentiation agent, induces the expression of RARRES1 and a differentiation phenotype in colon cancer cell lines [121]. Both down- and up-regulated genes presented here indicate very different responses and functions of those molecular pathways found in LI versus SI SCs.

4.3 DIFFERENCES IN THE WNT AND NOTCH PATHWAYS AND SELECTED DISEASE RELATION

Since the Wnt and Notch pathways play such pivotal roles in intestinal homeostasis, we sifted through the significantly changed pathway associated transcripts and found an interesting pattern. Of the many receptors, intermediaries and targets, we chose twelve Wnt-related transcripts that were significantly different between SI and LI SCs (**Figure 11**). Of those twelve, nine of them were upregulated in the LI, indicating Wnt hyperactivity. Other less direct regulatory mechanisms may explain the lower expression of some Wnt factors in the LI.

Interestingly, four Notch factors were also found to be significantly different between SI and LI SCs. Differentiation factors ChrA, ATOH1 and Muc2 indicate a higher degree of differentiation in SI SCs while increased Notch2, a receptor for the Notch pathway known to play a role in intestinal crypt progenitor cells indicates higher SC activity in LI SCs (**Figure 11B**) [63]. Differential responses to the same environment indicate that these are inherited characteristics of the different SCs.

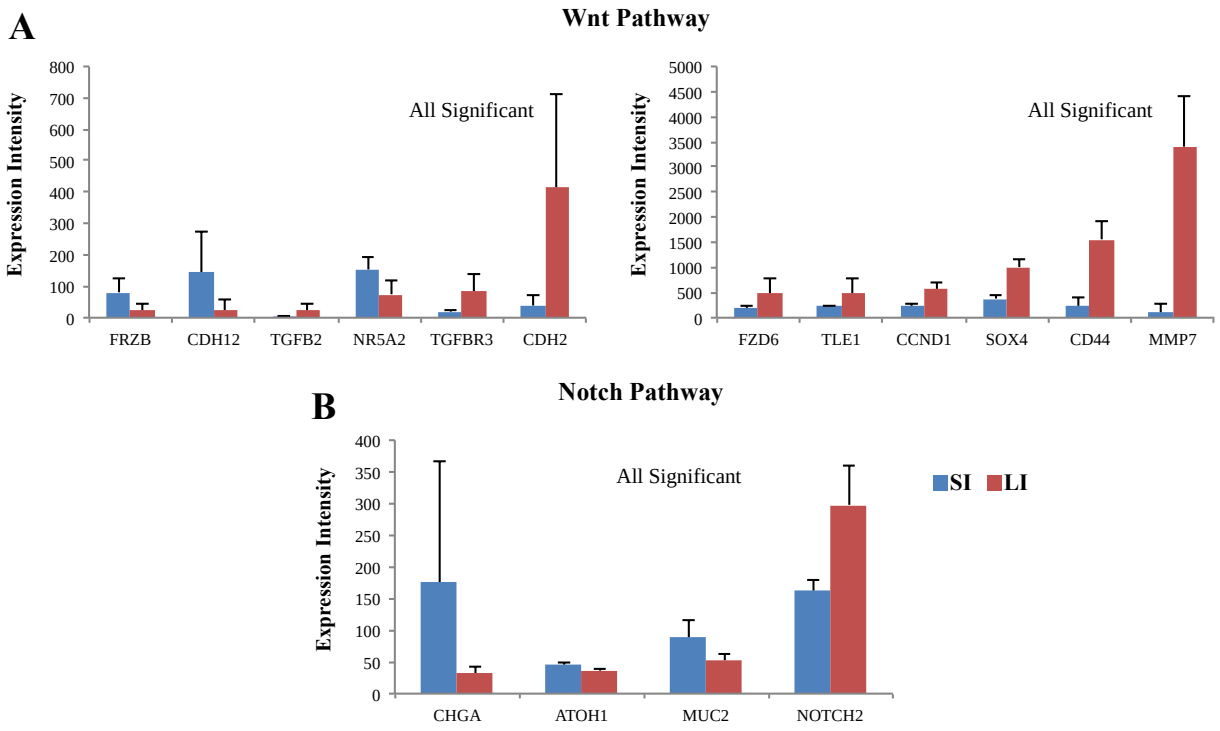

Figure 11: Wnt and Notch pathway gene expression differences between SI and LI SCs. Histograms depict significant ($q<0.05$) differential expression of individual genes between SI and LI samples classified into canonical pathways using Ingenuity Pathways Analysis (see Methods). All values are reported as mean (box) plus standard deviation (error bar) of raw intensity for each transcript. The ordinate depicts expression intensity values with (A) Wnt Pathway transcripts displayed on 2 graphs with different scale maximum to accurately reflect the intrinsic biological range among these samples and (B) Notch pathway participants. FRZB: frizzled-related protein, CDH12: cadherin 12, TGFB2: transforming growth factor, beta 2 NR5A2: nuclear receptor subfamily 5, group A, member 2, TGFBR3: transforming growth factor, beta receptor III, CDH2: cadherin 2, FZD6: frizzled homolog 6, TLE1: transducin-like enhancer of split 1 (E(sp1) homolog, CCND1: cyclin D1, SOX4: SRY (sex determining region Y)-box 4, CD44: CD44 molecule (Indian blood group), MMP7: matrix metallopeptidase 7, CHGA: chromogranin A, ATOH1: atonal homolog 1, MUC2: Mucin2, NOTCH2: notch 2.

Tumor related transcripts indicate that LI SCs may have an inherently greater predisposition to form tumors in general and colon tumors in particular compared to SI SCs

(**Figure 12A**). The differential regulation of these molecular pathways may contribute to the difference in cancer incidence between SI and LI as well as other intestinal diseases such as Crohn's disease, ulcerative colitis and celiac disease (**Figure 12B**).

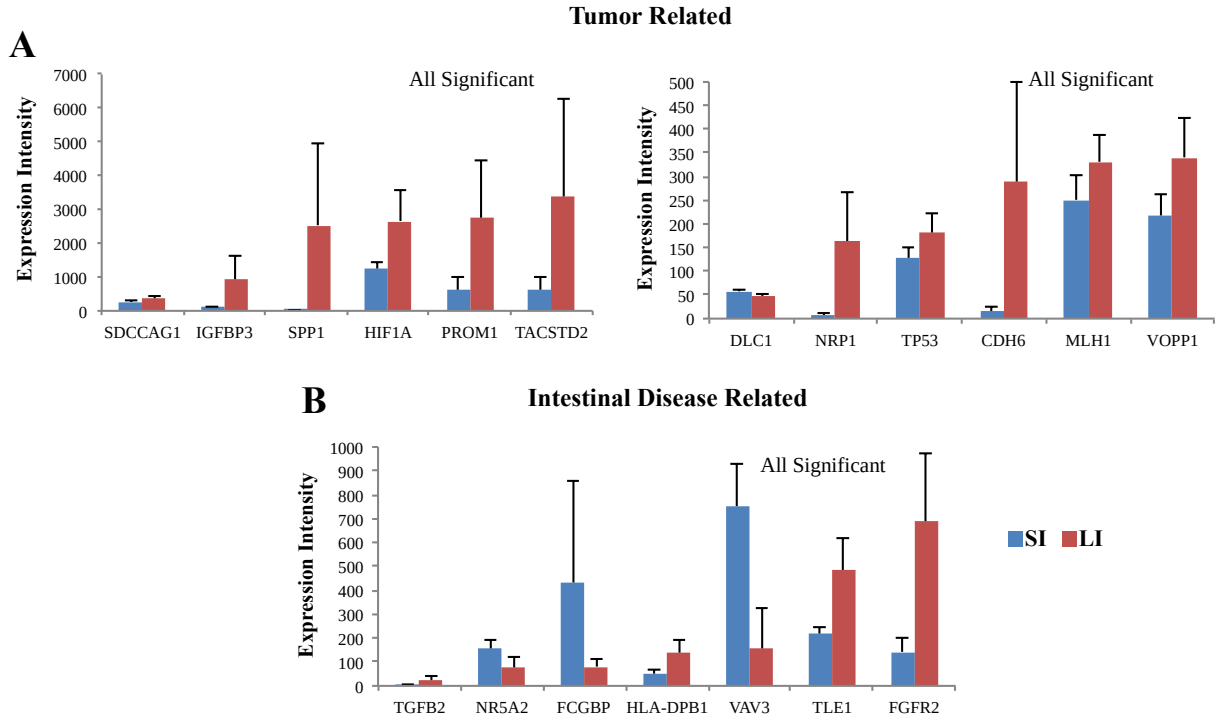

Figure 12: Tumor and disease related gene expression differences between SI and LI SCs. Histograms depict significant ($q<0.05$) differential expression of individual genes between SI and LI samples classified into canonical pathways using Ingenuity Pathways Analysis (see Methods). All values are reported as mean (box) plus standard deviation (error bar) of raw intensity for each transcript. The ordinate depicts expression intensity values with (A) Tumor Related transcripts displayed on 2 graphs with different scale maximum to accurately reflect the intrinsic biological range among these samples. (B) Intestinal Disease Related genes are those previously thought to be involved in either Crohn's disease, ulcerative colitis or celiac disease. SDCCAG1: serologically defined colon cancer antigen 1, IGFBP3: insulin-like growth factor binding protein 3, SPP1: secreted phosphoprotein 1, HIF1A: hypoxia inducible factor 1, alpha subunit, PROM1: prominin 1, TACSTD2: tumor-associated calcium signal

transducer 2, DLC1: deleted in liver cancer 1, NRP1: neuropilin 1, TP53: tumor protein p53, CDH6: cadherin 6, MLH1: mutL homolog 1, VOPP1: vesicular, overexpressed in cancer, prosurvival protein 1, TGFB2: transforming growth factor, beta 2, NR5A2: nuclear receptor subfamily 5, group A, member 2, FCGBP: Fc fragment of IgG binding protein, HLA-DPB1: major histocompatibility complex, class II, DP beta 1, VAV3: vav 3 guanine nucleotide exchange factor, TLE1: transducin-like enhancer of split 1 (E(sp1) homolog, FGFR2: fibroblast growth factor receptor 2.

4.4 DISCUSSION

Overall, the gene array analysis confirmed that SI and LI SCs have different molecular signatures and that they cluster well, but separately from each other (**Figure 10**). This would be expected of total tissue when considering the different structure and function of these two segments of the intestine. However, we detected differences in the SCs expanded from the two segments, indicating that the information is provided within the different SC populations and determines structure and function.

The predictive function analysis performed in Ingenuity software agreed with past studies that normal intestinal SCs share many characteristics with cancer, among them, functions in metastasis and cell growth and differentiation [79, 81]. It is plausible from this and previous data that normal SCs may be the origin of LI cancer [4].

The differential expression of the molecules with the highest fold change shows a tendency for LI SCs to be more closely related to cancer and possibly more susceptible to cancer than their SI SC counterparts. This is particularly evident when considering Wnt and Notch pathway participants as well as well-known tumor-related molecules (**Figure 11 & Figure 12**). The Wnt pathway is a diverse and multifactorial pathway that includes cadherins (important for

cell-cell interactions), the transforming growth factor beta (TGFβ) family (contributes to proliferation and differentiation), cyclin D (CCND1) (drives the G1/S phase of the cell cycle), as well as Wnt targets such as CD44 and MMP7, and a Wnt receptor (FZD6). In addition, Sox 4, increased here in LI SCs, was found to enhance B-catenin/TCF-LEF activity and proliferation of colon cancer cells [122]. Finally, FRZB (aka SFRP-3), decreased in LI SCs, inhibits Wnt activation and acts as a tumor suppressor [123]. Having a lower expression of a tumor suppressor may increase the susceptibility of LI SCs to transformation.

Many of the tumor-related transcripts in **Figure 12** have functions in tumorigenesis and cancer cell growth and survival. MutL homolog 1 (MLH1) and p53 are involved in genomic stability [124, 125] while hypoxia inducible factor 1 (HIF1A) [126], vesicular, overexpressed in cancer, prosurvival protein 1 (VOPP1) and neuropilin 1 (NRP1) have functions in angiogenesis, cell survival and growth. Interestingly, deleted in liver cancer 1 (DLC1) is a tumor suppressor [127] that is down-regulated in LI SCs, suggesting a higher susceptibility for transformation. Insulin-like growth factor binding protein 3 (IGFBP3) is involved in intestinal epithelium homeostasis [128]. An increase of expression in LI SCs indicates differential regulation of homeostatic processes between SI and LI SCs. Furthermore, Prom1, also known as CD133, is a well-known CSC marker discussed above [104]. OPN/SPP1 is the transcript with the highest fold change between the LI and SI SCs and will be discussed at length below. Two transcripts, serologically defined colon cancer antigen 1 (SDCCAG1) and tumor-associated calcium signal transducer 2 (TACSTD2) are defined by their presence and association with cancer. From this limited list of the significantly different tumor-related transcripts, it is obvious that the SI and LI SCs have intrinsic differences regulating these important pathways.

Aside from cancer, many of the differentially regulated genes are involved in other intestinal-related diseases. Celiac disease, Crohn's disease and ulcerative colitis plague the intestines with uncontrolled inflammation. While these diseases span both the SI and LI we found significant differences in several molecules when comparing SI to LI SCs. Transforming growth factor-β (TGF-β) increases in the active phase of ulcerative colitis and Crohn's disease [129]. Nuclear receptor 5A2 (NR5A2), Fc-γ binding protein (FCGBP) and fibroblast growth factor receptor (FGF) are protective against the development of inflammatory bowel disorders [40, 130, 131]. It is thought that certain HLA-D molecules can even serve as predictors of susceptibility of Celiac disease [132]. Finally transducin-like enhancer of split 1 (TLE1) and vav 3 guanine nucleotide exchange factor (Vav3) both play a role in Crohn's and colitis respectively [133, 134]. Collectively, the differential expression in SI versus LI SCs may play a role in the susceptibility of these two intestinal segments to diseases other than cancer.

Above, we identified significant differences based on known pathways and diseases of the intestine. However, the molecules with the highest fold change between SI and LI SCs define functional and relational differences as well as confirm their tissue origin. OPN, with 142-fold increase in LI SCs, is thought to have clinical significance in CRC patients. Not only is OPN expression higher in CRC cell lines than normal intestinal cell lines, but it is higher in tumor tissue in comparison to normal tissue [135, 136]. It also correlates with lymph node metastasis, lymphatic or venous invasion and TNM stage (classification of malignant tumors). Patients with a higher expression of OPN had lower 5-year survival rates and it is thought to be an independent prognostic factor. Therefore, it may play a role in CRC progression and could be a prognostic marker for patients [136]. In 2003, OPN was identified as the leading candidate clinical marker from a screen of approximately 12,000 named genes and later as a marker of tumor

progression in CRC [137, 138]. The protein-protein interaction of OPN and CD44, another transcript in the list of highest fold changes, has long been thought to promote metastatic spread [139]. Some have found that CD44 is expressed on hepatocytes and it is through its binding to OPN on CRC cells that liver metastasis occurs [135]. Others have found that CD44 expressing CRC cells, or the CSCs of a tumor, enhance the expression and secretion of OPN by tumor-associated macrophages (TAM). This expression then promotes CRC cell clonogenicity [140]. Therefore, OPN and CD44 expression are not only associated with metastasis, but also the CSC phenotype and poor patient outcomes due to a vicious cycle. CD44 signaling can activate the JNK pathway, known for its involvement in not only oncogenic transformation and tumor development, but also in its cross-talk with the Wnt pathway and homeostatic control [141]. Normal control of CD44, OPN and the Wnt pathway may be very important in the maintenance of crypt homeostasis in the LI as its perturbation has detrimental effects [139]. Since SI SCs have much less expression of OPN and CD44, this balance may be an important homeostatic and protective factor.

As mentioned earlier, CD44 itself has been implicated in adhesion, migration and CRC metastasis [108, 109]. Our flow panel analysis indicated that normal intestinal SCs in our culture system do not express CD44 on their surface. While CD44 has many isoforms, the antibody used in this study recognizes all isoforms. However, the gene expression seen in the microarray analysis may not be translated into proteins at this stage. While both LI and SI SCs are negative for cell surface protein CD44, LI SCs may have a greater propensity to express CD44 at the cell surface compared to SI SCs. This poses a dangerous scenario if transformation does occur, allowing CD44 transcript translation.

The last in this group of highly up regulated genes is MMP7. Matrix metalloproteinases (MMP) are zinc- or calcium-dependent endopeptidases that degrade matrix glycoproteins.

However, it is becoming increasingly known that several members, including MMP-7, are also involved in normal cell growth, differentiation and cell regulation. MMP-7 is upregulated in 85% of colorectal adenomas and are associated with poor prognosis [142]. The down regulation of MMP-7 caused a subsequent decrease in proliferation and colony formation of colon cancer cells as well as an enhanced susceptibility to 5-fluorouracil and X-ray irradiation, indicating the promotion of carcinogenesis of colon cancer [143]. It is thought that MMP-7 may play a role in the early stages of CRC because it is a target of beta-catenin/TCF-LEF, downstream of the often-mutated Wnt pathway member APC [144, 145]. Interactions have been seen between MMP-7 and the genes involved in the pathways of CRC development [146]. The LI SCs from our culture system showed 37-fold higher expression of MMP-7 compared to SI SCs. This higher expression in normal cells may make the LI SCs more susceptible to increased proliferation and metastatic spread once the initial APC mutation occurs. In addition, if this mutation occurs in normal SCs, CSCs will inherit the enhanced drug resistance, a dangerous scenario for patients [143].

On the other hand, the transcripts with the highest negative fold changes when comparing LI to SI SCs had much less interesting or well-known functions. CPS1 is a molecule localized to the mitochondria that is responsible for the conversion of ammonia to carbamoyl phosphate in the urea cycle. This process is limited to hepatocytes and SI enterocytes [147]. A less well-understood function is the conversion of arginine into citrulline and nitric oxide (NO), whose absence was implicated in the pathophysiology of necrotizing enterocolitis [148, 149]. Not only can CPS1 be a specific marker for SI mucosa, but it is seen to diminish on the pathway from adenoma to adenocarcinoma in the SI. 70% of all adenocarcinomas examined had lost CPS1 expression [120]. These studies confirm that the intestinal SCs propagated in our culture system are

indeed two different SCs, one from the SI, expressing higher amounts of CPS1 and one from the LI, expressing lower amounts.

RARRES1, found here to have low expression in LI SCs, is expressed at high levels in the differentiated cells of the normal SI and LI as well as adenomas and well-differentiated adenocarcinomas [150]. Its expression progressively decreases in poorly-differentiated tumors and with disease progression. RARRES1 has also been found to reduce invasion and tumorigenicity [151]. This tumor suppressive role may, in part, explain the 10-fold down-regulation in LI SCs compared to SI SCs. Since SI SCs have a higher expression of RARRES1 than LI SCs, they may be more protected from transformation and contribute to a lower incidence of SI cancer over LI cancer. In addition, a more recent study indicated that RARRES1 might be a controller of SC differentiation [152]. Its higher expression in SI SCs may make them easier to differentiate if a transformative event does occur, deeming them less likely to perpetuate a CSC phenotype.

These expression studies demonstrate a robust examination of the molecular signatures of SI and LI SCs. Not only do intrinsic differences between SCs determine structure and function, but they also may determine both cancer and other disease susceptibility.

5.0 MULTIPOTENTIALITY OF SMALL AND LARGE INTESTINAL STEM CELLS

Next, because intestinal SCs are defined by their multipotentiality, we investigated the ability of intestinal SCs to differentiate into various cell lineages. We adapted a previously defined three-dimensional culture system to promote SC differentiation *in vitro* [5]. This system provides an environment that simulates the SC niche and by changing exogenous cues, they respond in varying ways. The Matrigel™ matrix provides extracellular matrix proteins such as laminin and collagen. Many exogenous factors were added in order to recreate factors normally seen in the intestinal crypt (See Methods, Chapter 6.6). R-spondins are known for their enhancement of epithelial proliferation as well as their activation of the Wnt pathway as ligands for the LGR family of receptors [153, 154]. Epidermal growth factor (EGF) is involved in intestinal proliferation and Noggin in the expansion of crypt numbers [155, 156]. Nicotinamide, a precursor of oxidized nicotinamide adenine dinucleotide that inhibits sirtuin, blocks differentiation [157]. A83-01, an Alk4/5/7 inhibitor and SB202190, a p38 inhibitor, were included to improve plating efficiency [12]. Wnt3A was previously found to cause ISCs to adopt a proliferative progenitor phenotype, signifying its importance in the SC media [158]. By removing Nicotinamide, Wnt3A and SB202190, differentiation ensues, thus providing evidence that the cells retain their multipotentiality as well as highlight any regulatory differences between SI and LI SC responses.

5.1 SMALL AND LARGE INTESTINAL STEM CELLS FORM ORGANOIDS IN VITRO

5.1.1 Small and large intestinal SC organoids differ in morphology

After expansion on the feeder layer, cells were embedded in Matrigel™ and given media containing growth factors known to be important for the proliferation and differentiation of intestinal SCs [12] (**Table 8**). Cells were initially plated in Stem Cell (SC) media for 5-10 days. After small organoids were established, cells were switched to Differentiation (Diff) media or maintained in SC media. After at least 5 days in Diff media, cells were maintained in Diff media or supplemented with N-[N-(3,5-difluorophenacetyl)-1-alanyl]-S-phenylglycine t-butyl ester (DAPT), a γ-secretase inhibitor (GSI) (**Figure 13A**). Activation of the Notch pathway represses secretory cell differentiation [66], but inhibition of Notch leads to activation of ATOH1 promoting goblet cell differentiation in intestinal crypts and adenomas (see **Figure 3**) [48, 67]. Even though the intestinal cells have been removed from their native environment and expanded *in vitro*, they retained the ability to differentiate and form a layer of epithelial cells around a central lumen with a similar architecture and cellular hierarchy as found *in vivo* (**Figure 13B** compared to **Figure 4A**). Once the organoids began to grow, they matured rather rapidly, as can be seen in daily pictures taken of the same organoids sequentially treated with the three types of media (**Figure 14**). Similar spherical structures were seen for SI and LI in SC media. However, we observed morphological differences between the SI and LI SC derived organoids in the Diff and Diff+DAPT treatments (**Figure 13B & Figure 14**). SI structures became more differentiated, with the obvious appearance of vacuolated goblet cells in Diff treated organoids and even an increased amount with the addition of DAPT. However, LI structures remained spherical without

the obvious appearance of goblet cells (**Figure 13B**). Similarly assayed colon CSCs formed structures comparable to the observed LI structures (**Figure 15**).

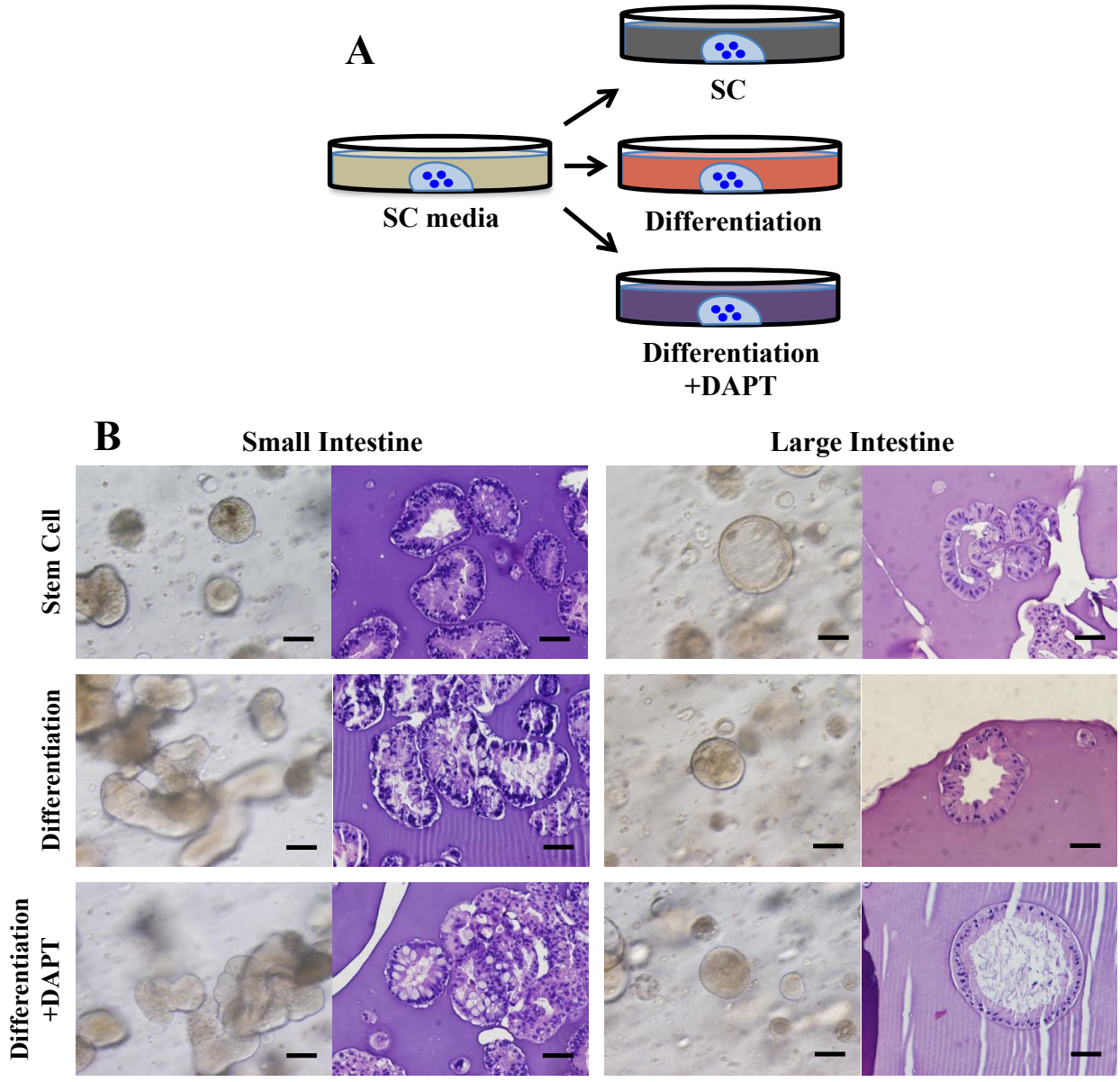

Figure 13: Three-dimensional differentiation assay for small and large intestinal SCs. (A) Experimental design of three-dimensional differentiation assay. Expanded intestinal SCs were embedded as single cells in Matrigel™, first expanded in SC media, then treated further with SC media, Differentiation media or Differentiation media +

DAPT. (B) *In vitro* and H&E pictures of organoids from SI and LI SCs in each of the three treatments. One pair of SI and LI organoids is representative of three sets examined. Scale bar = 50µm.

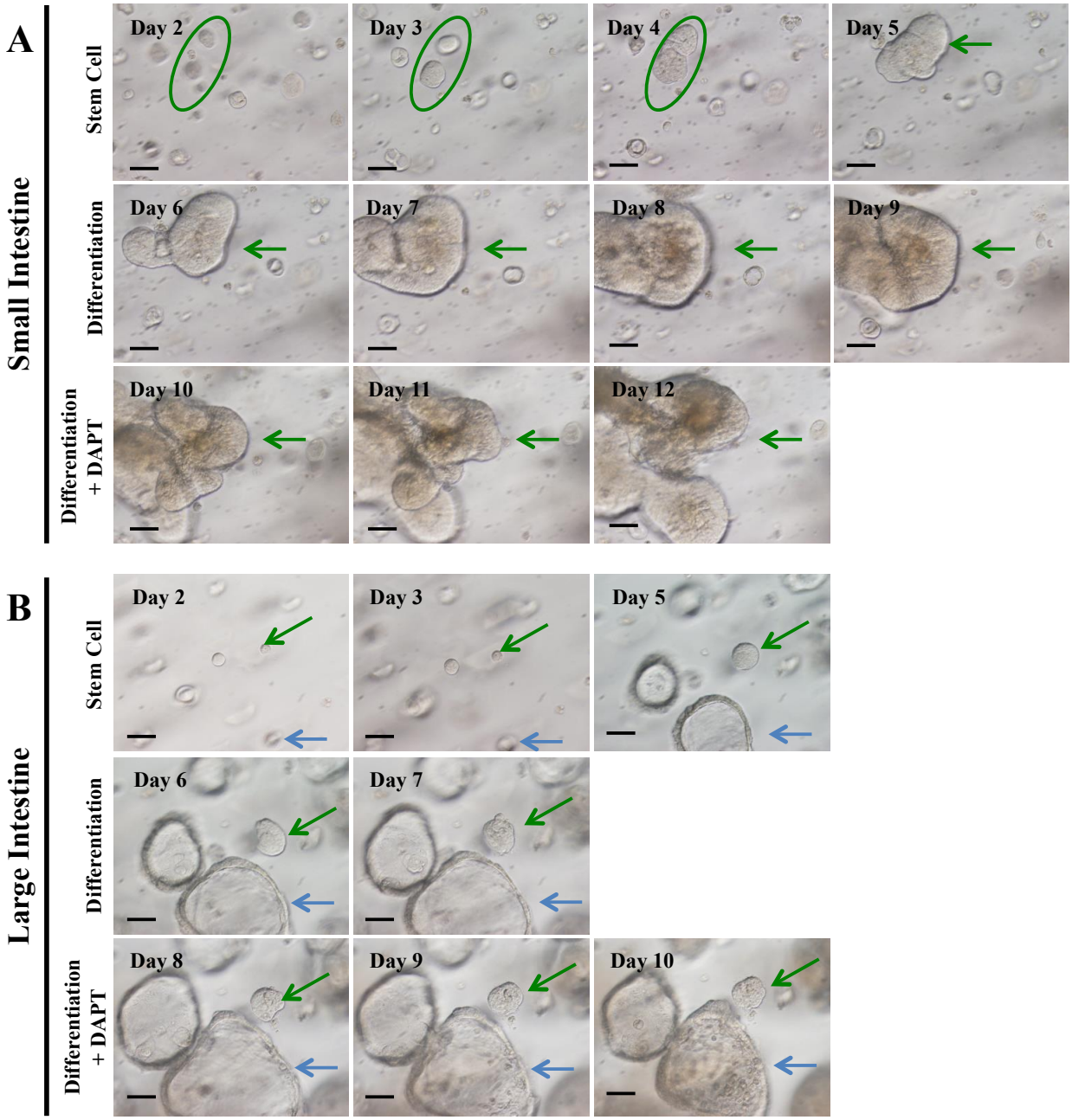

Figure 14: Daily growth of small and large intestinal organoids. (A) SI organoids grown in SC media, Differentiation media and Differentiation media supplemented with DAPT for the last three days. (B) LI organoids

grown in SC media, Differentiation media and Differentiation media with DAPT for the last three days. Scale = 50µm.

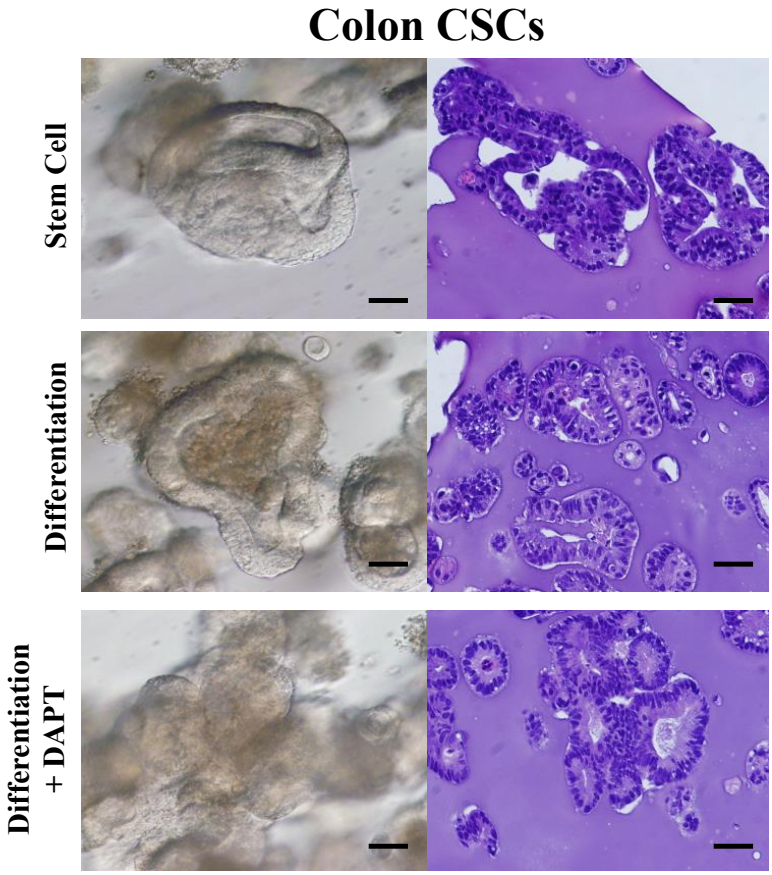

Figure 15: Colon CSCs form organoids in the differentiation assay. Previously characterized colon CSCs (Tu22) [98] grown in three-dimensional system form organoids *in vitro* and can be seen in H&E staining. Scale bar = 50µm.

5.1.2 Intestinal organoids harbor a small population of proliferating cells

As another indication of heterogeneity in the organoids, a modified nucleoside, EdU (5-ethynyl-2´-deoxyuridine), was used to mark the proliferating cells present in the organoids. This

compound is incorporated during DNA synthesis, resulting in a direct measurement of proliferating cells. In **Figure 16**, representative pictures of each treatment group of SI and LI intestinal organoids are depicted. Abundant positive cells are present with SC media in both SI and LI samples. Upon treatment with either Differentiation media or with the addition of DAPT, a dramatic decrease in EdU+ cells was seen (**Figure 16A&B**). Quantification showed statistically significant differences between SC media and both Differentiation and Differentiation + DAPT media (**Figure 16C**).

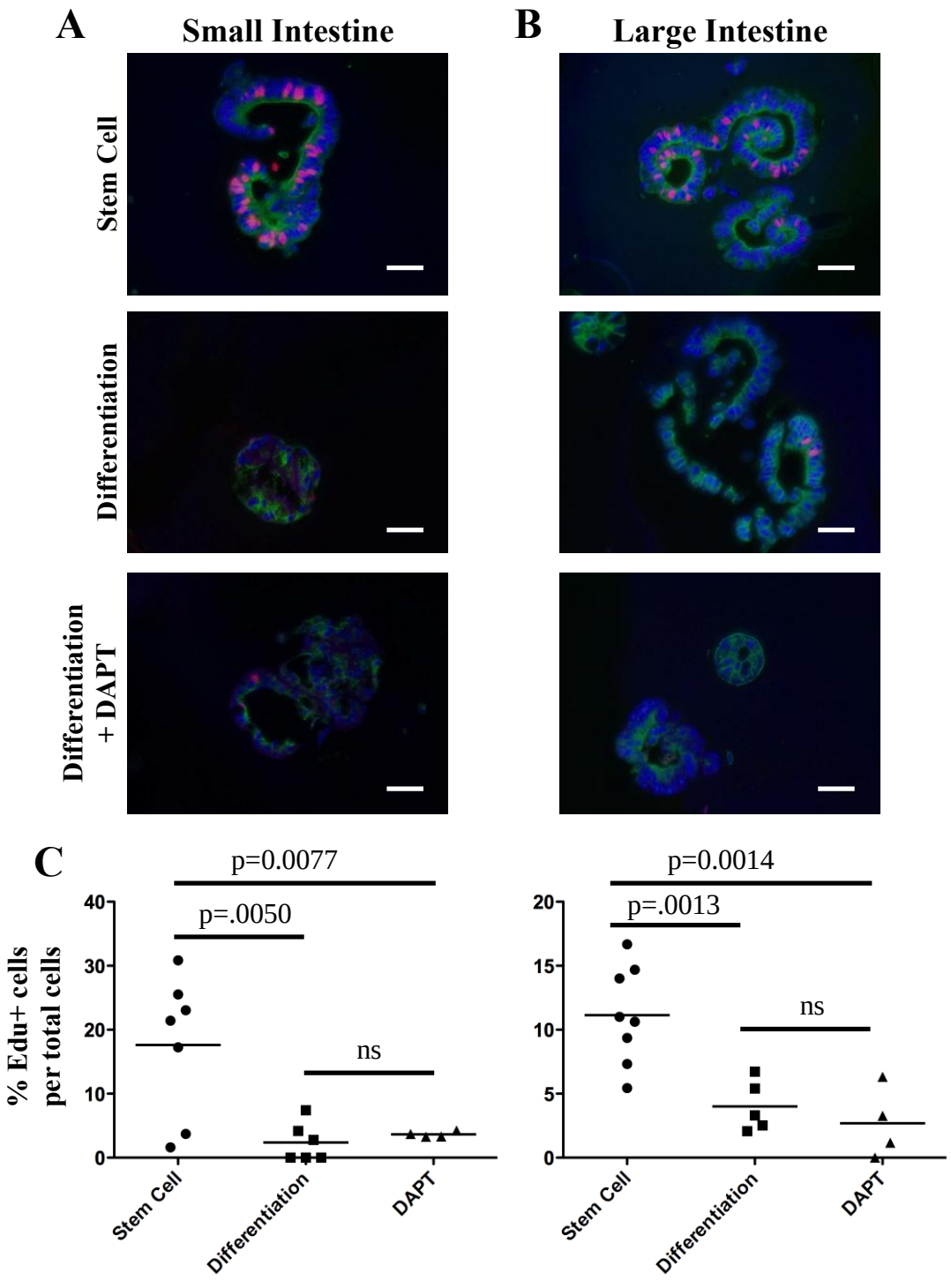

Figure 16: A small subset of cells in intestinal organoids are capable of proliferating and decrease upon differentiation cues. Immunofluorescence of EdU^{+} (red) cells in (A) small and (B) large intestinal organoids in the

three treatments. Stained for epithelial marker, EpCAM (green). Counterstain Hoechst 33342 (blue). (C) Quantification of percent EdU^+ cells per total cells for small (left) and large (right) intestinal organoids. Scale = 50μm.

In contrast, when colon CSCs were subjected to EdU treatment, the result showed a statistically significant increase in proliferation with each differentiation treatment indicated by an increase in the percent of cells that were EdU^+ (**Figure 17A & B**).

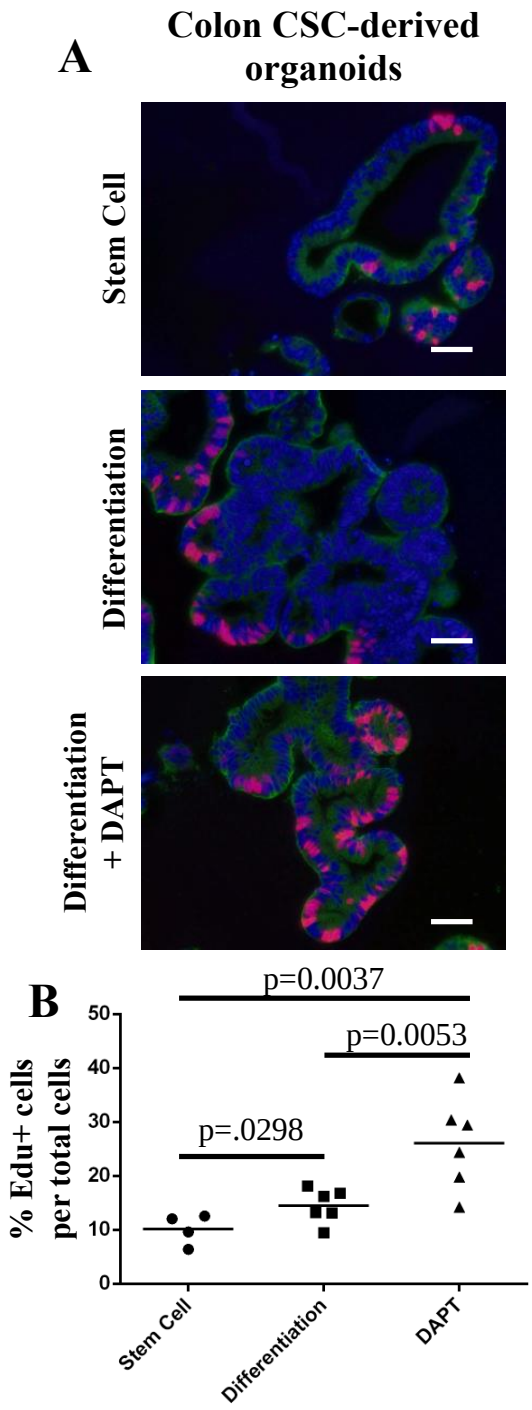

Figure 17: Colon CSC-derived organoids increase percent of proliferating cells with differentiation treatment. (A) Immunofluorescence of EdU^{+} (red) cells in three-dimensional organoids derived from previously characterized colon CSCs (Tu25) [98] in the three treatments. Stained for EpCAM (green). Counterstain Hoechst

33342 (blue). (B) Quantification of percent EdU^+ cells per total cells for colon CSC-derived organoids. Scale = 50μm.

5.1.3 Small intestinal organoids have more potential for goblet and enteroendocrine cells than large intestinal organoids

Using immunofluorescent staining and quantification of differentiation markers, we analyzed SI and LI organoids generated in Matrigel™. The expression of Muc2, a marker of mature goblet cells, significantly increased upon Diff and Diff+DAPT treatment in both SI and LI organoids (**Figure 18**). In addition, SI organoids showed increased expression of ChromograninA (ChrA), a marker for enteroendocrine cells, with differentiation cues (**Figure 18A&C**). This phenomenon has been observed previously after treatment with a GSI [159]. However, under the same conditions, LI organoids failed to express any measurable amounts of ChrA (**Figure 18B**).

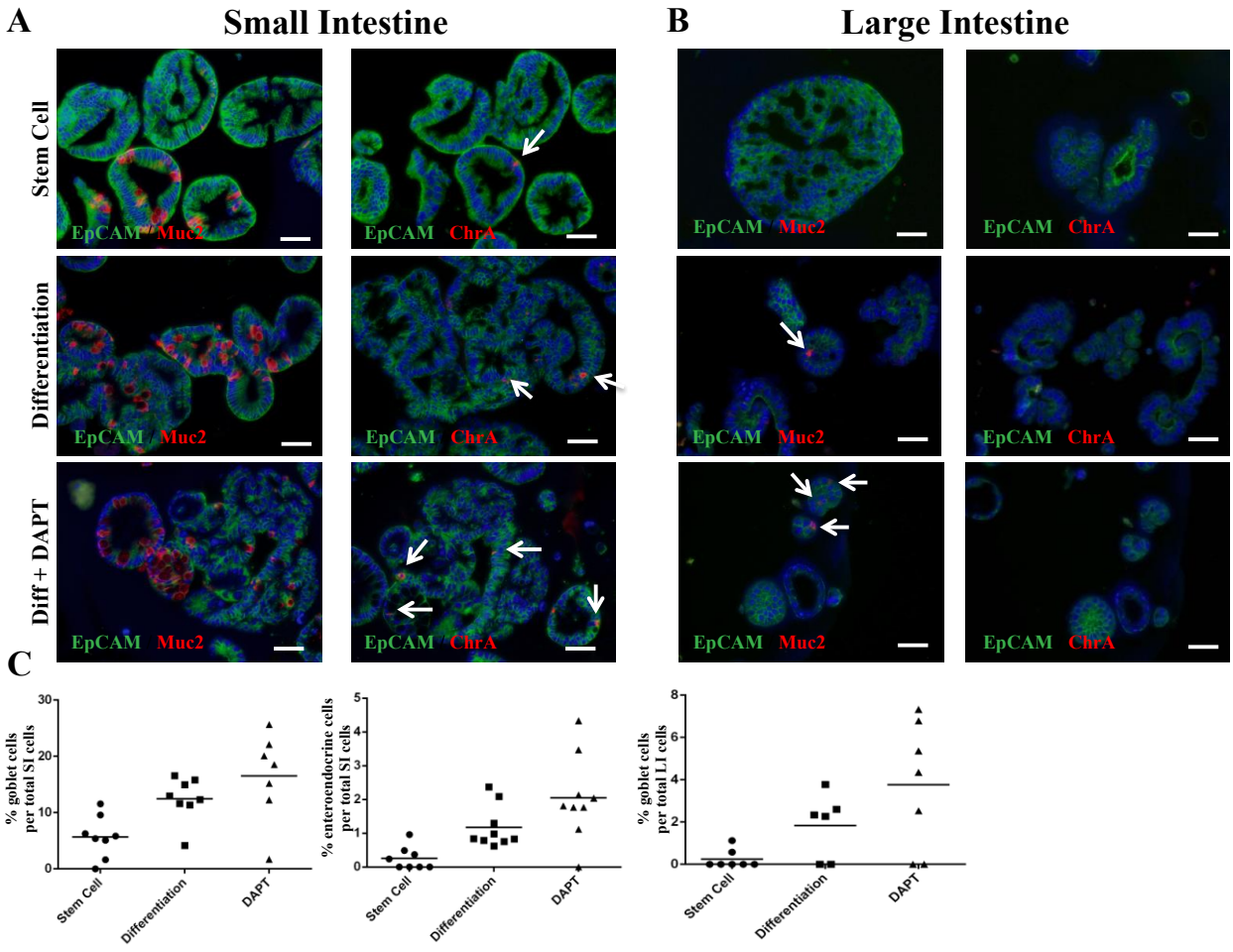

Figure 18: Immunofluorescent staining of intestinal organoids indicating mulitpotentiality and response to differentiation cues. (A) SI and (B) LI organoids from paired samples stained for EpCAM (green), goblet cell marker, Muc2 (red) and enteroendocrine marker, ChrA (red). Counterstain, Hoechst 33342 (blue). Scale bar = 50µm. (C) Quantification of percent goblet or enteroendocrine cells per total cells counted. This paired set serves as a representative of two sets examined.

A similar phenomenon was also seen *in vivo* where a significantly higher number of $ChrA^+$ cells was observed in SI compared to LI (**Figure 19**).

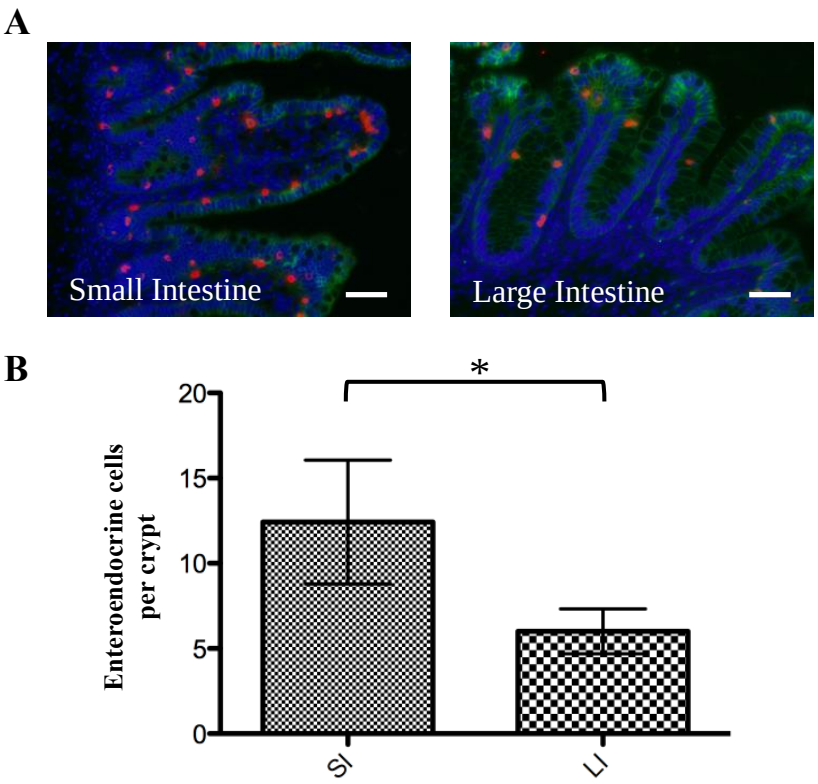

Figure 19: Enteroendocrine cells are found more frequently in the SI than in the LI *in vivo*. (A) Immunofluorescent staining of enteroendocrine cells, ChrA (red), EpCAM (green) in normal human fetal intestine. Counterstain, Hoechst 33342 (blue). Scale bar = 50μm. (B) Cells were counted as cells per crypt and depicted in a bar graph (*$p<0.05$).

Furthermore, enterocyte expression of Villin in SI organoids was lower and dispersed throughout the cell but was localized on the cell apical surface in differentiated LI organoids (**Figure 20**).

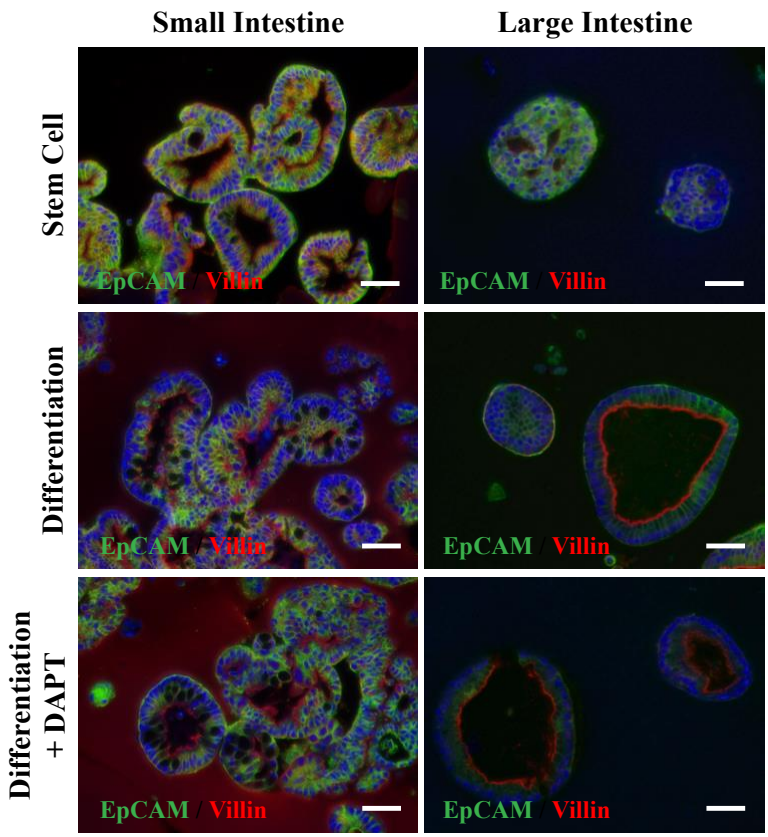

Figure 20: Differential expression of Villin in intestinal organoids. Immunofluorescent staining of SI and LI organoids for EpCAM (green) and enterocyte marker, Villin (red). Counterstain, Hoechst 33342 (blue). Scale bar = 50μm.

Interestingly, Muc2, ChrA and Villin expression in colon CSC organoids resembled that of normal LI organoids, with even less expression of all differentiation markers in all treatment groups (**Figure 21**). Less expression of Muc2 is seen in xenograft tumors derived from colon CSCs when compared to normal human fetal colon (**Figure 22**) (not quantified). These data provide further evidence that intrinsic differences between human SI and LI SCs regulate their differentiation potential and that colon CSCs share more characteristics with normal LI SCs than with SI SCs.

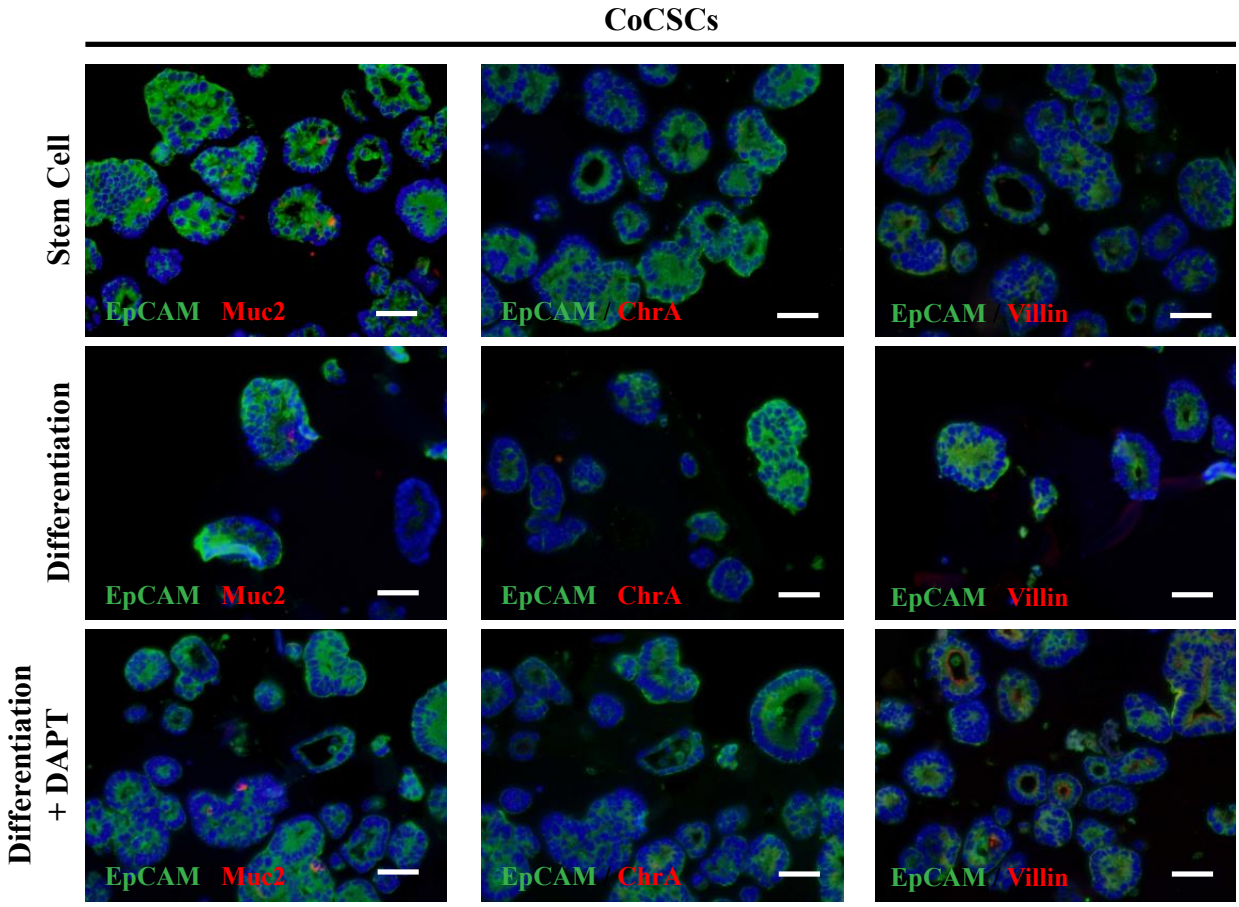

Figure 21: Immunofluorescence of colon CSCs in differentiation assay. Previously characterized colon CSCs (Tu22) [98] grown as organized in three-dimensional system and stained for EpCAM (green) goblet cell marker, Muc2 (red), enteroendocrine marker, ChrA (red) and enterocyte marker, Villin (red). Counterstain, Hoechst 33342 (blue). Scale bar = 50μm.

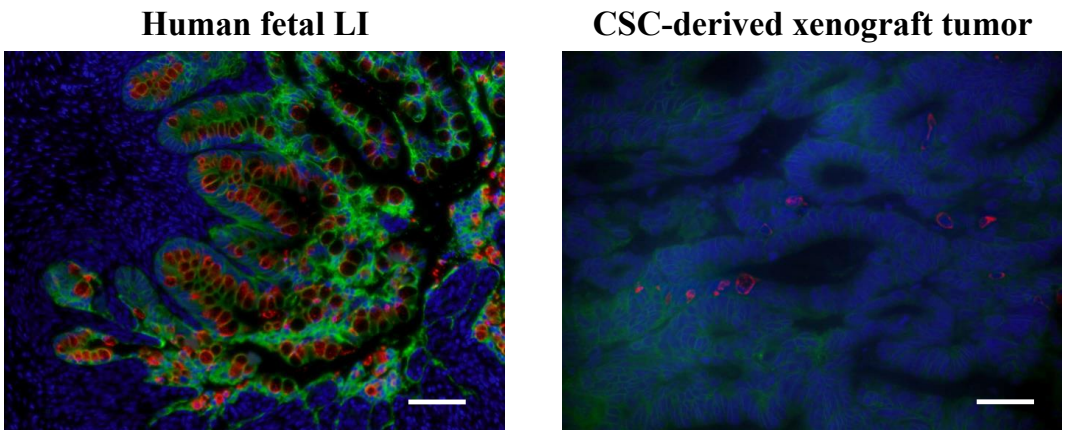

Figure 22: Tumor tissue is less differentiated than normal large intestine. Immunofluorescent staining of normal human fetal LI and xenograft tumor derived from previously characterized human colon CSCs (Tu22) [98] for EpCAM (green) and goblet cell marker, Muc2 (red). Counterstain Hoechst 33342 (blue). Scale = 50μm.

5.2 STEM CELL AND DIFFERENTIATION RELATED GENES DIFFER BETWEEN SMALL AND LARGE INTESTINAL SC-DERIVED ORGANOIDS

5.2.1 The Notch pathway is differentially regulated in SI and LI organoids

Real-time PCR showed increased mRNA expression of ATOH1, Muc2 and ChrA in SI organoids upon exposure to differentiation signals (**Figure 23A**). In LI organoids, Muc2 expression increased upon exposure to differentiation cues, while ATOH1 and ChrA expression was negligible (**Figure 23B**). This confirmed the absence of ChrA protein expression in LI organoids shown in **Figure 18**. Since ATOH1 is upstream of Muc2, this observation suggests the presence of an alternative goblet cell differentiation pathway in LI SCs. These Notch pathway differences were also seen in the gene array analysis of LI and SI SCs from two-dimensional

cultures, indicating these characteristics are inherited by the different SC populations (**Figure 11B**). Interestingly, colon CSC-derived organoids resulted in an increase in Muc2, and even small amounts of ChrA transcript expression following differentiation treatment, indicating that differentiation pathways remain after transformation (data not shown).

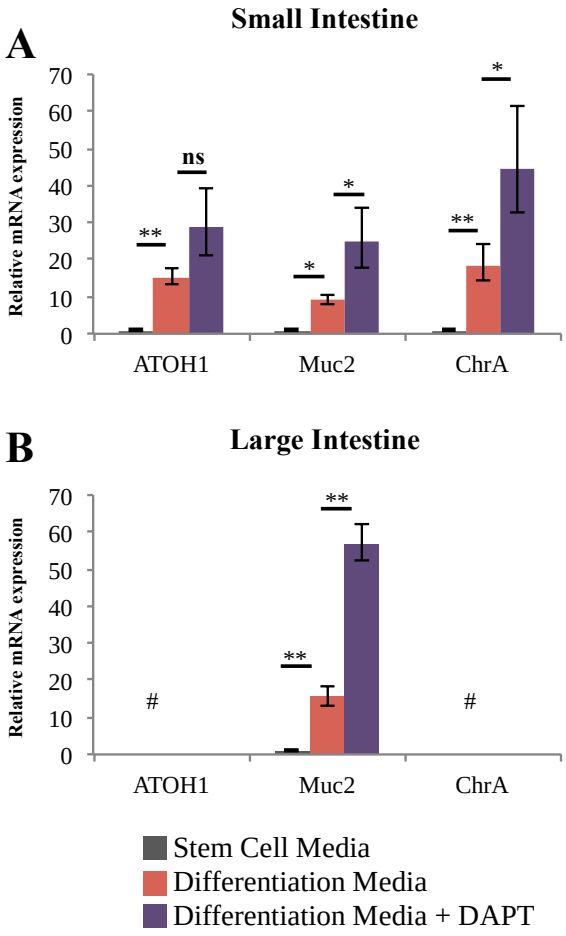

Figure 23: The Notch pathway is differentially regulated in SI and LI organoids. Real-time PCR analysis of (A) small and (B) large intestinal organoids derived from intestinal SCs and treated with SC media, Differentiation or Differentiation media + DAPT. Expression in SC treated organoids was used as control and set to 1. Differentiation media and Differentiation media + DAPT expression values are relative to SC media. Expression was normalized to glyceraldehyde-3-phosphate dehydrogenase (*GAPDH)* mRNA. Error bars represent upper and lower error limits

based on replicate variability (*p<0.05, **p<0.01, ***p<0.001, ns=not significant, # no expression detected). (n=3 wells per sample/primer pair). One paired SI and LI set serves as a representative of at least two paired sets examined.

5.2.2 SC related gene expression differs between SI and LI organoids

We also found differences in SC related gene expression between Matrigel^{TM} organoids derived from SI and LI SCs. As expected, the expression of SC marker and Wnt pathway participant LGR5 decreased in SI organoids upon differentiation treatment. Surprisingly, however, LGR5 reproducibly increased in LI organoids after the addition of Diff media, and only returned to SC media levels after treatment with DAPT (**Figure 24A & B**). This result shows that the SCs of the SI and LI have intrinsic differences in their ability to respond to the same environmental cues. We also found EphrinB2 (EphB2), another putative intestinal SC marker [160], consistently increased upon Diff treatment of LI organoids. In SI organoids, EphB2 remained unchanged in Diff media but subsequently decreased with the addition of DAPT. In addition, Myc, a Wnt target gene, also decreased as expected upon exposure to differentiation cues in SI organoids but a significant change in LI organoids was not observed. This confirms the gene array analysis of LI and SI SCs expanded in the two-dimensional system displaying significantly different Wnt pathway transcript expression with generally more Wnt activity seen in the LI SCs, again indicating that these are inherited characteristics of the different SCs (**Figure 11A**).

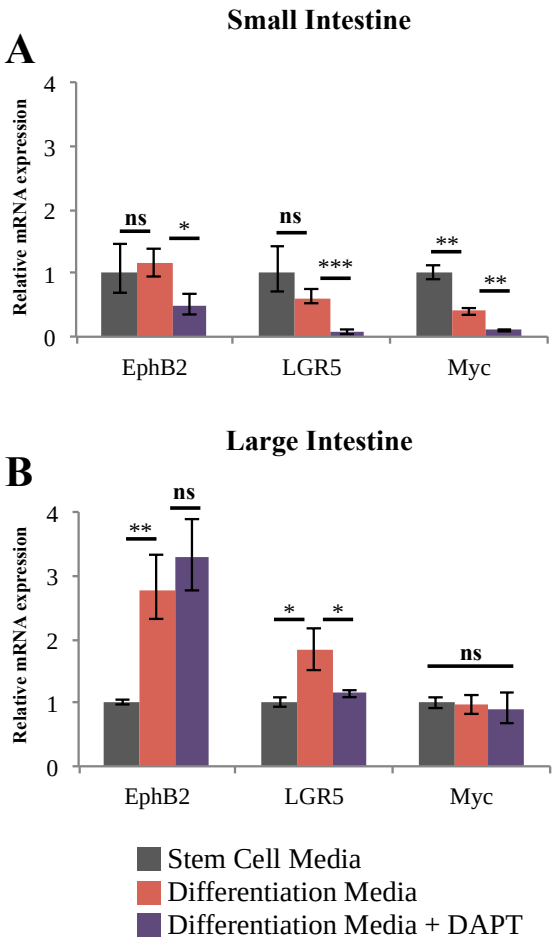

Figure 24: SC related genes are differentially regulated in SI and LI organoids. Real-time PCR analysis of (A) small and (B) large intestinal organoids derived from intestinal SCs and treated with SC media, Differentiation or Differentiation media + DAPT. Expression in SC treated organoids was used as control and set to 1. Differentiation media and Differentiation media + DAPT expression values are relative to SC media. Expression was normalized to *GAPDH* mRNA. Error bars represent upper and lower error limits based on replicate variability (*p<0.05, **p<0.01, ***p<0.001, ns=not significant). (n=3 wells per sample/primer pair). One paired SI and LI set serves as a representative of at least two paired sets examined.

To further understand how colon CSCs compare to normal LI SCs, we also assayed these SC related genes in colon CSC-derived organoids (data not shown). In correlation with the LI

organoid results, colon CSCs had an increase in LGR5 and EphB2 upon differentiation. Unlike their normal counterparts (**Figure 24)**, colon CSC-derived organoids had an increase in Myc expression, acting as a tribute to their transformed identity and differential response to differentiation cues.

To better understand the expression differences in genes of interest, we compared SI and LI organoids directly at each treatment step and again found undetectable expression of ATOH1 in LI organoids (**Figure 25**). LGR5 and Myc were significantly higher in LI organoids compared to SI, indicating dramatically different responses in the SCs of the SI and LI (**Figure 25**). The observation that SC and differentiation genes have opposing expression under the same environmental cues reveals important differences between the SCs of the SI and LI.

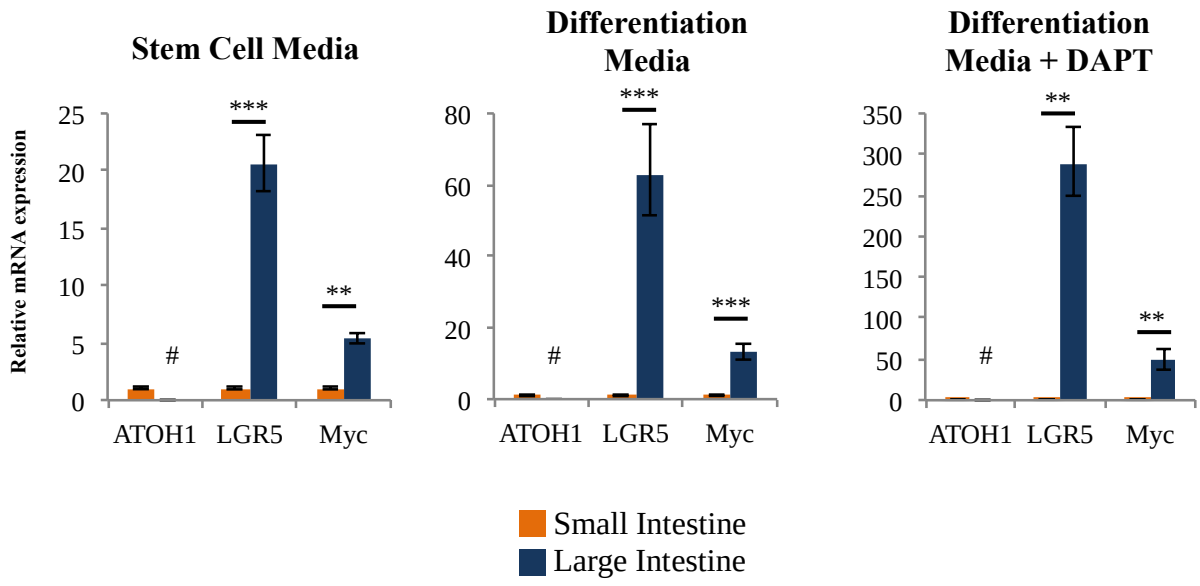

Figure 25: Select gene expression in SI versus LI organoids. Real-time PCR analysis of SI and LI organoids derived from intestinal SCs and treated with SC media, Differentiation or Differentiation media + DAPT. Select marker expression comparison between SI and LI organoids in the three treatments. SI values used as control and set to 1. LI expression values are relative to SI. Expression was normalized to *GAPDH* mRNA. Error bars represent upper and lower error limits based on replicate variability (*p<0.05, **p<0.01, ***p<0.001, # no expression

detected). (n=3 wells per sample/primer pair). One paired SI and LI set serves as a representative of at least two paired sets examined.

5.3 DISCUSSION

SI and LI SCs were subjected to identical sets of environmental stimuli to determine differences in differentiation responses. Wnt and Notch factors were carefully controlled in a three-dimensional system as a way of recreating the intestinal environment and SC niche to allow differentiation [12]. Any differences observed were due to inherent instructions in the cells in response to defined exogenous cues. Although both SI and LI organoids responded to differentiation treatment with a decrease in proliferation (**Figure 15 & Figure 16**), morphological differences implied that differences did exist (**Figure 13 & Figure 14)**. Further characterization confirmed this observation with differential expression of markers for the three cells types in the intestine, enterocytes (Villin), goblet cells (Muc2) and enteroendocrine cells (ChrA) (**Figure 18 & Figure 20**). Not only does the lack of expression of ChrA in LI organoids highlight an important mechanistic difference between the SI and LI, but it also mimicked that which is found *in vivo*, confirming that this *in vitro* system has provided the cells with an environment similar to that found *in vivo* (**Figure 19**). The difference in Muc2 expression was initially a concern since goblet cells are often more abundant in the LI than the SI. However, upon QPCR analysis, Muc2 transcript was abundant in LI organoids and increased upon differentiation treatment.

Upon differentiation, it is expected that an increase in ATOH1 will lead to an increase in Muc2, as part of the Notch pathway [48]. SI organoids had abundant ATOH1 and Muc2 transcripts, however, ATOH1 was not detected in LI organoids, possibly explaining the limited expression of Muc2 seen with immunofluorescence. The gene array analysis (**Chapter 4.3**) of SI and LI SCs indicated that this differentiation pattern is inherited from SCs (**Figure 11**). The differential regulation of the Notch pathway between SI and LI SCs and organoids may reflect a yet unknown phenomenon in the LI (**Figure 11 & Figure 23**). While numerous studies have elucidated the many players in the Notch pathway, including ATOH1, most *in vivo* studies have been performed in the SI of mice. As the SI and LI share many characteristics, researchers often assume that phenomena seen in the SI would carry into the LI. However, in the current study, while the expected results were seen in the SI in all cases, the LI samples followed a different pattern, providing reason for caution when classifying the intestines as one organ.

Interestingly, ATOH1 is important in intestinal cell homeostasis [161] and is required for the efficacy of GSIs [162, 163]. This may further explain the limited Muc2 protein expression seen in DAPT treated LI organoids. In addition, 70% of CRC patient samples were shown to have significantly decreased mRNA expression of ATOH1 compared to tissue-matched normal LI samples [164]. If GSIs require active ATOH1 expression to elicit their differentiation effect, the decreased expression of ATOH1 may explain the poor results of differentiation therapies. Previous studies also showed that ATOH1 has tumor suppressive effects. Increased expression limited tumor cell growth *in vitro* and loss of expression increased tumor formation *in vivo* [164]. Therefore, the lack of detectable ATOH1 in LI SC-derived organoids could make them more susceptible to transformation than their SI counterparts.

Parallel studies in colon CSCs demonstrate an ability to form disorganized organoids (**Figure 15**). When assessing their differentiation capability, it looks as though they have limited capability, similar to normal LI organoids. As LI organoids mimic the *in vivo* structure of the LI, organoids derived from CSCs mimic xenograft tumors from the same origin (**Figure 21 & Figure 22**). While normal LI tissue is well-organized and follows a defined differentiation pattern, CSC-derived xenografts are poorly organized with random differentiation patterns throughout the tumor tissue. This serves as confirmation that the original characteristics of the cells, normal- or cancer-derived have been retained in *in vitro* organoids. Similarities are expected if mutations in normal LI SCs give rise to colon CSCs [4].

Surprisingly, even though the colon CSC-derived organoids showed an increase in Muc2 expression with differentiation treatment, they also responded with a significant increase in proliferation (**Figure 17**), setting them apart from their untransformed normal LI SC counterparts (**Figure 16**). Although LI SCs seem to have characteristics that would make them more susceptible to transformation, there are still well defined controls present, limiting their proliferation and inhibiting them from forming tumors (**Table 2**). CSC-derived organoids not only lack these controls, but also have alternate signaling that opposes homeostatic responses present in normal tissue. The dramatic increase in proliferation upon differentiation treatment may be another reason that GSIs have failed in the clinic. Although many *in vitro* studies have indicated that GSIs increase differentiation [66] (as appears in this study as well), when SC and proliferation experiments accompany such studies, contradictions arise. Even in the study that identified ATOH1 as being required for the effect of GSIs, notch activation and growth inhibition seen in human cell lines of CRC were variable [162]. GSI treatment of wild-type murine intestines caused a significant decrease in BrdU incorporation compared to vehicle treated.

However, in ATOH1-null mice, there was a significant increase in BrdU incorporation in the LI with GSI treatment, demonstrating that loss of ATOH1 can enhance proliferation in response to GSIs. This proliferative response was not seen in the SI of ATOH1-null mice. Furthermore, GSI treatment of APC^{min} adenoma-bearing mice reduced adenoma proliferation [67, 162], but ATOH1 status was not assessed. Combined with previous results, our study indicates that a lack of ATOH1 may be inherited from LI SCs to colon CSCs upon transformation, explaining the increased susceptibility of LI SCs to transformation and subsequent failure of GSIs to treat colon cancer in the clinic.

The differences seen between SI and LI organoids extended to the expression of SC related genes. EphB2, LGR5 and Myc all decreased in SI organoids upon differentiation treatment. However, this general trend was not seen in LI organoids (**Figure 24**). The differential regulation of genes involved in cell proliferation, self-renewal and the Wnt pathway highlight key regulatory changes governing SI versus LI determination and likeness to cancer. Quite unexpected, LGR5 increased significantly upon differentiation treatment and did not return to SC treatment levels until after DAPT treatment. This novel result may reveal a yet unknown molecular pathway that distinguishes LI SCs form SI SCs. LGR5 may serve a different role in the LI that is not paralleled in the SI. LGR5 was also expressed at a significantly higher level in LI versus SI at each treatment step (**Figure 25**). The higher expression of SC marker LGR5 could mean the presence of cells with higher resistance, DNA repair and growth advantage that if transformed, could give rise to CSCs ready to rapidly fuel cancer growth [165]. In fact, CSC-derived organoids also demonstrated an increase in EphB2 and LGR5 upon differentiation treatment, however, this was also accompanied by an increase in Myc. This indicated over

activation of the Wnt pathway and suggested again that LI SCs are more susceptible to transformation due to their similarities with colon CSCs.

The expected results obtained from these experiments in SI samples confirm that the combined systems of two-dimensional SC expansion and three-dimensional differentiation assays reproducibly create an environment similar to that found *in vivo*. The unexpected results seen with the LI samples identify key intrinsic differences between human SI and LI SCs and their relation to cancer.

6.0 METHODS

6.1 TISSUE PREPARATION AND CELL CULTURE

6.1.1 Cell isolation and cell culture

Small and large intestines were obtained from 19-23 week fetuses from elective abortions performed at Magee Women's Hospital, Pittsburgh, PA. Intestines were cut longitudinally in HBSS, contents rinsed, cut into 1-inch pieces, transferred to EBSS/10mM EGTA/1% HEPES (Life Technologies, NY/Sigma-Aldrich, MO/Mediatech, VA) and minced. Tissue was then transferred to a tube and incubated for 5 min at room temperature. After an EBSS wash, the tissue was treated three times with a cocktail containing 1mg/mL collagenase II (Life Technologies, NY), 1mg/mL hyaluronidase (Sigma-Aldrich, MO), and 20μg/mL DNase I (Roche, IN) in HBSS/1% HEPES for 20 min. Tissue/cell suspensions were passed through a 100μm cell strainer (Fisher, PA) to isolate single cells from undigested tissue. Cells were plated on irradiated feeders at ~80,000 cells/cm^2 in DMEM/F12 supplemented with 0.5% FBS, 25μg/mL gentamicin (Sigma-Aldrich, MO), 1% Insulin-Transferrin Selenium (ITS) (Mediatech, VA) and 0.1ng/μL human R-Spondin2 (R&D, MN). When single cells were plated, 10μM ROCK inhibitor, Y-27632 (Reagents Direct, CA), was added to the media for ~24 hours.

Cultures were passaged at 2-3 weeks post-plating (~70% confluency) by incubating with EBSS/10mM EGTA/1% HEPES followed by 0.25% Trypsin/0.1% EDTA.

6.1.2 Preparation of feeder cells

LA7 (ATCC: CRL-2283™) cells were grown in DMEM/F12 (Mediatech, VA) supplemented with 5% FBS, 1% Pen/Strep (Mediatech, VA), 50nM hydrocortisone (Sigma-Aldrich, MO) and 5μg/mL Insulin (Sigma-Aldrich, MO. Cells were detached from the plate with 0.25% Trypsin/0.1% Ethylenediaminetetraacetic acid (EDTA) (Mediatech, VA) and γ-irradiated at 17,000 rads. Cell culture flasks were seeded at ~300,000 cells/cm^2 to generate a confluent monolayer of feeder cells.

6.1.3 Tumor Cell Analysis

Colon CSCs, originally obtained from tumors surgically removed from the liver of patients with metastatic colon cancer, were maintained in the feeder cell system as previously reported [98]. Colon CSCs were subsequently cultured as organoids in matrigel as described above for normal intestinal SCs.

6.2 XENOGRAFT TUMOR ANALYSIS

Rag-2/$\gamma c^{-/-}$ mice were anesthetized and transplanted with normal SI and LI SCs or colon CSCs. Cells were mixed 1:1 with HBSS/Matrigel and 0.5-1.0e6 cells were injected into the subcutaneous space. 1-4 months later, the mice were opened to observe tumor formation.

6.3 GROWTH CURVE ANALYSIS

Small and large intestinal SCs were assayed for difference in their growth rates using cell culture and flow cytometry. Three paired SI and LI samples were independently compared using the same number of starting cells on day 0 (SI and LI 1 at 18,750 cells/well, SI and LI 2 and 3 at 93,750 cells/well) in a 24-well plate seeded with feeder cells. Wells were analyzed in triplicate on days 1, 4, 8 and 11 to determine the absolute number of EpCAM+ cells in a defined volume using the MACSQuant™ (Mitleyi Biotec, CA) cell analyzer. Triplicates were averaged and plotted against time on a line graph to reflect growth rate. A repeated measures ANOVA was performed followed by a Student's t-test. Significance was defined as $p<0.05$.

6.4 MRNA EXPRESSION ASSAYS

6.4.1 Eukaryotic target preparation

Total RNA was extracted from frozen cell pellets comprising feeder cells (LA7 feeder cells; n=5) and human fetal small or large intestine (SI; n=6 and LI; n=6) putative stem cells. Total RNA was isolated using the Qiagen miRNeasy kit (Qiagen Inc., Valencia, CA) according to the manufacturer's protocol. Only RNA of highest quality and integrity was subjected to further processing after purification as defined by an absorption ratio 260/280$\geq$1.8 obtained by spectrophotometry on the NanoDrop 1000 (NanoDrop Inc., Wilmington, DE) and a RIN value $\geq$8.0 via electrophoretic analysis on the Bioanalyzer 2100 (Agilent Technologies, Santa Clara, CA).

6.4.2 Hybridization

In vitro transcription (IVT) was performed using the Ambion MessageAmp Premier Enhanced assay protocol (Ambion Inc, Austin, TX) starting with 500ng of purified total RNA. Confirmation of cRNA diversity was obtained using the Bioanalyzer 2100 to generate an electrophoretogram for the products of each IVT reaction regarding sample yield, integrity, and size diversity against transcripts derived from a Universal Human Reference RNA (Stratagene, La Jolla, CA). Fifteen micrograms of purified, amplified, biotin labeled cRNA were fragmented and hybridized on to Affymetrix Human Genome HGU133A 2.0 arrays (Affymetrix Corp. Santa Clara, CA) for 18 hours. Washing, staining and scanning of arrays was performed on the

Affymetrix Fluidics Station 450 and Scanner 3000 immediately after completion of hybridization according to the manufacturer's protocol.

6.4.3 Data processing

Microarray data were processed using the Robust Multi-array Average by importing raw CEL files into Partek software (Partek Genomics Suite, St. Louis, MO) resulting in RMA background correction, log base 2 transformation, quantile normalization, and median polish probe set summarization. A 2 way ANOVA was performed across the three groups (LI, SI, LA) versus gene expression and post-hoc testing was performed using the Students T test to identify transcripts that were significantly changed between groups. A q-value correction adjusted for false discovery rate (FDR) was established ($q<0.05$) to control for Type 1 errors arising from multiple tests. Expression data (q value<0.05, 2 fold change) was imported into Ingenuity software (Ingenuity Pathways Analysis, Ingenuity Systems Inc, Redwood City, CA) for pathway analysis. All figures are plotted using unlogged data to maintain the original biological distribution of expression.

6.5 FLUORESCENCE-ACTIVATED CELL CORTING AND ANALYSIS

Single cell suspensions were stained with appropriate antibodies (**Table 7**) at 200,000 cells per tube and analyzed on the MACSQuant™ or BD FACSAriaII™ (BD Biosciences, MA). Singlet discrimination was performed as described by Wersto et al. [166]. Post-acquisition analysis was carried out in FlowJo (http://www.treestar.com). Staining index was calculated as D/W, where D

is the distance between the positive and negative populations and W is two standard deviations of the negative population. Limiting Dilution Analyses (LDA) were performed by sorting 1, 10, 25, 50, 100, 250, 500, 1000 cells per well into respective rows of 96-well plates (Corning, NY) seeded with irradiated feeder cells. Plates were counted at four weeks and the number of wells with colonies was input into L-Calc® (Stem Cell Technologies, Vancouver, BC, Canada).

Table 7: Comprehensive list of antibodies for flow cytometry

Antibody	Manufacturer	Concentration
Epcam-FITC	Milteyni Biotec	1:100
CD24-FITC	BD Biosciences	1:50
CD227FITC	BD Biosciences	1:20
CD49b-FITC	BD Biosciences	1:10
CD49f-FITC	BD Biosciences	1:10
CD34-FITC	Milteyni Biotec	1:10
CD9-FITC	BD Biosciences	1:5
EpCAM-PE	Milteyni Biotec	1:50
CD66c-PE	BD Biosciences	1:50
CD13-PE	BD Biosciences	1:25
CD133.1-PE	Milteyni Biotec	1:50
CD133.2-PE	Milteyni Biotec	1:5
CD166-PE	BD Biosciences	1:10
CD26-PE	BD Biosciences	1:5
EpCAM-APC	Milteyni Biotec	1:50
CD81-APC	BD Biosciences	1:10
CD29-APC	BD Biosciences	1:5
CD90-APC	BD Biosciences	1:10
CD44-APC	BD Biosciences	1:10
CD49f-APC	BioLegend	1:10
CD54-APC	BD Biosciences	1:50
EpCAM-PerCP-Cy5.5	iCyt	1:50
HLA-Biotin	Ancell	1:100
SAV-APC-Cy7	BD Biosciences	1:25

6.6 MATRIGEL DIFFERENTIATION ASSAY AND ANALYSIS

6.6.1 Culturing in Matrigel

The differentiation assay was originally found in Sato, et. al. with slight modifications [12]. Single intestinal cells previously cultured on feeder cells were suspended in 50μL Growth Factor Reduced (GFR), phenol-red free Matrigel™ (BD Bioscience, CA) and plated in tissue culture dishes at low density (~50,000 cells/well of 48-well plate). After solidification at 37°C for 30 min, the matrigel was overlaid with Stem Cell media (SC) (**Table 8**). For the first 24 hours, the media included Y-27632 to prevent anoikis. After initial plating in SC media and the formation of small organoids, two-thirds of the wells were switched to Differentiation (Diff) media to allow differentiation of the organoids to occur. After further growth of the organoids, DAPT (Reagents Direct, CA), a γ-secretase inhibitor, was added to half the wells containing Diff media at 10μmol/mL for three days. Media was changed on all wells three times a week. Resulting organoids were isolated using 0.2% dispase (Life Technologies, NY), 0.1% collagenase II and 20μg/mL DNase I. Organoids were then rinsed in PBS (Mediatech, VA) for downstream applications.

If DNA synthesis was to be detected after paraffin embedding, EdU (5-ethynyl-2'-deoxyuridine) (Life Technologies, NY) was added directly to matrigel media at 1μM two hours prior to collection of organoids.

Table 8: List of matrigel media components

Matrigel media components:	Final Conc.	Manufacturer	SC media	Diff Media
Adv DMEM/F12	1x	Life Technologies	X	X
Pen/Strep	100/100 U/mL	Mediatech	X	X
HEPES	10mM	Mediatech	X	X
N2	1x	Life Technologies	X	X
B27	1x	Life Technologies	X	X
Glutamax	2mM	Life Technologies	X	X
Nacetyl-L-Cysteine	1mM	Sigma	X	X
[Leu15]-Gastrin I human	100μM	Sigma	X	X
Y-27632	10μM	Reagents Direct	X	X
Murine EGF	50ng/mL	Peprotech	X	X
Human R-Spondin2	0.1ng/μL	R&D	X	X
Noggin	100ng/mL	Peprotech	X	X
A 83-01	500nM	Tocris	X	X
Human Wnt-3a	100ng/mL	R&D	X	
Nicotinamide	10mM	Sigma	X	
SB 202190	10μM	Sigma	X	

6.6.2 Paraffin embedding of matrigel organoids

Organoids were treated with 4% PFA (Sigma-Aldrich, MO) for 20 min at 4°C, rinsed in PBS and embedded in 5% gelatin (Sigma-Aldrich, MO) in PBS and solidified on ice for 20 min. The gelatin was fixed in 4% PFA for 1 hour at 4°C, rinsed in PBS and submitted for paraffin embedding. Freshly isolated tissue was fixed in 4% PFA for 2 hours at 4°C, rinsed in PBS and submitted for paraffin embedding.

6.6.3 RNA isolation and quantitative real-time PCR

Organoids were lysed and RNA isolated using the RNeasy kit (Qiagen, CA). RNA was quantified with the Nanodrop (Thermo Scientific, IL). Reverse transcription was performed using iScript RT Supermix followed by PCR with SsoADV SYBR Green (Bio-Rad, CA) on an ABI StepOne Plus Real-Time PCR machine (Applied Biosystems, CA). Primers were designed using Primer Express software (Applied Biosystems, CA) and purchased from Life Technologies (NY) (**Table 9**). Expression was normalized to GAPDH. Error bars represent upper and lower error limits based on replicate variability. Statistical analysis was performed using Student's t-test ($p<0.05$ was considered significant).

Table 9: Comprehensive list of real-time PCR primers

Target	Sequence
ChrA-Fwd	CGCTGTCCTGGCTCTTCTG
ChrA-Rev	CCTTTATTCATAGGGCTGTTCACA
LGR5-Fwd	CCTGCGTCTGGATGCTAACC
LGR5-Rev	GGAATGCAGGCCACTGAAA
Myc-Fwd	CGTCTCCACACATCAGCACAA
Myc-Rev	TCTTGGCAGCAGGATAGTCCTT
Muc2-Fwd	TGGCTGGATTCTGGAAAACC
Muc2-Rev	TGGCTCTGCAAGAGATGTTAGC
ATOH1-Fwd	GCAATGTTATCCCGTCGTTCA
ATOH1-Rev	CCATCTGCAGGGTCTCATATTTG
GAPDH-Fwd	GGCATCCTGGGCTACACTGA
GAPDH-Rev	GGAGTGGGTGTCGCTGTTG

6.7 IMMUNOFLUORESCENT STAINING

Antibodies against EpCAM, Chromogranin A, Mucin2 and Villin were used at the appropriate dilution in PBS containing 0.5% Bovine Serum Albumin (BSA) (Fisher, PA) (**Table 10**). Paraffin sections were deparaffinized and rehydrated, permeabilized with 0.1% Triton X100 (Sigma-Aldrich, MO) for 10 min, blocked with 5% BSA for 30 min, stained with primary antibodies for one hour followed by either anti-mouse or anti-rabbit Alexa Fluor® secondaries (Life Technologies, NY) for 30 minutes. Images were taken using an IX71 Inverted microscope (Olympus, PA).

Table 10: Comprehensive list of antibodies for immunofluorescent staining

Antibody	Manufactureer	Conentration
CD133.1 (AC133)	Miltenyi Biotech	1:100
ChrA	Millipore	1:400
Epcam	Abcam	1:50
Lysozyme	Novus Biologicals	1:200
Muc2	Santa Cruz	1:150
Villin	AbD SeroTec	1:100
Alexa Fluor 488 secondary (anti-Rb)	Life Technologies	1:300
Alexa Fluor 594 secondary (anti-Ms)	Life Technologies	1:300

For detection of EdU incorporation into cells of matrigel organoids, the Click-iT EdU Assay (Life Technologies, NY) was used according to manufacturer's protocol. In brief, after permeabilization as stated above, the sections were rinsed in PBS and incubated for 30 minutes with Click-iT reaction cocktail containing the Alexa Fluor 594 azide that reacts with the alkyne of EdU to allow detection. The sections were rinsed with Click-iT reaction rinse buffer before continuing with blocking and staining with antibodies as noted above.

7.0 CONCLUSIONS

Few methods allow for the expansion of primitive cells from the human intestine. Here we have described methods by which to expand primary human SI and LI epithelial SCs. We identified the need to alter the culture conditions used **previously** for the expansion of colon CSCs [98] by adding a Wnt agonist, R-spondin2, without the evidence of transformation. SI and LI SCs were enriched for SC markers CD133.1, CD24, CD166 and CD49f, while being negative for CSC marker CD44. We subsequently characterized the cells as having SC characteristics of self-renewal and differentiation using the two-dimensional SC culture as well as a three-dimensional differentiation assay. During this characterization, many differences between SI and LI SCs were observed and further analyzed. Initially, both two- and three-dimensional cultures showcased the different morphologies of SI and LI cells and their structures, a reflection of their *in vivo* characteristics. Furthermore, CD66c identified two opposing populations in expanded SI and LI cells with high self-renewal ability.

The intricate regulation of the cells was examined by gene array, highlighting the differences in proliferation, migration and other disease-related pathways. SI and LI SCs clustered well within themselves but very distinct from one another, confirming that their differences are rooted in their intrinsic molecular signatures. Notch and Wnt pathway regulation revealed differences in fundamental pathways, predicting a higher Wnt activity in LI SCs and a more differentiated phenotype in SI SCs. The highest positive fold changes occurred in

transcripts with roles in metastasis and CRC progression, while those with the highest negative fold changes occurred in transcripts with tumor suppressor roles or an association with a differentiation phenotype. These results indicate that LI SCs are more closely related to cancer and possibly more susceptible to transformation than SI SCs, owing to the inherent differences in LI versus SI SCs.

Lastly, the organoid differentiation assay confirmed differential regulation of the Notch pathway in a system that mimics the *in vivo* condition. While SI organoids responded as expected to environmental changes, LI organoids lacked detectable expression of ATOH1, a key player in goblet cell specification. In addition, the dramatic increase in LGR5, the most accepted SC marker of the intestine, after differentiation treatment of LI organoids demonstrated a yet unobserved phenomenon that may have implications in susceptibility to transformation and therapy resistance of transformed cells.

Many differences between the SI and LI have been observed in recent years, but only one study observed differences in SI and LI and attributed it to resident SCs with an implication for susceptibility to disease [167]. This study used a novel label and chase technique to follow intestinal SCs over time. These label-retaining cells were absent from the LI and the difference is thought to reflect the different functional requirements of the SI and LI as well as their susceptibility to cancer. Likewise, the SC marker Bmi1 was mapped to the +4 stem cell position in SI, but was absent in LI [35, 168]. Both of these studies may identify a compensatory SC in the SI that is absent in the LI. Without a second SC population, LI SCs receive the full burden of transformative insults. However, LI SCs required eight times the dose of irradiation required to reach similar levels of apoptosis as their SI SC counterparts, indicating differential responses to a specific type of injury [73]. The increased resistance of LI SCs may be attributed to lower expression of p53 and

higher expression of Bcl-2 [72, 74, 75, 169]. When transformation occurs, these resistant behaviors are inherited by the newly formed CSCs, fueling a cancer that is difficult to eradicate.

Our characterization of human fetal SI and LI SCs revealed critical intrinsic differences, underscoring the importance of carefully distinguishing between SI and LI, as regulation of differentiation and SC pathways show dramatic disparities. This becomes particularly important when considering the various models of intestinal cancer that utilize murine small intestine. Results derived from such models may not directly correlate to human colon cancer in light of SI and LI SC differences reported in this study. These differences may also account for the increased prevalence of LI cancer compared to SI cancer, as well as highlight crucial protective mechanisms present in the SI that could be exploited to improve the prevention and treatment of colon cancer.

8.0 FUTURE DIRECTIONS

The novel characterization in this study comparing human SI and LI SCs *in vitro* identified many important differences that warrant further investigation.

8.1 ADULT INTESTINAL STEM CELLS

This study focused solely on the characterization and manipulation of human fetal SI and LI SCs. While cancer formation often depicts a return to the developmental state [170], making the use of fetal cells relevant to cancer studies, colon cancer is very much an old-age disease with the highest cancer rates in people aged 75-84 years [2]. Therefore, it is important to compare the SI and LI SCs from adult origin in order to see differences in the SCs that are at risk for transformation. Prior to identifying the proper culture conditions for fetal intestinal SCs, attempts were made to culture adult intestinal SCs, but without success. Now that the culture conditions have been defined, it is likely that they will also aid in the expansion of normal adult intestinal SCs.

8.2 REGULATION OF APOPTOSIS

Previous observations have suggested that LI SCs are more resistant to apoptosis in response to irradiation [72, 74, 75]. While this phenomenon was not directly assessed in the current work, the idea that LI SCs have high resistance to irradiation may determine the resistance of their transformed counterparts, CSCs, to cancer therapies. Therefore, it is important to assess apoptosis in SI and LI SCs and determine if there is a specific resistance mechanism present in the LI SCs compared to SI SCs. This may be the reason for the higher 5-year survival rate in SI cancers, indicating that patients respond more favorably to cancer treatments (**Table 1**). Higher levels of Bcl-2 and lower levels of p53 likely increase the resistance of LI SCs to DNA-damage-induced apoptosis [72, 74]. Their level of expression should be assessed to see if this phenomenon is also true in human cells, as previous studies have assessed their role in murine models. If their mechanism of resistance can be elucidated, therapies targeting CSCs can be improved. Once the anti-apoptotic mechanisms have been identified in normal cells, colon CSCs can be used to assess the efficacy of such directed targeting.

8.3 INTESTINAL REGENERATION AND WOUND HEALING

Previous studies in mice have indicated that intestinal organoids can be used to heal damaged tissue in the intestinal epithelium and promote regeneration [171]. Therefore, it is important to assess if human intestinal SC-derived organoids are capable of the same phenomenon. Wounds in the LI of immunocompromised mice could be transplanted with human LI SC-derived organoids and compared to the transplantation of SI SC-derived organoids. The detection of

engraftment could be aided with the expression of CMV-EGFP in normal SI and LI SCs prior to organoid formation. In preliminary studies, we found that LI SCs can be infected with viruses for expression purposes. When CMV-EGFP was introduced into LI SCs, EGFP was well incorporated and expressed. While it would be interesting to do the same engraftment experiment in SI tissue with both SI and LI SC-derived organoids, this would be more technically challenging with a higher risk of infection. These experiments would confirm that human intestinal SC-derived organoids could help the regeneration of intestinal epithelium after damage.

8.4 LI STEM CELLS VERSUS CSCS

While the current study focused on the differences between SI and LI SCs, some results indicated similarities between LI SCs and colon CSCs. To truly understand what makes a normal SC cancerous, comparison studies between the cell of origin and the cell produced must be done. For example, results found in this study indicated cell surface expression of CD44 on CSCs but absent on normal LI SCs (**Figure 7B**). It is likely that the overexpression of CD44 protein in normal LI SCs may cause the cells to adopt more of a CSC phenotype, assayed by LDA or tumorigenicity assays. Alternatively, a reduction in the expression of CD44 in colon CSCs may reduce their ability to form colonies or tumors. As mentioned earlier in the text, previous studies have shown that a reduction in CD44 lowers the tumorigenicity and clonogenicity of cells *in vitro* [109]. It is important to confirm this result in CSCs expanded from patients with metastatic disease. It is also important to note that according to the gene array results, CD44 transcript is

abundant in normal LI SCs, indicating translational repression that may be removed upon transformation, allowing the expression of CD44 and enhancement of migration and adhesion.

8.5 TRANSFORMATION OF NORMAL INTESTINAL STEM CELLS

Throughout this work, there were many evidences that the normal intestinal SCs expanded in our culture system were not transformed. In Chapter 3.1.2 we found that LI and SI SCs did not express CD44, while colon CSCs did. In Chapter 2.2.1, we found that the cells are not tumorigenic upon transplantation into mice. Lastly, in Chapter 5.1.2 we showed that intestinal organoids respond to differentiation cues with a decrease in proliferation, unlike CSC-derived organoids that increase their proliferation. If normal LI SCs are the initiating cells of cancer, it may be possible to transform them *in vitro*. Similar to the viral approach used to express CMV-EGFP, discussed above, virus could be used to introduce a mutated beta-catenin to promote transformation, such as beta-catenin with S33A mutation, rendering it stable [172]. Although mutations in beta-catenin are rare in colon cancer, the result is similar to mutations in APC; accumulation of beta-catenin in the nucleus with enhanced Wnt signaling [57]. Alternatively, siRNA targeted to APC would also lead to the increased translocation of beta-catenin into the nucleus and enhance Wnt signaling. Other components of the Wnt pathway can be targeted pharmacologically. GSK3-beta can be catalytically inhibited by CHIR99021, releasing beta-catenin from the destruction complex [172]. HLY78 activates Wnt signaling upstream of beta-catenin by modulating the interaction between Axin-LRP5/6 [173]. These experiments should be performed in both SI and LI SCs, with subsequent assessment of changes in proliferation (LDA and organoid incorporation of EdU) and response to differentiation cues (matrigel organoids).

However, forced transformation will likely cause transformation in both SI and LI (as in Barker 2009 [4]), which does not mimic what happens *in vivo*. From the results presented here, it is the increased susceptibility of LI SCs that causes a higher incidence of LI cancer, therefore, introducing a forced genetic alteration is likely to result in transformation of both SCs.

8.6 DETERMINE THE CONSEQUENCES OF MANIPULATING SI AND LI SC GENE EXPRESSION

Significant differences in gene expression were identified in SI and LI SCs, but it is not clear if these differences play key roles distinguishing SI from LI SCs and relation to disease. In the gene array studies, Chapter 4, expression of OPN and CD44 was found to be higher in LI SCs and is linked to metastasis and cancer progression [139]. High expression of CPS1 and RARRES1 in SI SCs is linked to differentiation and tumor suppression [120, 151]. Therefore, if the expression patterns were altered using gene knockdown or over expression, the effects could be assessed using growth curves, surface marker assessment (CD133.1, CD66c, CD13), LDA and matrigel assays. If OPN or CD44 were over expressed or CPS1 or RARRES1 were knocked down in SI SCs, we would expect to see an adoption of LI SC characteristics. Likewise, if OPN or CD44 were knocked down or CPS1 or RARRES1 were over expressed in LI SCs we would expect to see an adoption of SI SC characteristics.

Following the lack of detection of ATOH1 in LI-derived organoids in Chapter 5.2, ATOH1 could be expressed in LI-derived organoids. Resulting organoids could be assessed for Muc2 and ChrA expression both at RNA and protein levels to see if LI-derived organoids took on the phenotype of SI-derived organoids. Likewise, ATOH1 could be knocked down in SI-

derived organoids and results similarly assessed. LGR5 levels should also be assessed in matrigel organoids after changing the expression of ATOH1, since its increase upon differentiation treatment of LI-derived organoids (**Figure 24B**) was an unexpected and yet undocumented phenomenon. These experiments would determine if ATOH1 levels are responsible for the differences seen in SI- and LI-derived organoids. Subsequently, due to their tumor-suppressor roles, ATOH1 and RARRES1 could be knocked down in colon CSCs to see its effect on colony formation and tumor formation [151, 164]. Characterizing the differences between SI and LI SCs and CSCs are needed to identify new therapeutic opportunities to improve the prevention and treatment of colon cancer.

BIBLIOGRAPHY

1. Siegel R, Naishadham D, Jemal A. Cancer statistics, 2012. CA Cancer J Clin. 2012;62: 10-29.
2. Howlander N, Noone, A.M., Krapcho, M., Garshell, J., Neyman, N., Altekruse, S.F., Kosary, C.L., Yu, M., Ruhl, J., Tatalovich, Z., Cho, H., Mariotto, A., Lewis, D.R., Chen, H.S., Feuer, E.J., Cronin, K.A. (eds). SEER Cancer Statistics Review, 1975-2010, National Cancer Institute. Bethesda, MD, http://seer.cancer.gov/csr/1975_2010/, based on November 2012 SEER data submission, posted to the SEER web site, 2013.
.
3. Fearon ER, Vogelstein B. A genetic model for colorectal tumorigenesis. Cell. 1990;61: 759-767.
4. Barker N, Ridgway RA, van Es JH, et al. Crypt stem cells as the cells-of-origin of intestinal cancer. Nature. 2009;457: 608-611.
5. Sato T, Vries RG, Snippert HJ, et al. Single Lgr5 stem cells build crypt-villus structures in vitro without a mesenchymal niche. Nature. 2009;459: 262-265.
6. Barker N, van Es JH, Kuipers J, et al. Identification of stem cells in small intestine and colon by marker gene Lgr5. Nature. 2007;449: 1003-1007.
7. Potten CS, Owen G, Booth D. Intestinal stem cells protect their genome by selective segregation of template DNA strands. J Cell Sci. 2002;115: 2381-2388.
8. Potten CS, Kellett M, Roberts SA, Rew DA, Wilson GD. Measurement of in vivo proliferation in human colorectal mucosa using bromodeoxyuridine. Gut. 1992;33: 71-78.
9. Sato T, van Es JH, Snippert HJ, et al. Paneth cells constitute the niche for Lgr5 stem cells in intestinal crypts. Nature. 2011;469: 415-418.
10. Chandler JM, Lagasse E. Cancerous stem cells: deviant stem cells with cancer-causing misbehavior. Stem Cell Res Ther. 2010;1: 13.
11. Schofield R. The relationship between the spleen colony-forming cell and the haemopoietic stem cell. Blood Cells. 1978;4: 7-25.
12. Sato T, Stange DE, Ferrante M, et al. Long-term expansion of epithelial organoids from human colon, adenoma, adenocarcinoma, and Barrett's epithelium. Gastroenterology. 2011;141: 1762-1772.
13. Farin HF, Van Es JH, Clevers H. Redundant sources of Wnt regulate intestinal stem cells and promote formation of Paneth cells. Gastroenterology. 2012;143: 1518-1529 e1517.
14. Kosinski C, Li VS, Chan AS, et al. Gene expression patterns of human colon tops and basal crypts and BMP antagonists as intestinal stem cell niche factors. Proc Natl Acad Sci U S A. 2007;104: 15418-15423.
15. Geiser J, Venken KJ, De Lisle RC, Andrews GK. A mouse model of acrodermatitis enteropathica: loss of intestine zinc transporter ZIP4 (Slc39a4) disrupts the stem cell niche and intestine integrity. PLoS Genet. 2012;8: e1002766.

16. Altmann GG. Morphological observations on mucus-secreting nongoblet cells in the deep crypts of the rat ascending colon. Am J Anat. 1983;167: 95-117.
17. Leblond CP, Messier B. Renewal of chief cells and goblet cells in the small intestine as shown by radioautography after injection of thymidine-H3 into mice. Anat Rec. 1958;132: 247-259.
18. Quastler H, Sherman FG. Cell population kinetics in the intestinal epithelium of the mouse. Exp Cell Res. 1959;17: 420-438.
19. Walker BE, Leblond CP. Sites of nucleic acid synthesis in the mouse visualized by radioautography after administration of C14-labelled adenine and thymidine. Exp Cell Res. 1958;14: 510-531.
20. Cheng H, Leblond CP. Origin, differentiation and renewal of the four main epithelial cell types in the mouse small intestine. I. Columnar cell. Am J Anat. 1974;141: 461-479.
21. Cheng H, Leblond CP. Origin, differentiation and renewal of the four main epithelial cell types in the mouse small intestine. V. Unitarian Theory of the origin of the four epithelial cell types. Am J Anat. 1974;141: 537-561.
22. Winton DJ, Blount MA, Ponder BA. A clonal marker induced by mutation in mouse intestinal epithelium. Nature. 1988;333: 463-466.
23. Bjerknes M, Cheng H. Clonal analysis of mouse intestinal epithelial progenitors. Gastroenterology. 1999;116: 7-14.
24. Potten CS, Hume WJ, Reid P, Cairns J. The segregation of DNA in epithelial stem cells. Cell. 1978;15: 899-906.
25. Marshman E, Booth C, Potten CS. The intestinal epithelial stem cell. Bioessays. 2002;24: 91-98.
26. Escobar M, Nicolas P, Sangar F, et al. Intestinal epithelial stem cells do not protect their genome by asymmetric chromosome segregation. Nat Commun. 2011;2: 258.
27. Schepers AG, Vries R, van den Born M, van de Wetering M, Clevers H. Lgr5 intestinal stem cells have high telomerase activity and randomly segregate their chromosomes. EMBO J. 2011;30: 1104-1109.
28. Steinhauser ML, Bailey AP, Senyo SE, et al. Multi-isotope imaging mass spectrometry quantifies stem cell division and metabolism. Nature. 2012;481: 516-519.
29. Hayflick L. The Limited in Vitro Lifetime of Human Diploid Cell Strains. Exp Cell Res. 1965;37: 614-636.
30. Korinek V, Barker N, Moerer P, et al. Depletion of epithelial stem-cell compartments in the small intestine of mice lacking Tcf-4. Nat Genet. 1998;19: 379-383.
31. Schuijers J, Clevers H. Adult mammalian stem cells: the role of Wnt, Lgr5 and R-spondins. EMBO J. 2012;31: 2685-2696.
32. Yan KS, Chia LA, Li X, et al. The intestinal stem cell markers Bmi1 and Lgr5 identify two functionally distinct populations. Proc Natl Acad Sci U S A. 2012;109: 466-471.
33. Glinka A, Dolde C, Kirsch N, et al. LGR4 and LGR5 are R-spondin receptors mediating Wnt/beta-catenin and Wnt/PCP signalling. EMBO Rep. 2011;12: 1055-1061.
34. Carmon KS, Gong X, Lin Q, Thomas A, Liu Q. R-spondins function as ligands of the orphan receptors LGR4 and LGR5 to regulate Wnt/beta-catenin signaling. Proc Natl Acad Sci U S A. 2011;108: 11452-11457.
35. Sangiorgi E, Capecchi MR. Bmi1 is expressed in vivo in intestinal stem cells. Nat Genet. 2008;40: 915-920.

36. Tian H, Biehs B, Warming S, et al. A reserve stem cell population in small intestine renders Lgr5-positive cells dispensable. Nature. 2011;478: 255-259.
37. Snoeck V, Goddeeris B, Cox E. The role of enterocytes in the intestinal barrier function and antigen uptake. Microbes Infect. 2005;7: 997-1004.
38. Falk P, Roth KA, Gordon JI. Lectins are sensitive tools for defining the differentiation programs of mouse gut epithelial cell lineages. Am J Physiol. 1994;266: G987-1003.
39. Dharmani P, Srivastava V, Kissoon-Singh V, Chadee K. Role of intestinal mucins in innate host defense mechanisms against pathogens. J Innate Immun. 2009;1: 123-135.
40. Kim YS, Ho SB. Intestinal goblet cells and mucins in health and disease: recent insights and progress. Curr Gastroenterol Rep. 2010;12: 319-330.
41. Roth KA, Hertz JM, Gordon JI. Mapping enteroendocrine cell populations in transgenic mice reveals an unexpected degree of complexity in cellular differentiation within the gastrointestinal tract. J Cell Biol. 1990;110: 1791-1801.
42. Lievin-Le Moal V, Servin AL. The front line of enteric host defense against unwelcome intrusion of harmful microorganisms: mucins, antimicrobial peptides, and microbiota. Clin Microbiol Rev. 2006;19: 315-337.
43. Moran GW, Leslie FC, Levison SE, Worthington J, McLaughlin JT. Enteroendocrine cells: neglected players in gastrointestinal disorders? Therap Adv Gastroenterol. 2008;1: 51-60.
44. Jenny M, Uhl C, Roche C, et al. Neurogenin3 is differentially required for endocrine cell fate specification in the intestinal and gastric epithelium. EMBO J. 2002;21: 6338-6347.
45. Skipper M, Lewis J. Getting to the guts of enteroendocrine differentiation. Nat Genet. 2000;24: 3-4.
46. Jensen J, Pedersen EE, Galante P, et al. Control of endodermal endocrine development by Hes-1. Nat Genet. 2000;24: 36-44.
47. van Es JH, Jay P, Gregorieff A, et al. Wnt signalling induces maturation of Paneth cells in intestinal crypts. Nat Cell Biol. 2005;7: 381-386.
48. Fre S, Huyghe M, Mourikis P, Robine S, Louvard D, Artavanis-Tsakonas S. Notch signals control the fate of immature progenitor cells in the intestine. Nature. 2005;435: 964-968.
49. Fre S, Pallavi SK, Huyghe M, et al. Notch and Wnt signals cooperatively control cell proliferation and tumorigenesis in the intestine. Proc Natl Acad Sci U S A. 2009;106: 6309-6314.
50. Rubinfeld B, Souza B, Albert I, et al. Association of the APC gene product with beta-catenin. Science. 1993;262: 1731-1734.
51. Su LK, Vogelstein B, Kinzler KW. Association of the APC tumor suppressor protein with catenins. Science. 1993;262: 1734-1737.
52. Korinek V, Barker N, Morin PJ, et al. Constitutive transcriptional activation by a beta-catenin-Tcf complex in APC-/- colon carcinoma. Science. 1997;275: 1784-1787.
53. Clevers H. Wnt/beta-catenin signaling in development and disease. Cell. 2006;127: 469-480.
54. Tetsu O, McCormick F. Beta-catenin regulates expression of cyclin D1 in colon carcinoma cells. Nature. 1999;398: 422-426.
55. He TC, Sparks AB, Rago C, et al. Identification of c-MYC as a target of the APC pathway. Science. 1998;281: 1509-1512.
56. Powell SM, Zilz N, Beazer-Barclay Y, et al. APC mutations occur early during colorectal tumorigenesis. Nature. 1992;359: 235-237.
57. Morin PJ, Sparks AB, Korinek V, et al. Activation of beta-catenin-Tcf signaling in colon cancer by mutations in beta-catenin or APC. Science. 1997;275: 1787-1790.

58. Kwong LN, Dove WF. APC and its modifiers in colon cancer. Adv Exp Med Biol. 2009;656: 85-106.
59. Kinzler KW, Nilbert MC, Su LK, et al. Identification of FAP locus genes from chromosome 5q21. Science. 1991;253: 661-665.
60. Groden J, Thliveris A, Samowitz W, et al. Identification and characterization of the familial adenomatous polyposis coli gene. Cell. 1991;66: 589-600.
61. Schroeter EH, Kisslinger JA, Kopan R. Notch-1 signalling requires ligand-induced proteolytic release of intracellular domain. Nature. 1998;393: 382-386.
62. Heitzler P, Bourouis M, Ruel L, Carteret C, Simpson P. Genes of the Enhancer of split and achaete-scute complexes are required for a regulatory loop between Notch and Delta during lateral signalling in Drosophila. Development. 1996;122: 161-171.
63. Riccio O, van Gijn ME, Bezdek AC, et al. Loss of intestinal crypt progenitor cells owing to inactivation of both Notch1 and Notch2 is accompanied by derepression of CDK inhibitors p27Kip1 and p57Kip2. EMBO Rep. 2008;9: 377-383.
64. Kageyama R, Ohtsuka T, Tomita K. The bHLH gene Hes1 regulates differentiation of multiple cell types. Mol Cells. 2000;10: 1-7.
65. Pellegrinet L, Rodilla V, Liu Z, et al. Dll1- and dll4-mediated notch signaling are required for homeostasis of intestinal stem cells. Gastroenterology. 2011;140: 1230-1240 e1231-1237.
66. Sikandar SS, Pate KT, Anderson S, et al. NOTCH signaling is required for formation and self-renewal of tumor-initiating cells and for repression of secretory cell differentiation in colon cancer. Cancer Res. 2010;70: 1469-1478.
67. van Es JH, van Gijn ME, Riccio O, et al. Notch/gamma-secretase inhibition turns proliferative cells in intestinal crypts and adenomas into goblet cells. Nature. 2005;435: 959-963.
68. Hoey T, Yen WC, Axelrod F, et al. DLL4 blockade inhibits tumor growth and reduces tumor-initiating cell frequency. Cell Stem Cell. 2009;5: 168-177.
69. Thenappan A, Li Y, Shetty K, Johnson L, Reddy EP, Mishra L. New Therapeutics Targeting Colon Cancer Stem Cells. Curr Colorectal Cancer Rep. 2009;5: 209.
70. Hua G, Thin TH, Feldman R, et al. Crypt base columnar stem cells in small intestines of mice are radioresistant. Gastroenterology. 2012;143: 1266-1276.
71. Blanpain C, Mohrin M, Sotiropoulou PA, Passegue E. DNA-damage response in tissue-specific and cancer stem cells. Cell Stem Cell. 2011;8: 16-29.
72. Merritt AJ, Potten CS, Watson AJ, et al. Differential expression of bcl-2 in intestinal epithelia. Correlation with attenuation of apoptosis in colonic crypts and the incidence of colonic neoplasia. J Cell Sci. 1995;108 (Pt 6): 2261-2271.
73. Potten CS, Grant HK. The relationship between ionizing radiation-induced apoptosis and stem cells in the small and large intestine. Br J Cancer. 1998;78: 993-1003.
74. Merritt AJ, Potten CS, Kemp CJ, et al. The role of p53 in spontaneous and radiation-induced apoptosis in the gastrointestinal tract of normal and p53-deficient mice. Cancer Res. 1994;54: 614-617.
75. Hendry JH, Cai WB, Roberts SA, Potten CS. p53 deficiency sensitizes clonogenic cells to irradiation in the large but not the small intestine. Radiat Res. 1997;148: 254-259.
76. Korinek V, Barker N, Willert K, et al. Two members of the Tcf family implicated in Wnt/beta-catenin signaling during embryogenesis in the mouse. Mol Cell Biol. 1998;18: 1248-1256.
77. Shy BR, Wu CI, Khramtsova GF, et al. Regulation of Tcf7l1 DNA binding and protein stability as principal mechanisms of Wnt/beta-catenin signaling. Cell Rep. 2013;4: 1-9.

78. Angus-Hill ML, Elbert KM, Hidalgo J, Capecchi MR. T-cell factor 4 functions as a tumor suppressor whose disruption modulates colon cell proliferation and tumorigenesis. Proc Natl Acad Sci U S A. 2011;108: 4914-4919.
79. Reya T, Morrison SJ, Clarke MF, Weissman IL. Stem cells, cancer, and cancer stem cells. Nature. 2001;414: 105-111.
80. Vogelstein B, Kinzler KW. Cancer genes and the pathways they control. Nat Med. 2004;10: 789-799.
81. Sell S. Stem cell origin of cancer and differentiation therapy. Crit Rev Oncol Hematol. 2004;51: 1-28.
82. Al-Hajj M, Clarke MF. Self-renewal and solid tumor stem cells. Oncogene. 2004;23: 7274-7282.
83. Schepers AG, Snippert HJ, Stange DE, et al. Lineage tracing reveals Lgr5+ stem cell activity in mouse intestinal adenomas. Science. 2012;337: 730-735.
84. Merlos-Suarez A, Barriga FM, Jung P, et al. The intestinal stem cell signature identifies colorectal cancer stem cells and predicts disease relapse. Cell Stem Cell. 2011;8: 511-524.
85. Ziskin JL, Dunlap D, Yaylaoglu M, et al. In situ validation of an intestinal stem cell signature in colorectal cancer. Gut. 2012.
86. Loupakis F, Cremolini C, Fontanini G, Stasi I, Salvatore L, Falcone A. Beyond KRAS: perspectives on new potential markers of intrinsic and acquired resistance to epidermal growth factor receptor inhibitors in metastatic colorectal cancer. Ther Adv Med Oncol. 2009;1: 167-181.
87. Kosa P, Szabo R, Molinolo AA, Bugge TH. Suppression of Tumorigenicity-14, encoding matriptase, is a critical suppressor of colitis and colitis-associated colon carcinogenesis. Oncogene. 2012;31: 3679-3695.
88. Fodde R, Brabletz T. Wnt/beta-catenin signaling in cancer stemness and malignant behavior. Curr Opin Cell Biol. 2007;19: 150-158.
89. Pinto D, Clevers H. Wnt control of stem cells and differentiation in the intestinal epithelium. Exp Cell Res. 2005;306: 357-363.
90. Ashley N. Regulation of intestinal cancer stem cells. Cancer Lett. 2012.
91. Snippert HJ, van der Flier LG, Sato T, et al. Intestinal crypt homeostasis results from neutral competition between symmetrically dividing Lgr5 stem cells. Cell. 2010;143: 134-144.
92. Clevers H. The intestinal crypt, a prototype stem cell compartment. Cell. 2013;154: 274-284.
93. De Wever O, Nguyen QD, Van Hoorde L, et al. Tenascin-C and SF/HGF produced by myofibroblasts in vitro provide convergent pro-invasive signals to human colon cancer cells through RhoA and Rac. FASEB J. 2004;18: 1016-1018.
94. Rasola A, Fassetta M, De Bacco F, et al. A positive feedback loop between hepatocyte growth factor receptor and beta-catenin sustains colorectal cancer cell invasive growth. Oncogene. 2007;26: 1078-1087.
95. Vermeulen L, De Sousa EMF, van der Heijden M, et al. Wnt activity defines colon cancer stem cells and is regulated by the microenvironment. Nat Cell Biol. 2010;12: 468-476.
96. Heijmans J, Buller NV, Hoff E, et al. Rage signalling promotes intestinal tumourigenesis. Oncogene. 2013;32: 1202-1206.
97. Ehmann UK, Peterson WD, Jr., Misfeldt DS. To grow mouse mammary epithelial cells in culture. J Cell Biol. 1984;98: 1026-1032.
98. Odoux C, Fohrer H, Hoppo T, et al. A stochastic model for cancer stem cell origin in metastatic colon cancer. Cancer Res. 2008;68: 6932-6941.

99. Burgess AW, Faux MC, Layton MJ, Ramsay RG. Wnt signaling and colon tumorigenesis--a view from the periphery. Exp Cell Res. 2011;317: 2748-2758.
100. Munz M, Kieu C, Mack B, Schmitt B, Zeidler R, Gires O. The carcinoma-associated antigen EpCAM upregulates c-myc and induces cell proliferation. Oncogene. 2004;23: 5748-5758.
101. Balzar M, Winter MJ, de Boer CJ, Litvinov SV. The biology of the 17-1A antigen (Ep-CAM). J Mol Med (Berl). 1999;77: 699-712.
102. Ricci-Vitiani L, Lombardi DG, Pilozzi E, et al. Identification and expansion of human colon-cancer-initiating cells. Nature. 2007;445: 111-115.
103. Munz M, Baeuerle PA, Gires O. The emerging role of EpCAM in cancer and stem cell signaling. Cancer Res. 2009;69: 5627-5629.
104. Kemper K, Sprick MR, de Bree M, et al. The AC133 epitope, but not the CD133 protein, is lost upon cancer stem cell differentiation. Cancer Res. 2010;70: 719-729.
105. Levin TG, Powell AE, Davies PS, et al. Characterization of the intestinal cancer stem cell marker CD166 in the human and mouse gastrointestinal tract. Gastroenterology. 2010;139: 2072-2082 e2075.
106. von Furstenberg RJ, Gulati AS, Baxi A, et al. Sorting mouse jejunal epithelial cells with CD24 yields a population with characteristics of intestinal stem cells. Am J Physiol Gastrointest Liver Physiol. 2011;300: G409-417.
107. Tani H, Morris RJ, Kaur P. Enrichment for murine keratinocyte stem cells based on cell surface phenotype. Proc Natl Acad Sci U S A. 2000;97: 10960-10965.
108. Huang X, Sheng Y, Guan M. Co-expression of stem cell genes CD133 and CD44 in colorectal cancers with early liver metastasis. Surg Oncol. 2012;21: 103-107.
109. Park YS, Huh JW, Lee JH, Kim HR. shRNA against CD44 inhibits cell proliferation, invasion and migration, and promotes apoptosis of colon carcinoma cells. Oncol Rep. 2012;27: 339-346.
110. Glebov OK, Rodriguez LM, Nakahara K, et al. Distinguishing right from left colon by the pattern of gene expression. Cancer Epidemiol Biomarkers Prev. 2003;12: 755-762.
111. Weilbaecher K, Weissman I, Blume K, Heimfeld S. Culture of phenotypically defined hematopoietic stem cells and other progenitors at limiting dilution on Dexter monolayers. Blood. 1991;78: 945-952.
112. Waldmann H, Lefkovits I, Quintans J. Limiting dilution analysis of helper T-cell function. Immunology. 1975;28: 1135-1148.
113. O'Brien CA, Pollett A, Gallinger S, Dick JE. A human colon cancer cell capable of initiating tumour growth in immunodeficient mice. Nature. 2007;445: 106-110.
114. Gemei M, Mirabelli P, Di Noto R, et al. CD66c is a novel marker for colorectal cancer stem cell isolation, and its silencing halts tumor growth in vivo. Cancer. 2012.
115. Johnson RL, Fleet JC. Animal models of colorectal cancer. Cancer Metastasis Rev. 2013;32: 39-61.
116. Moser AR, Pitot HC, Dove WF. A dominant mutation that predisposes to multiple intestinal neoplasia in the mouse. Science. 1990;247: 322-324.
117. Leclerc D, Deng L, Trasler J, Rozen R. ApcMin/+ mouse model of colon cancer: gene expression profiling in tumors. J Cell Biochem. 2004;93: 1242-1254.
118. Ullman TA, Itzkowitz SH. Intestinal inflammation and cancer. Gastroenterology. 2011;140: 1807-1816.

119. Van der Flier LG, Sabates-Bellver J, Oving I, et al. The Intestinal Wnt/TCF Signature. Gastroenterology. 2007;132: 628-632.
120. Cardona DM, Zhang X, Liu C. Loss of carbamoyl phosphate synthetase I in small-intestinal adenocarcinoma. Am J Clin Pathol. 2009;132: 877-882.
121. Wood RJ, Tchack L, Angelo G, Pratt RE, Sonna LA. DNA microarray analysis of vitamin D-induced gene expression in a human colon carcinoma cell line. Physiol Genomics. 2004;17: 122-129.
122. Sinner D, Kordich JJ, Spence JR, et al. Sox17 and Sox4 differentially regulate beta-catenin/T-cell factor activity and proliferation of colon carcinoma cells. Mol Cell Biol. 2007;27: 7802-7815.
123. Kongkham PN, Northcott PA, Croul SE, Smith CA, Taylor MD, Rutka JT. The SFRP family of WNT inhibitors function as novel tumor suppressor genes epigenetically silenced in medulloblastoma. Oncogene. 2010;29: 3017-3024.
124. Cunningham JM, Christensen ER, Tester DJ, et al. Hypermethylation of the hMLH1 promoter in colon cancer with microsatellite instability. Cancer Res. 1998;58: 3455-3460.
125. Leslie A, Pratt NR, Gillespie K, et al. Mutations of APC, K-ras, and p53 are associated with specific chromosomal aberrations in colorectal adenocarcinomas. Cancer Res. 2003;63: 4656-4661.
126. Quintero M, Mackenzie N, Brennan PA. Hypoxia-inducible factor 1 (HIF-1) in cancer. Eur J Surg Oncol. 2004;30: 465-468.
127. Dai Z, Jin Y. Promoter methylation of the DLC1 gene and its inhibitory effect on human colon cancer. Oncol Rep. 2013.
128. Modica S, Morgano A, Salvatore L, et al. Expression and localisation of insulin receptor substrate 2 in normal intestine and colorectal tumours. Regulation by intestine-specific transcription factor CDX2. Gut. 2009;58: 1250-1259.
129. Babyatsky MW, Rossiter G, Podolsky DK. Expression of transforming growth factors alpha and beta in colonic mucosa in inflammatory bowel disease. Gastroenterology. 1996;110: 975-984.
130. Coste A, Dubuquoy L, Barnouin R, et al. LRH-1-mediated glucocorticoid synthesis in enterocytes protects against inflammatory bowel disease. Proc Natl Acad Sci U S A. 2007;104: 13098-13103.
131. Saksena S, Priyamvada S, Kumar A, et al. Keratinocyte growth factor-2 stimulates P-glycoprotein expression and function in intestinal epithelial cells. Am J Physiol Gastrointest Liver Physiol. 2013;304: G615-622.
132. Megiorni F, Pizzuti A. HLA-DQA1 and HLA-DQB1 in Celiac disease predisposition: practical implications of the HLA molecular typing. J Biomed Sci. 2012;19: 88.
133. Nimmo ER, Stevens C, Phillips AM, et al. TLE1 modifies the effects of NOD2 in the pathogenesis of Crohn's disease. Gastroenterology. 2011;141: 972-981 e971-972.
134. Levison SE, Fisher P, Hankinson J, et al. Genetic analysis of the Trichuris muris-induced model of colitis reveals QTL overlap and a novel gene cluster for establishing colonic inflammation. BMC Genomics. 2013;14: 127.
135. Huang J, Pan C, Hu H, Zheng S, Ding L. Osteopontin-enhanced hepatic metastasis of colorectal cancer cells. PLoS One. 2012;7: e47901.
136. Likui W, Hong W, Shuwen Z. Clinical significance of the upregulated osteopontin mRNA expression in human colorectal cancer. J Gastrointest Surg. 2010;14: 74-81.

137. Yeatman TJ, Chambers AF. Osteopontin and colon cancer progression. Clin Exp Metastasis. 2003;20: 85-90.
138. Agrawal D, Chen T, Irby R, et al. Osteopontin identified as colon cancer tumor progression marker. C R Biol. 2003;326: 1041-1043.
139. Weber GF, Ashkar S, Cantor H. Interaction between CD44 and osteopontin as a potential basis for metastasis formation. Proc Assoc Am Physicians. 1997;109: 1-9.
140. Rao G, Wang H, Li B, et al. Reciprocal interactions between tumor-associated macrophages and CD44-positive cancer cells via osteopontin/CD44 promote tumorigenicity in colorectal cancer. Clin Cancer Res. 2013;19: 785-797.
141. Sancho R, Nateri AS, de Vinuesa AG, et al. JNK signalling modulates intestinal homeostasis and tumourigenesis in mice. EMBO J. 2009;28: 1843-1854.
142. Clapper ML, Hensley HH, Chang WC, Devarajan K, Nguyen MT, Cooper HS. Detection of colorectal adenomas using a bioactivatable probe specific for matrix metalloproteinase activity. Neoplasia. 2011;13: 685-691.
143. Zhang W, Li Y, Yang L, et al. Knockdown of MMP-7 inhibits cell proliferation and enhances sensitivity to 5-fluorouracil and X-ray irradiation in colon cancer cells. Clin Exp Med. 2012.
144. Brabletz T, Jung A, Dag S, Hlubek F, Kirchner T. beta-catenin regulates the expression of the matrix metalloproteinase-7 in human colorectal cancer. Am J Pathol. 1999;155: 1033-1038.
145. Zeng ZS, Shu WP, Cohen AM, Guillem JG. Matrix metalloproteinase-7 expression in colorectal cancer liver metastases: evidence for involvement of MMP-7 activation in human cancer metastases. Clin Cancer Res. 2002;8: 144-148.
146. Leeman MF, Curran S, Murray GI. New insights into the roles of matrix metalloproteinases in colorectal cancer development and progression. J Pathol. 2003;201: 528-534.
147. Van Beers EH, Rings EH, Posthuma G, et al. Intestinal carbamoyl phosphate synthase I in human and rat. Expression during development shows species differences and mosaic expression in duodenum of both species. J Histochem Cytochem. 1998;46: 231-240.
148. Blachier F, Darcy-Vrillon B, Sener A, Duee PH, Malaisse WJ. Arginine metabolism in rat enterocytes. Biochim Biophys Acta. 1991;1092: 304-310.
149. Moonen RM, Paulussen AD, Souren NY, Kessels AG, Rubio-Gozalbo ME, Villamor E. Carbamoyl phosphate synthetase polymorphisms as a risk factor for necrotizing enterocolitis. Pediatr Res. 2007;62: 188-190.
150. Wu CC, Shyu RY, Chou JM, et al. RARRES1 expression is significantly related to tumour differentiation and staging in colorectal adenocarcinoma. Eur J Cancer. 2006;42: 557-565.
151. Jing C, El-Ghany MA, Beesley C, et al. Tazarotene-induced gene 1 (TIG1) expression in prostate carcinomas and its relationship to tumorigenicity. J Natl Cancer Inst. 2002;94: 482-490.
152. Oldridge EE, Walker HF, Stower MJ, et al. Retinoic acid represses invasion and stem cell phenotype by induction of the metastasis suppressors RARRES1 and LXN. Oncogenesis. 2013;2: e45.
153. Kim KA, Zhao J, Andarmani S, et al. R-Spondin proteins: a novel link to beta-catenin activation. Cell Cycle. 2006;5: 23-26.
154. Yoon JK, Lee JS. Cellular signaling and biological functions of R-spondins. Cell Signal. 2012;24: 369-377.
155. de Lau W, Barker N, Low TY, et al. Lgr5 homologues associate with Wnt receptors and mediate R-spondin signalling. Nature. 2011;476: 293-297.

156. Dignass AU, Sturm A. Peptide growth factors in the intestine. Eur J Gastroenterol Hepatol. 2001;13: 763-770.
157. Denu JM. Vitamin B3 and sirtuin function. Trends Biochem Sci. 2005;30: 479-483.
158. van de Wetering M, Sancho E, Verweij C, et al. The beta-catenin/TCF-4 complex imposes a crypt progenitor phenotype on colorectal cancer cells. Cell. 2002;111: 241-250.
159. Milano J, McKay J, Dagenais C, et al. Modulation of notch processing by gamma-secretase inhibitors causes intestinal goblet cell metaplasia and induction of genes known to specify gut secretory lineage differentiation. Toxicol Sci. 2004;82: 341-358.
160. Jung P, Sato T, Merlos-Suarez A, et al. Isolation and in vitro expansion of human colonic stem cells. Nat Med. 2011;17: 1225-1227.
161. Shroyer NF, Helmrath MA, Wang VY, Antalffy B, Henning SJ, Zoghbi HY. Intestine-specific ablation of mouse atonal homolog 1 (Math1) reveals a role in cellular homeostasis. Gastroenterology. 2007;132: 2478-2488.
162. Kazanjian A, Noah T, Brown D, Burkart J, Shroyer NF. Atonal homolog 1 is required for growth and differentiation effects of notch/gamma-secretase inhibitors on normal and cancerous intestinal epithelial cells. Gastroenterology. 2010;139: 918-928, 928 e911-916.
163. van Es JH, de Geest N, van de Born M, Clevers H, Hassan BA. Intestinal stem cells lacking the Math1 tumour suppressor are refractory to Notch inhibitors. Nat Commun. 2010;1: 18.
164. Bossuyt W, Kazanjian A, De Geest N, et al. Atonal homolog 1 is a tumor suppressor gene. PLoS Biol. 2009;7: e39.
165. Francipane MG, Chandler J, Lagasse E. Cancer Stem Cells: A Moving Target. Curr Pathobiol Rep. 2013;1: 111-118.
166. Wersto RP, Chrest FJ, Leary JF, Morris C, Stetler-Stevenson MA, Gabrielson E. Doublet discrimination in DNA cell-cycle analysis. Cytometry. 2001;46: 296-306.
167. Hughes KR, Gandara RM, Javkar T, et al. Heterogeneity in histone 2B-green fluorescent protein-retaining putative small intestinal stem cells at cell position 4 and their absence in the colon. Am J Physiol Gastrointest Liver Physiol. 2012;303: G1188-1201.
168. Lin SA, Barker N. Gastrointestinal stem cells in self-renewal and cancer. J Gastroenterol. 2011;46: 1039-1055.
169. Qiu W, Carson-Walter EB, Liu H, et al. PUMA regulates intestinal progenitor cell radiosensitivity and gastrointestinal syndrome. Cell Stem Cell. 2008;2: 576-583.
170. Cohnheim J. Ueber Entzundung und Eiterung. Virchows Arch Path Anat. 1867;40: 1-79.
171. Yui S, Nakamura T, Sato T, et al. Functional engraftment of colon epithelium expanded in vitro from a single adult Lgr5(+) stem cell. Nat Med. 2012;18: 618-623.
172. Kuhl SJ, Kuhl M. On the role of Wnt/beta-catenin signaling in stem cells. Biochim Biophys Acta. 2013;1830: 2297-2306.
173. Wang S, Yin J, Chen D, et al. Small-molecule modulation of Wnt signaling via modulating the Axin-LRP5/6 interaction. Nat Chem Biol. 2013;9: 579-585.